AD_____

Award Number: DAMD17-00-1-0361

TITLE: Breast Cancer Training Program

PRINCIPAL INVESTIGATOR: Doctor Kenneth H. Cowan
James D. Shull, Ph.D.

CONTRACTING ORGANIZATION: University of Nebraska Medical Center
Omaha, Nebraska 68198-6810

REPORT DATE: August 2004

TYPE OF REPORT: Annual Summary

PREPARED FOR: U.S. Army Medical Research and Materiel Command
Fort Detrick, Maryland 21702-5012

REPORT DOCUMENTATION PAGE

Form Approved
OMB No. 074-0188

1. AGENCY USE ONLY (Leave blank)	2. REPORT DATE	3. REPORT TYPE AND DATES COVERED
	August 2004	Annual Summary (1 Jul 00-1 Jul 04)

4. TITLE AND SUBTITLE
Breast Cancer Training Program

5. FUNDING NUMBERS
DAMD17-00-1-0361

6. AUTHOR(S)
Doctor Kenneth H. Cowan
James D. Shull, Ph.D.

7. PERFORMING ORGANIZATION NAME(S) AND ADDRESS(ES)
University of Nebraska Medical Center
Omaha, Nebraska 68198-6810

E-Mail: kcowan@unmc.edu / j.shull@unmc.edu

8. PERFORMING ORGANIZATION REPORT NUMBER

9. SPONSORING / MONITORING AGENCY NAME(S) AND ADDRESS(ES)
U.S. Army Medical Research and Materiel Command
Fort Detrick, Maryland 21702-5012

10. SPONSORING / MONITORING AGENCY REPORT NUMBER

11. SUPPLEMENTARY NOTES

12a. DISTRIBUTION / AVAILABILITY STATEMENT
Approved for Public Release; Distribution Unlimited

12b. DISTRIBUTION CODE

13. ABSTRACT (Maximum 200 Words)

The Breast Cancer Training Program (BCTP) in the Eppley Cancer Institute of the University of Nebraska Medical Center offers predoctoral and postdoctoral trainees a comprehensive training environment in breast cancer by supporting, in part, an outstanding breast cancer seminar program, a short course in cancer biology, a breast cancer focus group and by providing stipend support to trainees performing research that is highly relevant to breast cancer. In the four years of this award we have provided stipends to nine predoctoral and twelve postdoctoral trainees. Five of nine predoctoral trainees have completed their graduate training and have secured postdoctoral positions in outstanding laboratories in research areas directly related to breast cancer. Five postdoctoral trainees have moved to other institutions and seven remain in training. Publications in highly ranked journals are beginning to result from the research of the BCTP trainees. Though DOD funding for the BCTP is ending, the program will continue and the program faculty will seek resources elsewhere to continue student and postdoctoral training in breast cancer research.

14. SUBJECT TERMS
Breast cancer, institutional training grant, predoctoral training, postdoctoral training

15. NUMBER OF PAGES
93

16. PRICE CODE

17. SECURITY CLASSIFICATION OF REPORT	18. SECURITY CLASSIFICATION OF THIS PAGE	19. SECURITY CLASSIFICATION OF ABSTRACT	20. LIMITATION OF ABSTRACT
Unclassified	Unclassified	Unclassified	Unlimited

Table of Contents

Cover 1

SF 298 2

Table of Contents 3

Introduction ..... N/A

Body ..... N/A

Key Research Accomplishments 4-9

Reportable Outcomes 9-11

Conclusions ..... N/A

References ..... N/A

Appendices 12-59

1) mTIP 30 Deficiency Increases Susceptibility to Tumorigenesis 12-16

2) TIP 30 Interacts with an Estrogen Receptor *a*-interacting Coactivator CIA and Regulates c-*myc* Transcription 17-25

3) Cell cycle arrest and cell death are controlled by p53-dependant and p53-independent mechanisms in Tsg 101-deficient cells 26-59

4) Genetics of pituitary tumorigenesis 60

I. Key Accomplishments.

Task 1. **We will develop and maintain a Breast Cancer Training Program for graduate students and postdoctoral fellows that will include the following academic programs (programs and activities were detailed in application).** The Breast Cancer Focus Group continues to meet monthly and the Student/Fellow Research Forum continues to meet weekly during the academic year. The 2004 Short Course in Cancer Biology was held May 10-14 and the internationally recognized visiting scientists for this course are listed in Table 1. The Eppley Institute continues to sponsor an outstanding seminar program with a strong emphasis on breast cancer. Speakers on breast cancer in the 2000-04 academic years are listed in Table 2.

Table 1. Visiting Faculty for 2004 Short Course in Cancer Biology – Metastasis: Biology and Therapeutic Strategies.

Faculty	Institution	Title of Section
Dr. Danny Welch	University of Alabama, Birmingham	Metastasis Controlling Genes
Dr. Ruth Muschel	Children's Hospital of Philadelphia	Mechanisms of Metastasis
Dr. Patricia Steeg	National Institutes of Health	Translational Leads in Breast Cancer Metastasis
Dr. Lynn Matrisian	Vanderbilt University Eppley Visiting Professor of Oncology	What We've Learned from the Matrix Metalloproteinase Inhibitor Clinical Trials
Visiting Faculty for 2003 Short Course in Cancer Biology - Cell Biology of Breast Cancer		
Faculty	**Institution**	**Title of Section**
Dr. Jeffrey Holt	University of Colorado Health Science Center, Denver, CO	Pathobiology and Genetics of Breast Cancer
Dr. Nita Maihle	Mayo Clinic, Rochester,MN	Growth Factor Regulation of Breast Cancer
Dr. William Mueller	McGill University, Quebec, ON, Canada	Transgenic Models of Breast Cancer
Dr. Mary (Nora) Disis	Washington University, Seattle, WA	Novel Therapeutic for the Treatment of Breast Cancer
Visiting Faculty for 2002 Short Course in Cancer Biology – Cancer Genetics		
Faculty	**Institution**	**Title of Section**
Dr. Gerard Evan	University of California, San Francisco	Constructing and Deconstructing a Cancer Genetically
Dr. Donna Albertson	University of California, San Francisco	Micro array Based Comparative Genomic Hybridization to Assess Gene Copy Number
Dr. William Kaelin	Harvard University and Howard Hughes Med. Institute	Tumor Suppressor Genes and Gene Based Therapies
Dr. William Bennett	City of Hope, Beckman Research Institute	Cancer Epidemiology
Visiting Faculty for 2001 Short Course in Cancer Biology		
Faculty	**Institution**	**Title of Section**
Dr. Matthew Mescher	University of Minnesota	T Lymphocyte Response to Tumors
Dr. James Mule	University of Michigan Medical Center	Tumor Vaccines
Dr. Jeffrey Weber	University of Southern California, School of Medicine	Clinical Immunotherapy Trials
Dr. Ellen Vitetta	University of Texas southwestern Medical Center	Monoclonal Antibody Therapies for Cancer

Table 2. Eppley Institute Seminar Speakers on Breast Cancer, 2000-2004.

Date	Speaker	Institution	Topic
July 22, 2004	Dr. Emanuel F Petricoin	FDA-NCI Clinical Proteomics Program, Office of Cellular and Gene Therapies	Clinical Proteomics: Applications at the Bedside
May 24, 2004	Dr Evelyne Sage	CNRS Institute Curie , Centre Universitaire	Multiply damaged sites in DNA : a challenge for cellular repair processes?
May 1, 2004	Dr. Nancy E Davidson	Johns Hopkins University School of Medicine	Henry Lemon Memorial Lecture Epigenetic Gene Regulation in Breast Cancer
April 22, 2004	Dr. Michael Stallcup	University of Southern California Los Angeles	Role of protein methylation and protein-protein interactions in transcriptional activation by nuclear receptors and their co activators
April 8, 2004	Dr. Hallier Rui	Georgetown University, Lombardi Comprehensive Cancer Center	The role of Stat5 in human breast cancer progression
March 25, 2004	Dr. Guo-Min Li	University of Kentucky , Department of Pathology	Dissection of DNA mismatch repair in human cells
March 18, 2004	Dr. Paola Muti	Department of Social & Preventive Medicine University at Buffalo	Endogenous hormones and breast cancer risk and recurrence
February 5, 2004	Dr. Dawn Quelle	University of Iowa	Signaling pathways and partners of ARF
December 11, 2003	Dr. Scott Kaufmann	Mayo Clinic, Oncology Research	Apoptosis and the Response to Anticancer Drugs
November 13, 2003	Dr. Thomas Sutter	W. Harry Feinstone Center for Genomic Research, University of Memphis	Functional Genomic Approaches to Chemical Carcinogenesis and Chemoprevention
October 9, 2003	Dr. Jun Qin	Lerner Research Institute, The Cleveland Clinic Foundation	Integrin-Mediated Cell Adhesion Viewed at Three Dimensions
September 25, 2003	Dr. Scott Weed	University of Colorado Health Sciences Center	Cortactin: Integrating Tyrosine Kinase and Actin Cytoskeletal Signaling Pathways
September 18, 2003	Dr. Lewis Chodosh	University of Pennsylvania School of Medicine	Genetically Engineered Mouse Models for Breast Cancer and Breast Cancer Risk
May 1, 2003	Dr. Gail Prins	University of Illinois at Chicago	Estrogenic regulation of steroid receptors, morphogens and signaling pathways during prostate development
April 24, 2003	Dr. Jose Russo	Fox Chase Cancer Center	A new paradigm in the prevention of human breast cancer
April 17, 2003	Dr. Jerry Zambetti	St. Jude Children's Research Hospital	Regulators and mediators of the p53 tumor suppressor pathway.
April 10, 2003	Dr. Chu-Xia Deng	NIH	BRCA1 and Tumorigenesis
March 13, 2003	Dr. Donald Patrick McDonnell	Duke University Medical Center	Nuclear receptor-cofactor interactions: Points of convergence between multiple signaling pathways
February 6, 2003	Dr. Russell Reiter	The University of Texas Health Science Center	Actions of Melatonin
January 16, 2003	Dr. Robert Cardiff	University of California, Davis	Breast Cancer: Lessons from the mouse
November 14, 2002	Dr. Philip Thorpe	UT Southwestern Medical Center	Vascular Targeting Agents for the Treatment of Solid Tumors
November 7, 2002	Dr. Barbara Vonderhaar	NCI	Prolactin in Mammary Development and Tumorigenesis
October 31, 2002	Dr. Al Reynolds	The Vanderbilt-Ingram Cancer Center	p 120-Catenin: Tumor Suppressor or Metastasis Promoter
October 24, 2002	Dr. David Zava	ZRT Laboratory Beaverton, Oregon	Hormonal Imbalance and Cancer Risk: The Estrogen Matrix
October 10, 2002	Dr. Joe W. Gray	UCSF Comprehensive Cancer Center	Genome Evolution in Breast Cancer: Predictive Markers to Therapeutics Targets
September 26, 2002	Dr. Martin Privalsky	University of California at Davis	A Molecular Toggle Switch: Nuclear Hormone Receptors and Transcriptional Regulation

Table 2. continued Eppley Institute Seminar Speakers on Breast Cancer, 2000-2004.

Date	Speaker	Institution	Topic
May 9, 2002	Dr. Priscilla Furth	Georgetown Univ.	Hormonal signaling and mammary carcinogenesis
April 18, 2002	Dr. Michael Gould	Univ. Wisconsin	Genetics of mammary cancer susceptibility
March 28, 2002	Dr. Daniel Medina	Baylor College of Medicine	Hormones, aneuploidy and mammary carcinogenesis
March 14, 2002	Dr. Itamar Barash	Volcani Institute, Israel	Stat5, mammary carcinogenesis
February 21, 2002	Dr. Robert Callahan	NCI	Notch, mammary gland development
January 17, 2002	Dr. Larry Brody	NCHGR	BRCA1
November 15, 2001	Dr. Dihua Yu	U. Texas, M.D. Anderson	ErbB2 and breast cancer chemoresistance
November 8, 2001	Dr. David Soloman	NCI	Cripto, mammary gland morphogen
October 11, 2001	Dr. Wei Zheng	Vanderbilt Univ.	Breast cancer epidemiology
September 6, 2001	Dr. Gilbert Smith	NCI	Mammary stem cells
May 24, 2001	Dr. V. Craig Jordan	Northwestern University School of Medicine	Henry Lemon Memorial Lecture: Development of Antiestrogens for Breast Cancer Treatment and Prevention
April 12, 2001	Dr. Joachim Liehr	Stehlin Foundation	Genotoxic Mechanisms of estrogen Carcinogenesis
April 5, 2001	Dr. Jeffrey Rosen	Baylor College of Medicine	Transgenic and Knockout Mouse Models of Breast Cancer
March 22, 2001	Dr. Kathryn Horwitz	University of Colorado Health Science Center	Mechanisms of Hormonal Resistance in Breast Cancer
October 19, 2000	Dr. Douglas Yee	University of Minnesota	The IGF-I Axes and Breast Cancer

Task 2. **We will recruit qualified students and fellows to the Breast Cancer Training Program and, through the laboratories of the training faculty, provide a stimulating, comprehensive and multidisciplinary training experience pertaining directly to breast cancer.** Nine predoctoral and twelve postdoctoral trainees have been supported by this training grant during the four years of this award. Five of the predoctoral trainees and five of the twelve postdoctoral fellows supported by the award have now completed their training at the Eppley Institute and have moved to postdoctoral positions in internationally recognized laboratories. Seven of the twelve postdoctoral trainees supported by the award remain in training. A summary of the research of each fellow is presented below.

Predoctoral Fellows:

Djuana Harvell, Ph.D.; predoctoral trainee supported in year 1. Dr. Harvell demonstrated that a 40% restriction of dietary energy consumption inhibits estrogen-induced mammary carcinogenesis in the female ACI rat. This inhibition occurs at a step subsequent to development of focal regions of atypical hyperplasia. Two first author manuscripts were published in the past year (Appendices 1 and 2), and a third has been submitted for publication. Dr. Harvell is now a postdoctoral fellow in the laboratory of Dr. Kate Horwitz at the University of Colorado Health Sciences Center, where she is continuing to study the role of steroid hormones in breast cancer.

Michelle VanLith, Ph.D.; predoctoral trainee supported in year 1. Dr. VanLith defined the cellular bases of tumor-specific immune responses to MUC-1. She is first author of a manuscript, listed below, that has been accepted for publication. A second first author manuscript has been submitted for publication. Dr. VanLith is currently a postdoctoral fellow in the laboratory of Dr. V. Englehard at the University of Virginia, working in the area of tumor immunology.

Jennifer Brennan, Ph.D.; predoctoral trainee supported in year 1. Dr. Brennan demonstrated that kinase suppressor of ras (KSR) cycles through the nucleus in a phosphorylation dependent manner. Cellular localization was also impacted by specific interactions with MEK. A first author manuscript detailing this study was published in the J. Biol. Chem. Dr. Brennan is currently a postdoctoral fellow at St. Jude Children's Hospital working in the laboratory of Dr. John Cleveland.

Martin Tochacek, Ph.D.; predoctoral trainee supported in year 2. Dr. Tochacek mapped several genetic loci that determine susceptibility to estrogen-induced mammary cancer in crosses between the highly susceptible ACI strain and two different resistant rat strains. Dr. Tochacek contributed to one published manuscript and two first and one co-author submitted for publication. Dr. Tochacek is currently a postdoctoral fellow at Duke University, working in the laboratory of Dr. Donald McDonnell, studying steroid hormones action and breast cancer.

Kimberly Wielgus; predoctoral trainee supported in year 2. Ms. Wielgus is working toward the Ph.D. in nursing and is investigating fatigue in patients with advanced stage breast cancer. Her participation in the activities of the Breast Cancer Research Program has enabled her to gain a fundamental understanding of the disease process as well as its genetic and molecular bases. Ms. Wielgus competed successfully for a four-year Scholarship in Cancer Nursing from the American Cancer Society.

Scott Stoeger, BS; predoctoral trainee in year 03
Scott is an MD/PhD student working on understanding how the Kinase Suppressor of Ras (KSR) may play a role in determining cellular sensitivity to chemotherapeutic agents. In addition, he is examining the expression of KSR in a variety of cancer cell lines. He is an author on one manuscript that is submitted for publication.

Tracy Strecker, Ph.D.; predoctoral trainee in year 03
Mr. Strecker is nearing completion of his doctoral studies and has one manuscript submitted for publication at this time. He is currently working on 2 additional manuscripts. His work focused on the identification of genetic loci involved in estrogen-induced tumorigenesis in ACI and Copenhagen Rats. His first author paper has been published in Genetics see Appendix 4.

Chunhui Yi; predoctoral trainee supported in year 4. Ms. Yi demonstrated that the expression of an extracellular matrix protein fibulin-2 is lower in eight breast cancer cell lines compared to normal cells. She is studying the roles and mechanisms of fibulin-2 in breast cancer growth, invasion and metastasis. Currently, her work is focus on verifying the expression of fibulin-2 in patient samples. She is also working on establish fibulin-2 expression in those breast cancer cell lines in order to study how fibulin-2 expression affects cancer growth and invasion. Her work will be presented at the AACR meeting and her preliminary data and data to be collected will contribute to a manuscript describing the functions of fibulin-2 in breast cancer.

Marissa Carstens; predoctoral trainee supported in year 4. Ms. Carstens is working toward her Ph.D. in Pathology and Microbiology. In October of 2003, Marissa received an AACR Scholar-in-Training-Award for her poster presentation at the special conference "Advances in Breast Cancer Research: Genetics, Biology, and Clinical Implications" in Huntington Beach, CA. Her first paper has been published in J. Biol. Chem. see Appendix 3.

Postdoctoral Fellows:

Benjamin Xie, M.D., Ph.D.; postdoctoral trainee supported in year 1. Dr. Xie demonstrated that expression of progesterone receptor (PR) is much higher in the focal regions of atypical hyperplasia and mammary carcinoma induced in ACI rats by continuous treatment with estradiol than in normal or hyperplastic mammary glands. These data are included in two published manuscripts. Dr. Xie also demonstrated that expression of Cdkn2a is markedly down-regulated as an early event in estrogen-induced mammary carcinogenesis. A manuscript describing these data is in preparation.

Constance Dooley, Ph.D.; postdoctoral trainee supported in year 1. Dr. Dooley tested the hypothesis that ectopic Kinase Suppressor of Ras (KSR) will inhibit the transformation properties of human cancer cells in vitro and the tumorigenic potential of mammary tissue in vivo. Dr. Dooley successfully generated high-titer recombinant baculovirus for full-length KSR, KSR with two mutated phosphorylation sites, the carboxy terminal half of KSR, the amino terminal half of KSR, and two forms of KSR with reduced or absent activity. Dr. Dooley moved to a new postdoctoral training position at the University of Utah.

David Smith, Ph.D.; postdoctoral trainee supported in year 1. Dr. Smith investigated the regulation of the human *MUC1* gene. *MUC1* has been shown to be up-regulated in many forms of cancer including breast. He performed *in vivo* foot printing experiments to locate the positions of transcription factor binding sites in the promoter region of the *MUC1* gene. Finally, he initiated a translational study in which cDNA array technologies are being used to compare gene expression profiles in primary breast cancers and associated axillary lymph node metastasis.

Beverly Schaffer, Ph.D.; postdoctoral trainee supported in year 2. Dr. Schaffer joined the BCTP in December of 2001. She is generating congenic rat lines in which Brown Norway alleles for *Emca1*, *Emca2* and *Emca3* are carried on the ACI background. She has demonstrated that these *Emca* loci determine susceptibility to estrogen-induced mammary cancer in crosses between the ACI and BN rat strains. The congenic lines will be characterized to define the roles of each *Emca* locus in estrogen-induced mammary carcinogenesis and to fine map each *Emca* locus. She is working on 2 additional manuscripts currently.

Nicholas Moniaux, Ph.D.; postdoctoral trainee supported in year 2. Dr. Moniaux has cloned and characterized the MUC4 genes from rat and human and is defining the interactions between MUC4 and HER2. He is testing the hypothesis that MUC4/HER2 interactions contribute to pathogenesis of breast cancer.

Adrian Reber, Ph.D.; postdoctoral trainee supported in year 2. Dr. Reber investigated the role of invariant chain protein (Ii) on MHC class I molecules in different breast cancer cell lines from humans, rats and mice. He demonstrated that Ii binds only to folded, peptide free, class I molecules and results in increased cell surface expression of class I. Future experiments underway will test the hypothesis that Ii may be used to increase anti tumor immune responses in rat and mouse mammary cancer models.

Lois Beckerbauer, Ph.D.; postdoctoral trainee in year 03

Dr. Beckerbauer continues her training in Dr. Shull's laboratory and recently received an individual postdoctoral fellowship from the DOD BCRP. She is coauthor on Dr. Xie's manuscript that is nearing submission and is first author on a second manuscript nearing submission. She is working on 2 additional manuscripts currently. She had a poster presentation accepted at the 2003 meeting of the AACR.

Chao Jiang, BS, M.D. postdoctoral trainee in year 03 and 04
Dr. Jiang is currently studying the roles of the transcription cofactors in estrogen receptor-mediated transcription and tumorigenesis. She has given 3 presentations at the meetings of Cancer Genetics & Tumor Suppressor Genes at Cold Spring Harbor, New York in August 2002, AACR 95th Annual meeting in Orlando, FL, March, 2004 and AACR Special conference in Cancer Research in Hunting Beach, CA., October, 2003. She has published 2 papers see Appendix 1 and Appendix 2.

Yan Zhang, Ph.D.; postdoctoral trainee supported in year 4. Dr. Zhang has been pursuing her proposed research on the role of various cytochromes P450 isoforms in the metabolism of estradiol to form DNA adducts in relation to the initiation of breast cancer. She has given a presentation at the meeting of the American Association of Cancer Research at Orlando, Florida in March 2004.

Kimberly Hansen, Ph.D.; postdoctoral trainee supported in year 4. Dr. Hansen helped develop several congenic rat lines in which the COP allele at one of four Ept loci has been introgressed onto the ACI background. Dr. Hansen is currently characterizing the response of these congenic rat lines to estrogen-induced mammary carcinogenesis and pituitary tumorigenesis. Dr. Hansen predicts that these congenic rat lines will retain their susceptibility to estrogen-induced mammary carcinogenesis similar to that of the ACI rat, but that estrogen-induced pituitary tumorigenesis will be significantly reduced. These experiments are aimed at examining the following hypothesis: that the tumorigenic actions of administered E2 in the mammary gland and the pituitary gland of the ACI rat are genetically separable. Dr. Hansen is co-first author of two manuscripts currently in preparation.

Steve Schreiner Ph.D.; postdoctoral trainee supported in year 4. Dr. Schreiner is studying the role of the molecular scaffold KSR1 in regulating cell proliferation and motility. He is also studying interactions between the metastasis suppressor nm23 and KSR1. Dr. Schreiner is co-author on a submitted manuscript that demonstrates the role of KSR1 as a regulator of cell differentiation. He is first author on a manuscript in preparation demonstrating the ability of KSR1 to regulate cell motility and adhesion. He has presented his results at a National meeting on breast cancer in Orlando, FL

Masato Maeda Ph.D.; postdoctoral trainee supported in year 4. Dr. Maeda is studying the role of cadherin switching in TGF-ß1-mediated epithelial to mesenchymal transition in mammary epithelial cells. He has presented his findings at the BCTP meeting, Mar 14, 2003 Eppley Science Hall, the 43rd Annual Meeting of American Society for Cell Biology, December, 2003 San Francisco, CA, 95th Annual Meeting of American Association for Cancer Research March, 2004 Orlando, FL and Gordon Research Conference (Signaling By Adhesion Receptors) June, 2004 Bristol, RI. He also first-author on a manuscript that has been submitted.

Task 3. We will maintain oversight of the Breast Cancer Training Program to ensure that all progress reports and communications are submitted as required and that the training faculty and trainees fulfill their respective obligations to the program. All previous progress reports have been submitted as required. All activities associated with the Breast Cancer Training Program, as described in our application, have been organized and will continue beyond the term of the award.

II. Reportable Outcomes.

A. Published Manuscripts (funded trainees are underlined):

Chao Jiang, Mitsuhiro Ito, Hua Xiao et al., mTIP30 deficiency increases susceptibility to tumorigenesis. Cancer Res. 63: 8763-7, 2003.

A. Published Manuscripts continued (funded trainees are underlined):

Chao Jiang, Robert G. Roeder, Hua Xiao. TIP30 interacts with an ERa-interacting coactivator CIA and regulates c-myc transcription. J. Biol Chem. 279: 27781-9, 2004.

Carstens MJ, Krempler A, Triplett AA, Van Lohuizen M, Wagner KU. Cell cycle arrest and cell death are controlled by p53-dependent and p53-independent mechanisms in Tsg101-deficient cells. J. Biol Chem. Jun 21 [Epub ahead of print], 2004.

Tracy E. Strecker, Spady, T.J., Kaufman, A.E., Shen, F., McLaughlin, M.T., Pennington,K.L., Meza, J.L., Schaffer, B.S., Gould, K.A.,Shull, J.D. Genetics of pituitary tumorigenesis. Genetics(ahead of print) 2004.

Harvell, D.M.E., Buckles, L.K., Gould, K.A., Pennington, K.L., McComb, R.D. and Shull, J.D. Rat Strain Specific Attenuation of Estrogen Action in the Anterior Pituitary Gland by Dietary Energy Restriction. Endocrine 21:175-83, 2003.(Appendix of year 3)

Brennan, J.A., Volle, D.J., Chaika, O.V. and Lewis, R.E. Phosphorylation regulates the nucleocytoplasmic distribution of kinase suppressor of ras. J. Biol. Chem. 277:5369-5377, 2002. (Appendix of year 2)

Harvell, D.M.E., Strecker, T.E., Xie, B., Buckles, L.K., Tochacek, M., McComb, R.D. and Shull, J.D. Diet-gene interactions in estrogen-induced mammary carcinogenesis in the ACI rat. J. Nutrition 131: 3087S-3091S, 2001. (Appendix of year 2)

Harvell, D.M.E., Strecker, T.E., Xie, B., Pennington, K.L., McComb, R.D. and Shull, J.D. Dietary energy restriction inhibits estrogen-induced mammary, but not pituitary, tumorigenesis in the ACI rat. Carcinogenesis 23: 161-169, 2002. (Appendix of year 1)

Moniaux, N., Escande, F., Porchet, N., Aubert, J.P. and Batra, S.K. Structural organization and classification of the human mucin genes. Front. Bioscience 6: D1192-1206, 2001. (Appendix of year 2)

Shiraga, T., Smith, D., Nuthall, H.N., Hollingsworth, M.A. and Harris, A. Identification of two novel elements involved in human MUC1 gene expression in vivo. Mol. Med. 8: 33-41, 2002. (Appendix of year 2)

Shull, J.D., Pennington, K.L., Reindl, T.M., Snyder, M.C., Strecker, T.E., Spady, T.J., Tochacek, M. and McComb, R.D. Susceptibility to estrogen-induced mammary cancer segregates as an incompletely dominant phenotype in reciprocal crosses between the ACI and Copenhagen rat strains. Endocrinology 142: 5124-5130, 2001. (Appendix of year 2)

VanLith, M.L., Kohlgraf, K.G., Sivinski, C.L., Tempero, R., and Hollingsworth, M.A. MUC1-Specific Anti-Tumor Responses: Molecular Requirements for CD4 mediated responses. International Immunology 14: 873-82, 2002. (Appendix of year 2)

B. Degrees obtained:

Michelle VanLith, Ph.D.	degree granted August 2001.
Djuana Harvell, Ph.D.	degree granted December 2001.
Jennifer Brennan, Ph.D.	degree granted December 2001.
Martin Tochacek, Ph.D.	degree granted June 2002.
Tracy Strecker, Ph.D.	degree granted June 2004

C. Cell lines generated:

B. Xie/J. Shull	normal mammary epithelium, ACI rat
B. Xie/J. Shull	normal mammary epithelium, Copenhagen rat
B. Xie/J. Shull	estrogen-induced mammary carcinoma, ACI rat
C. Jiang/ H. Xiao	cultured these cell lines HepG2-TIP30 and HepG2-TIPM3

D. Related funding:

Beverly Schaffer received an individual postdoctoral fellowship from the DOD BCRP.
Lois Beckerbauer received an individual postdoctoral fellowship from the DOD BCRP.
Kim Wielgus, Scholarship in Cancer Nursing, American Cancer Society, 2002-2006 and an additional grant for her research studies from NASA.
Scott Stoeger has been awarded a graduate studies assistantship from UNMC.
Masato Maeda has been awarded the Research Fellowship from the Uehara Memorial Foundation 4/1/04 – 3/31/05

E. Employment received:

Dr. Michelle VanLith (Ph.D., June 2001) accepted a postdoctoral position in the laboratory of Dr. V. Englehard at the University of Virginia, working in the area of tumor immunology.

Djuana Harvell (Ph.D., December 2001) accepted a postdoctoral position in the laboratory of Dr. Kate Horwitz at the University of Colorado Health Science Center. She is studying steroid hormones and breast cancer.

Jennifer Brennan (Ph.D., December 2001) accepted a postdoctoral position in the laboratory of Dr. John Cleveland at St. Jude Children's Hospital.

Martin Tochacek (Ph.D., June 2002) accepted a postdoctoral position in the laboratory of Dr. Donald McDonnell at Duke University, working in the area of steroid hormone action.

Constance Dooley (postdoctoral trainee, 2000-2002) accepted a postdoctoral position in the laboratory of Monica Vetter at the University of Utah.

Nicholas Moniaux (postdoctoral trainee 2002-2003) accepted a research assistant professorship in the Department of Biochemistry and Molecular Biology at UNMC.

David Smith (postdoctoral trainee supported in 2001-2002) accepted a position of Instructor in the UNMC Department of Surgery.

Adrian Reber (postdoctoral trainee supported in year 2001-2002) accepted a position of Post-doctoral Fellow at the University of Georgia in the Department of Large Animal Medicine.

Chao Jiang (postdoctoral trainee supported in year 3 & 4 of the grant) accepted a position of Research Assistant in the UNMC Department of Biochemistry with Dr. Hua Xiao.

[CANCER RESEARCH 63, 8763–8767, December 15, 2003]

APPENDIX 1

TIP30 Deficiency Increases Susceptibility to Tumorigenesis

Mitsuhiro Ito,[1] Chao Jiang,[2] Kristy Krumm,[2] Xia Zhang,[4] Jill Pecha,[2,3] Jian Zhao,[4] Yajun Guo,[2,4] Robert G. Roeder,[1] and Hua Xiao[2,3]

[1]Laboratory of Biochemistry and Molecular Biology, The Rockefeller University, New York, New York; [2]Eppley Institute for Cancer Research, and [3]Department of Pathology and Microbiology, University of Nebraska Medical Center, Omaha, Nebraska; and [4]International Joint Cancer Institute and Eastern Hospital of Hepatobiliary Surgery, Shanghai, People's Republic of China

ABSTRACT

TIP30, also called CC3 or Htatip2, is a putative metastasis suppressor that promotes apoptosis and inhibits angiogenesis. Although TIP30 has several characteristic features of a tumor suppressor in *in vitro* analyses, tumor development as a result of TIP30 inactivation has not been demonstrated *in vivo*, and abnormal expression of TIP30 in human cancer has not been reported. Using genetically engineered mice and cells deficient in TIP30, we show that TIP30-deficient mice have a high incidence of hepatocellular carcinoma and other tumors, and loss of TIP30 enhances susceptibility of fibroblasts to transformation by the SV40 large T antigen. Furthermore, immunohistochemical analysis indicates that reduced TIP30 expression is associated with 33% of human hepatocellular carcinomas. Some of these carcinomas harbor missense mutations in the *Tip30* gene, which cause abnormal expression of TIP30. Together, these results demonstrate that the *Tip30* gene is a tumor susceptibility gene playing an important role in the suppression of hepatocarcinogenesis.

INTRODUCTION

HIV-1 Tat-interacting protein TIP30, identical to the putative metastasis suppressor CC3, has been implicated in the regulation of tumor cell growth and metastasis (1–4). Recent experiments demonstrated that a reduced level of *TIP30* mRNA has been found in a number of tumor cell lines that include variant-small cell lung carcinoma (V-SCLC), classic-SCLC, neuroblastoma, colon cancer, and melanoma cell lines (2–6). Ectopic expression of the *TIP30/CC3* gene in a variant SCLC line lacking TIP30/CC3 expression led to a significant suppression of the metastatic potential of these cells in SCID-hu mice. In addition, metastases in melanoma-bearing mice are significantly reduced after i.v. treatment with the *TIP30/CC3* gene-cationic liposome-DNA complex (6). Subsequent work has led to the proposal that the suppression of cell growth and metastasis by ectopic expression of TIP30 may result, in part, from a propensity of cells to undergo apoptosis (2–4).

TIP30 was believed to be a transcription cofactor because it was demonstrated to potentiate Tat-mediated transcription in cooperation with components of elongation factor P-TEFb in transient transfection assays and is essential for Tat-mediated transcription in cell-free transcription assays (1, 3). TIP30 displays a serine-threonine kinase activity that can phosphorylate the carboxyl terminal domain of RNA polymerase II in a Tat-dependent manner *in vitro* (3). The intrinsic kinase activity is essential for TIP30 to enhance Tat-activated transcription and to sensitize NIH3T3 and v-SCLC cells to apoptosis (3). Consistent with the role of TIP30 in the suppression of tumor growth and metastasis via transcription mechanisms, studies revealed that the ectopic expression of TIP30 in v-SCLC cells and other tumor cell lines up-regulates the expression of proapoptotic factors (3) and angiogenic inhibitors, and down-regulates expression of angiogenic stimulators (4). Therefore, TIP30 may function as a tumor suppressor or tumor modifier that controls expression of genes involved in tumor growth and metastasis.

Although TIP30 has several characteristic features of a tumor suppressor, tumor development as a result of TIP30 inactivation has not been established *in vivo*, and abnormal expression of TIP30 in human cancer has not been reported. In this study, the generation of mice lacking *Tip30* has allowed us to demonstrate a role of TIP30 in the suppression of tumor development *in vivo*. In addition, we have identified missense mutations in the *TIP30* gene in the clinical human hepatocellular carcinomas (HCCs), which resulted in aberrant expression of TIP30.

MATERIALS AND METHODS

Constructions of the *Tip30* Targeting Vector and TIP30-Expressing Plasmids. To isolate the mouse *Tip30* gene, a mouse 129SvJ genomic library (Stratagene, La Jolla, CA) was screened with a mouse *Tip30* cDNA probe. Fourteen overlapping clones contained a 49-kb genomic region that included five coding exons of the *Tip30* gene locus. The *Hind*III-*Sac*I 2.7-kb genomic fragment was replaced by *LacZ* in-frame and a phosphoglycerate kinase *neo*-cassette (Fig. 1*A*). This replacement ablated the two exons that encode the NH_2-terminal portion of TIP30, except for 10 amino acids after the translation start site. The targeting vector (7) included a 5.2-kb upstream homologous region and a 6.5-kb downstream region. Mutated *Tip30* cDNA were generated by using pRSET-TIP30 (1) as templates and a site-directed mutagenesis kit (Stratagene). Plasmids containing Flag tag at the NH_2 terminal of TIP30 were generated by cloning wild-type and mutant *Tip30* coding regions between *Nde*I and *Bam*HI pFlag-7 (8). pCIN4-flag-TIP30, pCIN4-flag-TIP30^{R106H}, and pCIN4-flag-TIP30^{G134V} expressing flag TIP30 proteins were generated by cloning Flag-tag TIP30 cDNA between *Eco*RI and *Bam*HI sites of pCIN4 (1). Plasmids expressing green fluorescent protein-tagged wild-type TIP30 fusion protein (GFP-TIP30), GFP-TIP30^{R106H}, and GFP-TIP30^{G134V} fusion proteins were generated by cloning wild-type and mutant TIP30 coding regions between *Eco*RI and *Bam*HI sites of pEGFP-C2 (Clontech Laboratories, Palo Alto, CA).

Generation of the *Tip30* Knockout Mice. E14 embryotic stem (ES) cells were electroporated with the linearized targeting vector and selected with geneticin on embryonic fibroblast feeder cells as described previously (7). In total, 348 G418-resistant clones were screened by Southern blot analysis using the 5′ external probe, and 65 clones displayed evidence for the homologous recombination of the disrupted *Tip30* gene. Ten ES clones were microinjected into blastocysts of C57BL6/J female mice. Germ-line chimeras were bred to C57BL6J mice to generate heterozygous mutant F1 mice. All of the animal experimentation was performed according to the NIH guidelines in the Rockefeller University Laboratory Animal Research Center and the University of Nebraska Medical Center.

For genotyping, the genomic DNA isolated from ES cells or mouse tails was subjected to Southern blot analysis with a 5′ or 3′ external probe for *lacZ* or used for PCR analysis (primer sequences available on request). Mouse embryotic fibroblasts (MEFs) were prepared from E14.5 embryos obtained by

Received 6/9/03; revised 9/18/03; accepted 10/3/03.

Grant support: Grants for Beginning Investigators RSG0216501GMC from American Cancer Society, and from the University of Nebraska Medical Center (H. X.), and by the NIH grant (R. G. R.). M. I. was supported by a Human Frontier Science Program (HFSP) long-term fellowship. C. J. is partly supported by a breast cancer research training fellowship DAMD17-00-1-0361 from Department of Defense. X. Z., J. Z., and J. G. were supported in part by Grants from Natural Science Foundation of China, and Shanghai Commission of Science and Technology.

The costs of publication of this article were defrayed in part by the payment of page charges. This article must therefore be hereby marked *advertisement* in accordance with 18 U.S.C. Section 1734 solely to indicate this fact.

Notes: Drs. Ito and Jiang contributed equally to this work.

Requests for reprints: Hua Xiao, Eppley Institute for Cancer Research, University of Nebraska Medical Center, 987696 Nebraska Medical Center, Omaha, NE 68198-7696. Phone: (402) 559-3323; Fax: (402) 559-3739; E-mail: hxiao@unmc.edu.

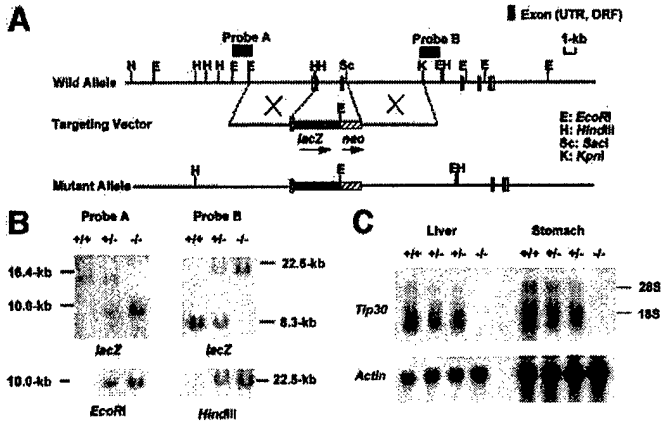

Fig. 1. Spontaneous development of tumors in TIP30-deficient mice. *A*, disruption of the *Tip30* gene. Wild-type allele of the mouse *Tip30* gene (*top*), the targeting vector with *LacZ* and phosphoglycerate kinase *neo* cassettes (*middle*), and the predicted mutant allele resulting from homologous recombination (*bottom*) are presented. *B*, Southern blot analysis of offspring obtained by a heterozygous cross. Genomic DNAs from wild-type (+/+), heterozygous (+/−), and homozygous (−/−) F2 tails, digested with *Eco*RI or *Hind*III, were hybridized with the 5′ or 3′ external probe or *lacZ*. *C*, Northern blot analysis of *Tip30* mRNA in liver and stomach of the indicated genotypes. The signals of two heterozygous mice represent a maternal or paternal allele each. The actin is shown as a control.

heterozygous crossings of mice that had been backcrossed 10 times with C57BL6/J mice.

Northern Blot Analysis. Northern blot analysis was performed as described previously (7). The full-length TIP30 cDNA was used as a probe, and labeled with [α^{32}p]dCTP and a random primer DNA labeling system (Invitrogen, Carlsbad, CA).

Growth and Soft Agar Assays of Immortalized MEFs. Primary *Tip30*$^{+/+}$, *Tip30*$^{+/-}$, and *Tip30*$^{-/-}$ MEFs in passage 2 were used to introduce the SV40 T-antigen expression vector by LipofectAMINE reagent (Invitrogen) and be immortalized after 20 passages. For growth curves, immortalized cells (10^4 per well of 12-well plates) were seeded, and cells were stained with trypan blue and counted daily. For soft agar assays, immortalized MEFs (5×10^3) were grown in DMEM supplemented with 10% fetal bovine serum and 0.53% agarose on top of a layer containing 0.4% agarose for 21 days. The clones were stained with crystal violet, and the clones with diameters >1 mm were counted.

Histology and Immunohistochemistry. Tissues were fixed with 10% buffered-formalin and embedded in paraffin blocks. Tissue sections were deparaffinized, rehydrated, and stained with H&E. For immunohistochemistry, rehydrated sections were incubated overnight at 4°C with affinity-purified antihuman TIP30 antibody. Staining was developed using VECTASTAIN Elite ABC kit (Vector Laboratories, Burlingame, CA).

Identification of *Tip30* Mutations. Genomic DNA was prepared from paraffin tissue blocks with the EX-WAX DNA extraction kit for paraffin-embedded tissue according to the manufacturer's instructions (Intergen Co., Purchase, NY). Exon 3 of the *Tip30* gene was amplified with Vent polymerase (New England Biolab. Inc., Beverly, MA). The primers used for amplification were 5′-GGCCTCCCAGCCTGCTAC-3′ and 5′-GTACTGCCAAAATAG-CTAG-3′. The primers for the nesting PCR were 5′-GCTACCCAAGCCAAG-TAGTAATC-3′ and 5′-GCTAGGGTTCTCCAAAGTG-3′. The first reactions were carried out for 25 cycles of 94°C, 30 s; 60°C, 30; and 72°C, 30 s. The nesting PCR reactions were carried out for 32 cycles of 94°C, 30 s; 60°C, 30; and 72°C, 30 s. The PCR products were incubated with Taq polymerase for 10 min at 72°C for adding A to the ends, and purified with Qiagen PCR purification columns (Qiagen, Valencia, CA), then cloned to the TA vector pCR2.1 (Invitrogen). Ten clones for each sample were sequenced for both DNA strands by the Eppley core facility at the University of Nebraska Medical Center using M13 reversal and universal primers. At least three clones containing identical mutations were sequenced for each patient. The HepG2 cell line was purchased from the American Type Culture Collection (Manassas, VA). Experiments in this study have been approved by the Institutional Review Board for the protection of human subjects at the University of Nebraska Medical Center.

Western Blot Analysis and Fluorescence Microscopy. For Western blot analysis in Fig. 3*B*, HepG2 cells were transfected with pCIN4-flag-TIP30 and pCIN4-flag-TIP30^{G134V} using SuperFect reagents (Qiagen). After 48-h transfection, cells were harvested and whole cell extracts were prepared as described previously (3). Whole cell extracts were incubated with anti-Flag M2-agarose (Sigma, St. Louis, MO) at 4°C overnight. After brief centrifugation, supernatants were removed for Western blots with anti-β-actin antibodies. Precipitated proteins were washed and subjected to Western blots with anti-TIP30 antibodies. Fluorescence microscopy was performed as described previously (9). Before being fixed with 4% buffered paraformaldehyde, cells were grown in DMEM supplemented with 10% fetal bovine serum in the presence or absence of 20 nM of Leptomycin B (LMB; Sigma) for 3 h.

Protein Stability Assay. HepG2 cells were cultured in 150-mm dishes and transfected with pCIN4-flag-TIP30 and pCIN4-flag-TIP30^{G134V} using FuGene 6 reagents (Roche Diagnostics Corp., Indianapolis, IN) according to the manufacturer's instruction. To inhibit protein synthesis, cycloheximade (100 μg/ml) was added to the medium, and cells were then harvested at the indicated time points. Cell lysates were subjected to immunoprecipitation and Western blot analysis as described above. Alexa Fluor 680 goat antirabbit IgG and goat antimouse IgG (Molecular Probes) were used for quantitative Western blot analysis. Li-Cor system was used to visualize and quantitate TIP30 protein and β-actin protein.

RESULTS AND DISCUSSION

To investigate the roles of TIP30 in both cultured cells and living animals, we generated mice carrying inactivated *Tip30* gene by homologous recombination. ES cell clones with a disrupted *Tip30* locus were used to obtain germ-line chimeras that, in turn, were used to generate heterozygous F1 mutant 129SvJ/C57BL6/J hybrid mice (Fig. 1*A*). Crosses between mice heterozygous for the *Tip30* gene led to the expected Mendelian ratios of live born progeny, thus indicating that the *Tip30* gene is not essential for development. The loss of TIP30 expression was confirmed by Southern blot analyses of tail genomic DNAs, and by Northern blot analyses of liver and stomach total RNAs (Fig. 1, *B* and *C*). Histological examinations of the *Tip30*$^{-/-}$ mice before the age of 1 year did not reveal obvious gross alterations or developmental abnormalities in organs other than the mammary glands.[5] Both *Tip30*$^{-/-}$ males and females were fertile and generated normal litter sizes.

To determine whether TIP30 is a tumor suppressor, we have kept a cohort of TIP30-deficient and wild-type animals (50% of C57BL6/J and 50% 129SvJ of genetic background) for long-term observation of the development of spontaneous malignancy. At the age of 18–20 months, 31 females and 16 males of the F2 littermates were sacrificed. Autopsy and histological analyses revealed tumor development in 9 of 18 (50%) TIP30-deficient female mice and 2 of 9 TIP30-deficient male mice. In contrast, none of the 13 female and 7 male wild-type mice displayed tumors (Table 1*A*; wild-type mice *versus* mutant mice; $P < 0.005$; $X^2 = 11.3$). The spectrum of tumor types in *Tip30*-mutant mice (Table 1*B*) is distinct from that seen in older wild-type mice described by others (10–12), as many of the tumors found in TIP30-deficient mice were carcinomas. Among those tumors, HCC showed the highest incidence, constituting 30% of the total tumors. The relatively high incidence of HCC indicates that TIP30 has a prevalent role in tumor suppression in hepatocytes. Interestingly, 1 *Tip30*$^{+/-}$ mouse had two tumors, a lipoid cell tumor at the right ovary and a neuroblastoma that arose at the right adrenal gland, with multiple metastases to tissues that included spleen, thymus, and salivary glands. The metastases were also found in the neck, mesenterium, and mediastinum. In addition, 1 mouse developed a transitional cell carcinoma in the urinary bladder, and exhibited metastases along the epithelium that involved the ureters and kidneys, whereas 2 male mice

[5] Jill Pecha and Hua Xiao, unpublished observations.

developed sarcomas that metastasized to the liver, spleen, and pancreas. These data demonstrate that TIP30-deficient mice are prone to tumor development.

To reveal the basis for the susceptibility of *Tip30*-mutant mice to tumor development, we analyzed *Tip30* wild-type and mutant MEFs. In an examination of the growth rates of MEFs, no significant difference was detected (data not shown). We then asked if TIP30-deficient MEFs may be more susceptible to transformation by SV40 large T antigen, which is able to inactivate p53 and retinoblastoma protein (reviewed in Ref. 13). These cells were immortalized by ectopic expression of the T antigen, and growth rates were measured. Immortalized $Tip30^{-/-}$ and $Tip30^{+/-}$ MEFs grew much faster than immortalized $Tip30^{+/+}$ MEFs (Fig. 2*A*). $Tip30^{-/-}$ and $Tip30^{+/-}$ MEFs also grew in a more disorganized fashion than$Tip30^{+/+}$ MEFs (data not shown). Therefore, we assessed the ability of each type of MEF to grow in soft agar. $Tip30^{-/-}$ and $Tip30^{+/-}$ MEFs showed a marked increase in the number and size of colonies as compared with $Tip30^{+/+}$ MEFs (Fig. 2, *B* and *C*). Western blot analysis revealed similar levels of T-antigen expression in $Tip30^{+/+}$ and $Tip30^{-/-}$ MEFs (Fig. 2*D*), and slightly higher expression of T antigen in $Tip30^{+/-}$ MEFs. These results demonstrate that a lack of TIP30 in cells enhances transformation by the SV40 T antigen.

To determine whether our studies in mice are relevant to human disease, we analyzed 24 surgical specimens of human HCC and compared the expression of TIP30 in cancerous cells with expression in adjacent benign hepatocytes on formalin-fixed, paraffin-embedded tissues with antihuman TIP30 antibody (1). Undetectable or significantly decreased TIP30 expression was found in cancerous cells in 8 specimens (33%) in comparison with the adjacent tissues. An example of the immunohistochemical analyses is shown (Fig. 3*A*). These data indicate that abnormal expression of TIP30 is implicated in human HCC. We next sought to examine whether these HCC cells harbor

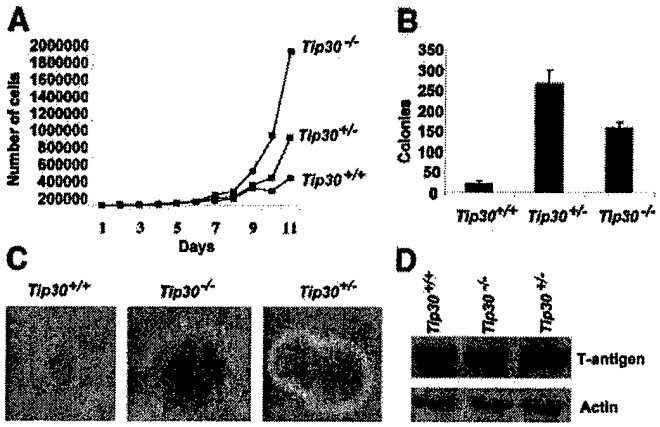

Fig. 2. Deletion of the TIP30 gene enhances fibroblast transformation by the SV40 large T antigen *A*, $TIP30^{-/-}$ and $TIP30^{+/-}$ mouse embryotic fibroblasts (MEFs) proliferate faster than wild-type MEFs after immortalization by SV40 T antigen. Immortalized $Tip30^{+/+}$, $Tip30^{+/-}$, and $Tip30^{-/-}$ MEFs were counted each day. Each value represents the mean of a representative experiment performed in triplicate. *B*, T antigen-immortalized $Tip30^{-/-}$ and $Tip30^{+/-}$ MEFs develop more colony foci than $TIP30^{+/+}$ immortalized MEFs in soft agars. Each value represents the mean of a representative experiment performed in triplicate; *bars*, ± SD. *C*, an example of a colony from each MEF genotype is shown. *D*, Western blot analysis of T-antigen expression in $Tip30^{+/+}$, $Tip30^{+/-}$, and $Tip30^{-/-}$ MEFs. Equivalent amounts of whole cell extracts from each of the indicated MEFs were analyzed by immunoblotting with an anti-T-antigen monoclonal antibody and antiactin monoclonal antibody.

Table 1 *TIP30*

A. *Tumor frequency in TIP30-deficient mice*

Genotype	Tumor rate		
	Total	Female	Male
$Tip30^{+/+}$	0/20 (0 %)	0/13 (0 %)	0/7 (0 %)
$Tip30^{+/-}$ or $-/-$	11/27 (41%)	9/18 (50%)	2/9 (22%)
$Tip30^{+/-}$	7/13	6/8	1/6
$Tip30^{-/-}$	4/13	3/10	1/3

B. *Spectrum of tumors in TIP30-deficient mice*

Sex	Genotype	Histological type	Anatomic site
F	+/−	Hepatocellular carcinoma	Liver
F	+/−	Hepatocellular carcinoma	Liver
F	−/−	Hepatocellular carcinoma	Liver
F	+/−	Thymoma	Thymus
F	+/−	Transitional cell carcinoma, grade III	Ureters, bladder, renal pelvis
F	+/−	Neuroblastoma lipoid cell tumor	Adrenal gland ovary
F	−/−	Adenocarcinoma	Duodenum
F	−/−	Leiomyoma	Uterus
M	+/−	Hemangiosarcoma	Retroperitoneum, liver, spleen, subcutis
M	−/−	Undifferentiated sarcoma	Retroperitoneum, liver, spleen, pancreas

C. *Amino acid substitutions in TIP30*

Name	Codon/nucleotide	Base change	Amino acid change
HLC 472	134/341	G → T	Gly → Val
HLC 485	109/325	C → T	Arg → stop
	106/316	C → A	Arg → Ser
	115/344	C → A	Ser → Tyr
HLC 583	106/316	C → A	Arg → Ser
	108/324	G → T	Asp → Tyr
	116/346	G → A	Ala → Thr
	144/430	C → A	Leu → Ile

mutations in the *TIP30* gene. Because the SNP database has listed four single nucleotide polymorphisms (SNPs) in the TIP30 coding regions, we first compared the *TIP30* cDNA sequences in National Center for Biotechnology Information databases (14) to identify bp changes other than these SNPs in the human *TIP30* coding region. Initially, we examined the sequences of TIP30 cDNA clones to identify insertion, deletion, or bp changes that will result in amino acid substitution. Besides those reported SNPs in the *TIP30* gene that were found in both normal and cancer cells, we only identify missense mutations in exon 3. We found that none of the normal cells in the database (0 of 75) harbored a single base-pair substitution in exon 3, and 24% of various types of cancer cells (21 of 52) harbored at least a single base-pair substitution in the same region. Interestingly, the amino acid sequences encoded by *Tip30* exon 3 are conserved among human, mouse, and *Caenorhabditis elegans* TIP30 proteins, and this region is important for the nuclear localization of TIP30.[6] Therefore, we focused our mutational study on *Tip30* exon 3 for those liver cancer patients who have abnormal TIP30 expression in their cancer cells. Three of 8 cancer samples contained at least a single bp change in the *Tip30* gene (Table 1*C*). These bp changes were not found in normal cells according to the National Center for Biotechnology Information database. In addition, whereas analyzing the sequences of cloned exon 3 DNA, we found that some of clones (20–80%) from the same cancer sample did not have any bp change, and individual clones from 1 HCC even harbored different bp changes. Importantly, we noted that 2 patients even had the same mutations in their carcinoma cells. Therefore, it is very likely that these base changes are somatic mutations that occurred during cancer development.

To explore the functional consequences of these amino acid substitutions in TIP30, we first investigated whether these mutations affected expression of TIP30 in cells. We transiently transfected a HCC cell line, HepG2, with mammalian expression plasmids encoding wild-type TIP30 and a mutant form of TIP30 with substitutions in G134V ($TIP30^{G134V}$) identified from the HCC showing in Fig. 3*A*. On Western blot analysis showed in Fig. 3*B*,

[6] C. Jiang and H. Xiao, unpublished observations.

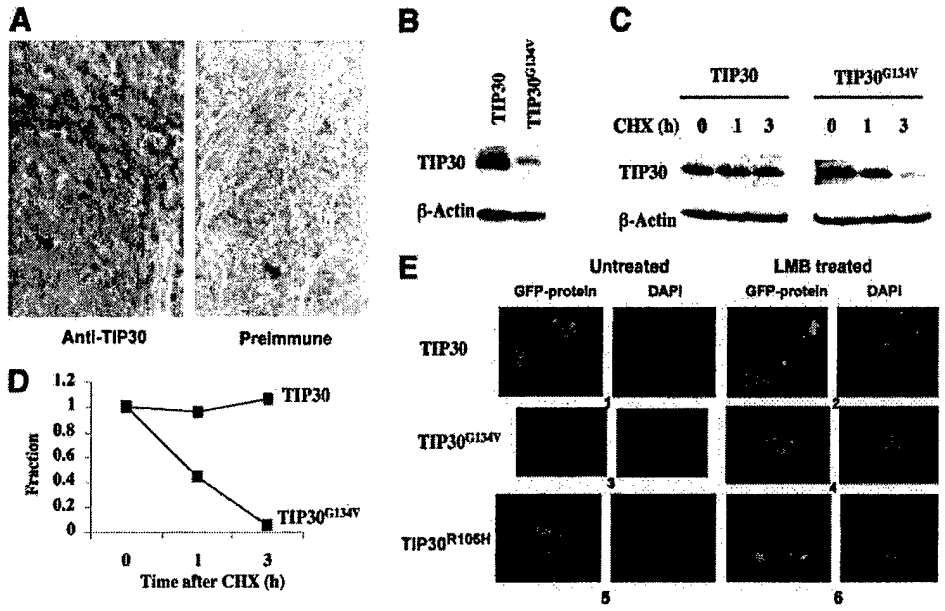

Fig. 3. Abnormal expression of TIP30 in human hepatocellular carcinoma. *A*, a representative immunohistochemical stain of human hepatocellular carcinoma with anti-TIP30 serum is presented in the *left*. It shows much decreased staining of TIP30 in tumor cells (*bottom red arrow*) compared with the strongly positive staining of TIP30 in the adjacent hepatocytes (*top green arrow*). A control analysis of a consecutive tissue section with preimmune serum is presented in the *right*. *B*, the levels of ectopic expression of wild-type *Tip30* and *Tip30* mutants in HepG2 cells. HepG2 cells were transiently transfected with plasmids expressing Flag-TIP30 and Flag-TIP30^{G134V}. Equivalent amounts of whole cell extracts made from these cells were subjected to immunoprecipitation with the anti-Flag M2 agarose. The precipitated proteins were then immunoblotted with anti-TIP30 antibodies. The supernatants were immunoblotted with anti-β-actin antibodies. *C* and *D*, G134V substitution reduces the half-life of TIP30 protein. HepG2 cells were transfected with plasmids expressing Flag-TIP30 and Flag-TIP30^{G134V}, treated with cycloheximade (*CHX*) and then harvested at various times. Cell extracts were subjected to immunoprecipitation with the anti-Flag M2 agarose. Precipitated TIP30 proteins and β-actin proteins in the supernatants were detected by Western blot analysis. Quantitation of the results was shown in *D*. *E*, cellular localization of GFP-TIP30, GFP-TIP30^{R106H}, and GFP-TIP30^{G134V} in HepG2 cells. Transfected HepG2 cells were treated with or without Leptomycin B (LMB), fixed on slide, and stained with 4′,6-diamidino-2-phenylindole. The representative images for both green fluorescent protein and DNA staining are presented as indicated. *Panels 1, 3,* and *5* are the untreated cells, and *panels 2, 4,* and *6* are LMB-treated cells.

TIP30^{G134V} was less expressed compared with the level of the wild-type TIP30. We then investigated whether this mutation affects the stability of the TIP30 protein in HepG2 cells. The relative level of TIP30 was monitored after addition of cycloheximide, a protein synthesis inhibitor. As shown in Fig. 3, *C* and *D*, G134V substitution markedly reduces the half-life of TIP30. This result suggests that G134V substitution reduces the stability of TIP30, thereby resulting in a lower level of TIP30 in cells. To investigate whether mutations affect the cellular localization of TIP30, we transfected HepG2 cells with mammalian expression vectors encoding GFP-TIP30 and mutant fusion proteins (GFP-TIP30^{R106H} and GFP-TIP30^{G134V}). The GFP tag had no influence on the cellular distribution of TIP30, because GFP-TIP30 had a subcellular distribution similar to endogenous TIP30 in HeLa and MCF7 cells (data not shown). In cells expressing wild-type GFP-TIP30 (Fig. 3*E*, *panel 1*), ~90% of transfected cells contained GFP-TIP30 in the cytoplasm, and 10% of transfected cells expressed GFP-TIP30 in the nucleus. When cells were treated with LMB, a CRM1-dependent nuclear export inhibitor (15), nuclear localization of GFP-TIP30 (Fig. 3*E*, *panel 2*) was increased to ~30% of transfected cells, suggesting that TIP30 is exported to the cytoplasm from the nucleus. However, cells expressing GFP-TIP30^{R106H} showed an exclusively cytoplasmic staining (Fig. 3*E*, *panel 5*), and LMB treatment did not increase the nuclear localization of GFP-TIP30^{R106H} (Fig. 3*E*, *panel 6*). This indicates that the R106H change may abrogate nuclear localization of TIP30 through inhibition of nuclear import. In contrast, GFP-TIP30^{G134V} (Fig. 3*E*, *panel 3*) was expressed in both the cytoplasm and nucleus similar to the expression of GFP alone, suggesting that this mutation may affect its nuclear export. However, LMB treatment did not increase accumulation of GFP-TIP30^{G134V} in the nucleus (Fig. 3*E*, *panel 4*), suggesting that the mutation may affect the nuclear import of TIP30. Therefore, it is possible that the mutation alters the protein structure, and results in abnormal nuclear import and export of TIP30. Given that TIP30 acts as a transcription cofactor in the nucleus and predisposes cells to apoptosis (1–5), it is conceivable that these mutations may impair the ability of TIP30 to regulate gene expression and apoptosis. Therefore, it is possible that TIP30 deficiency as a result of mutations in the *TIP30* gene may inhibit its function in the liver cells and contribute to the pathogenesis of human HCC.

Cellular gene products can function as tumor suppressors or tumor modifiers to regulate tumorigenesis (16, 17). In this study, we showed that TIP30-deficient mice spontaneously develop tumors in their second year of life. Some tumors were carcinomas such as HCC that rarely occurs in 129SvJ/C57BL6/J mice (18). In addition, 1 *Tip30* mutant mouse even had two different types of tumor. These data clearly represent a significant enhancement of susceptibility to tumorigenesis in TIP30-deficient mice. The same incidences of tumors in *Tip30*$^{-/-}$ and *Tip30*$^{+/-}$ mice is similar to the observations described in previous studies with DMP1, an Arf transcription activator, and p27^{kip1}, a potent tumor suppressor, that are haploinsufficient for tumor suppression (10, 19). We found that TIP30 mRNA and protein were expressed in both primary and metastatic sites of the neuroblastoma and hemangiosarcoma arisen in *Tip30*$^{+/-}$ mice by reverse transcription-PCR and immunohistochemical analyses (data not shown). Although we are not sure that the second allele in the tumors of *Tip30*$^{+/-}$ mice encodes a normal TIP30, based on the similar tumor incidence and latency in *Tip30*$^{+/-}$ and *Tip30*$^{-/-}$ mice, we suggest that TIP30 is haploinsufficient for tumor suppression.

The role of TIP30 in tumorigenesis is also suggested by the observation of reduced expression of TIP30 in human HCC and *Tip30* mutations in those HCC. One mutation results in significantly decreased expression of TIP30, and another mutation

changes cellular localization of TIP30. Therefore, it is possible that *Tip30* deficiency as a result of mutations in the *Tip30* gene may contribute to the pathogenesis of human HCC. Together, these results strengthen a conclusion that TIP30 plays an important role in tumorigenesis.

ACKNOWLEDGMENTS

We thank C. Yang and the Transgenic Facility of the Rockefeller University for help with ES cell manipulation and blastocyst injection, K. Ge for SV40 T-antigen expression vector, P-C. Cui, and K. Wagner for technical help and useful discussions, and C. Eischen and A. Diehl for critical reading of the manuscript.

REFERENCES

1. Xiao, H., Tao, Y., Greenblatt, J., and Roeder, R. G. A cofactor, TIP30, specifically enhances HIV-1 Tat-activated transcription. Proc. Natl. Acad. Sci. USA, *95:* 2146–2151, 1998.
2. Shtivelman, E. A link between metastasis and resistance to apoptosis of variant small cell lung carcinoma. Oncogene, *14:* 2167–2173, 1997.
3. Xiao, H., Palhan, V., Yang, Y., and Roeder, R. G. TIP30 has an intrinsic kinase activity required for up-regulation of a subset of apoptotic genes. EMBO J., *19:* 956–963, 2000.
4. NicAmhlaoibh, R., and Shtivelman, E. Metastasis suppressor CC3 inhibits angiogenic properties of tumor cells *in vitro*. Oncogene, *20:* 270–275, 2001.
5. Whitman, S., Wang, X., Shalaby, R., and Shtivelman, E. Alternatively spliced products CC3 and TC3 have opposing effects on apoptosis. Mol. Cell. Biol., *20:* 583–593, 2000.
6. Liu, Y., Thor, A., Shtivelman, E., Cao, Y., Tu, G., Heath, T. D., and Debs, R. J. Systemic gene delivery expands the repertoire of effective antiangiogenic agents. J. Biol. Chem., *274:* 13338–13344, 1999.
7. Ito, M., Yuan, C-X., Okano, H. J., Darnell, R. B., and Roeder, R. G. Involvement of the TRAP220 component of the TRAP/SMCC coactivator complex in embryonic development and thyroid hormone action. Mol. Cell, *5:* 683–693, 2000.
8. Chiang, C. M., and Roeder, R. G. Expression and purification of general transcription factors by FLAG epitope-tagging and peptide elution. Pept. Res., *6:* 62–64, 1993.
9. Alt, J. R., Gladden, A. B., and Diehl, J. A. p21 (Cip1) promotes cyclin D1 nuclear accumulation via direct inhibition of nuclear export. J. Biol. Chem., *277:* 8517–8523, 2002.
10. Inoue, K., Zindy, F., Randle, D. H., Rehg, J. E., and Sherr, C. J. Dmp1 is haploinsufficient for tumor suppression and modifies the frequencies of *Arf* and *p53* mutations in *Myc*-induced lymphomas. Genes Dev., *15:* 2934–2939, 2001.
11. Steele-Perkins, G., Fang, W., Yang, X. H., Van Gele, M., Carling, T., Gu, J., Buyse, I. M., Fletcher, J. A., Liu, J., Bronson, R., Chadwick, R. B., de la Chapelle, A., Zhang, X., Speleman, F., and Huang, S. Tumor formation and inactivation of RIZ1, an Rb-binding member of a nuclear protein-methyltransferase superfamily. Genes Dev., *15:* 2250–2262, 2001.
12. Hakem, R., and Mak, T. W. Animal models of tumor-suppressor genes. Annu. Rev. Genet., *35:* 209–241, 2001.
13. Levine, A. J. p53, the cellular gatekeeper for growth and division. Cell, *88:* 323–331, 1997.
14. Zhang, J., and Madden, T. L. Power BLAST: a new network BLAST application for interactive or automated sequence analysis and annotation. Genome Res., *7:* 649–656, 1997.
15. Harbers, M., Nomura, T., Ohno, S., and Ishii, S. Intracellular localization of the ret finger protein depends on a functional nuclear export signal and protein kinase C activation. J. Biol. Chem., *276:* 48596–48607, 2001.
16. Balmain, A. Cancer as a complex genetic trait: tumor susceptibility in humans and mouse models. Cell, *108:* 145–152, 2002.
17. Van Dyke, T., and Jacks, T. Cancer modeling in the modern era: progress and challenges. Cell, *108:* 135–144, 2002.
18. Ward, J. M., Mahler, J. F., Maronpot, R. R., Sundberg, J. P., and Frederickson, R. M., Pathology of mice commonly used in genetic engineering (C57BL/6; 129; B6, 129; and FVB/N). *In:* J. M. Ward, J. F. Mahler, R. R. Maronpot, J. P. Sundberg, and R. M. Frederickson, Pathology of Genetically Engineered Mice. First Edition, pp. 161–179. Ames: Iowa State University Press, 2000.
19. Philipp-Staheli, J., Payne, S. R., and Kemp, C. J. p27(Kip1): regulation and function of a haploinsufficient tumor suppressor and its misregulation in cancer. Exp. Cell Res., *264:* 148–168, 2001.

THE JOURNAL OF BIOLOGICAL CHEMISTRY
Vol. 279, No. 26, Issue of June 25, pp. 27781–27789, 2004
Printed in U.S.A.

TIP30 Interacts with an Estrogen Receptor α-interacting Coactivator CIA and Regulates c-*myc* Transcription*

Received for publication, February 18, 2004, and in revised form, April 5, 2004
Published, JBC Papers in Press, April 8, 2004, DOI 10.1074/jbc.M401809200

Chao Jiang‡§, Mitsuhiro Ito¶, Valerie Piening‡‖, Kristy Bruck‡, Robert G. Roeder, and Hua Xiao‡‖‡‡**

*From the ‡Eppley Institute for Cancer Research and the ‖Department of Pathology and Microbiology, University of Nebraska Medical Center, Omaha, Nebraska 68198-7696, the ¶Division of Hematology/Oncology, Department of Medicine, Kobe University School of Medicine, 751 Kusunoki-cho, Chuo-ku Kobe 650-0017, Japan, and the **Laboratory of Biochemistry and Molecular Biology, the Rockefeller University, New York, New York 10021*

Deregulation of c-*myc* expression is implicated in the pathogenesis of many neoplasias. Estrogen receptor α (ERα) can increase the rate of c-*myc* transcription through the recruitment of a variety of cofactors to the promoter, yet the precise roles of these cofactors in transcription and tumorigenesis are largely unknown. We show here that a putative tumor suppressor TIP30, also called CC3 or Htatip2, interacts with an ERα-interacting coactivator CIA. Using chromatin immunoprecipitation assays, we demonstrate that TIP30 and CIA are distinct cofactors that are dynamically associated with the promoter and downstream regions of the c-*myc* gene in response to estrogen. Both TIP30 and CIA are recruited to the c-*myc* gene promoter by liganded ERα in the second transcription cycle. TIP30 overexpression represses ERα-mediated c-*myc* transcription, whereas TIP30 deficiency enhances c-*myc* transcription in both the absence and presence of estrogen. Ectopic CIA cooperates with TIP30 to repress ERα-mediated c-*myc* transcription. Moreover, virgin TIP30 knockout mice exhibit increased c-*myc* expression in mammary glands. Together, these results reveal an important role for TIP30 in the regulation of ERα-mediated c-*myc* transcription and suggest a mechanism for tumorigenesis promoted by TIP30 deficiency.

Estrogen plays an important role in the development and maintenance of the mammary glands, as well as various other tissues, and in numerous human diseases that include breast and endometrial cancer, cardiovascular disease, and osteoporosis (1–5). Most of the effects of estrogen are facilitated by estrogen receptor α (ERα),[1] which controls the expression of a number of hormone-responsive genes (5, 6), including the c-*myc* gene, which is important for cell proliferation (7–10). ERα, like many other nuclear receptors, contains two intrinsic transcriptional activation domains, designated AF-1 and AF-2 (3, 11, 12). The function of AF-1 is estrogen-independent, whereas the activity of AF-2 is estrogen-dependent. AF-1 and AF-2 activities show promoter context and cell type specificity and can act synergistically to activate transcription (5).

Although the precise mechanisms by which ERα regulates gene expression are still not clearly defined, there is solid evidence suggesting that ERα executes its effects by directing cyclical and combinatorial recruitment of cofactors on promoters (13–17). Most ERα-interacting coactivators identified thus far are also able to interact with many other members of the nuclear receptor superfamily and have generalized functions, hence affecting transcriptional activation mediated by a wide spectrum of nuclear receptors (17–21). More recently, Giguere and co-workers (22) identified a novel nuclear receptor coactivator, called CIA (coactivator independent of AF-2 function). CIA was shown to interact with ERα and ERβ in a ligand-dependent manner but not with other members of the nuclear receptor family. Consistent with its binding specificity, CIA was found to potentiate transcriptional activation by the ER but not by other nuclear receptors (22). Nevertheless, the precise mechanism by which CIA enhances transcription remains unknown. CIA may represent a novel class of ligand-dependent ER coactivators that are independent of AF-2 function.

We previously purified a protein, TIP30 (Tat-interacting protein 30) that interacts specifically with the activation domain of Tat (23). TIP30 is identical to CC3, which is absent in highly metastatic human small cell lung carcinoma (24). TIP30/CC3 has been proposed to function as a metastasis suppressor via its ability to promote apoptosis and inhibit angiogenesis (24–27). Consistent with this hypothesis, ectopic expression of TIP30 was found to elevate the expression of a subset of pro-apoptotic genes (27) and angiogenic inhibitors and to down-regulate the expression of certain angiogenic stimulators (25). Moreover, deletion of one or both alleles of *Tip30* results in spontaneous development of hepatocellular carcinomas and other tumors in mice at a relatively long latency (28). Reduced expression of TIP30 is observed in 33% of human hepatocellular carcinomas, and mutations in the *Tip30* gene that caused the instability or abnormal cellular distributions of the TIP30

* This work was supported by American Cancer Society Research Scholar Grant for Beginning Investigators RSG0216501GMC, Department of Defense Breast Cancer Research Program Idea Award DAMD170210507, a University of Nebraska Medical Center start-up grant (to H. X.), and a National Institutes of Health grant (to R. G. R.). The costs of publication of this article were defrayed in part by the payment of page charges. This article must therefore be hereby marked "*advertisement*" in accordance with 18 U.S.C. Section 1734 solely to indicate this fact.

§ Supported in part by a breast cancer research training fellowship from the Department of Defense.

‡‡ To whom correspondence should be addressed: Eppley Institute for Research in Cancers & Allied Diseases, University of Nebraska Medical Center, 986805 Nebraska Medical Center, Omaha, NE 68198-7696. Tel.: 402-559-3323 or 402-559-3324; Fax: 402-559-3739; E-mail: hxiao@unmc.edu.

[1] The abbreviations used are: ER, estrogen receptor; MEF, mouse embryonic fibroblast; E2, 17β-estradiol; GST, glutathione *S*-transferase; ChIP, chromatin immunoprecipitation; RACE, rapid amplification of cDNA ends; RT, reverse transcriptase; TR, thyroid receptor; CBP, CREB-binding protein; CREB, cAMP-response element-binding protein; TRE, thyroid response element; GAL, yeast transcription factor GAL4 DNA-binding domain; RXR, retinoid X receptor; ERE, estrogen response element.

protein were identified in some of the human hepatocellular carcinoma specimens (28). These data further suggest that TIP30 is a tumor suppressor.

In this study, we describe the cloning and characterization of a TIP30-interacting protein identical to CIA and provide evidence that TIP30 is an important regulator of ERα-mediated c-*myc* transcription. This study defines a new pathway for regulating expression of the c-*myc* gene and possibly other ERα target genes that are involved in tumoriogenesis.

EXPERIMENTAL PROCEDURES

Protein Purification and Chromatography—The HeLa cell line (HeLa-fTIP30) stably expressing FLAG-tagged TIP30 was obtained by the introduction of pCIN4-FLAG-tagged TIP30 into HeLa S3 and selection in a G418-containing medium (27). Nuclear extracts were prepared as described previously (29) with the following modifications. During purification procedures, HEPES-HCl, pH 7.9, was used in buffers instead of Tris-HCl. Nuclear pellets were resuspended in a low salt buffer containing sulfosuccinimidylpropionate (Pierce), transferred to a homogenizer, and mixed with six strokes of a loose pestle. The suspensions were then transferred to glass beakers and dispersed with a stirring bar. The high salt buffer was slowly added into the mixtures. The cross-linking reactions were incubated at 4 °C for 2 h and then stopped by adding 1 M Tris-HCl, pH 8.0, to a final concentration of 20 mM. The extracts were centrifuged at 15000 rpm for 30 min and stored at −80 °C. For coimmunoprecipitation, 100 ml of nuclear extract prepared from the HeLa-f:TIP30 cells was mixed with 200 μl of anti-FLAG epitope immunoaffinity matrix M2 (Sigma) in BC450 containing 0.1% Nonidet P-40 and 0.45 M KCl. The matrix was washed extensively with BC500 plus 0.1% Nonidet P-40 and 0.5 M KCl and eluted with 1 ml of BC1000 containing 200 μg/ml FLAG peptide and 1 M KCl. The eluted proteins were concentrated and resolved on SDS-PAGE and stained with silver or Coomassie Blue. The indicated bands were excised from the gel and digested with endoproteinase C. The resulting peptides were isolated by high pressure liquid chromatography and subjected to microsequencing analysis (Core Facility, Rockefeller University). Affinity chromatography was carried out as described previously (23).

Cloning of the CIA Gene—An expressed sequence tag clone (DKFZp434J208) was initially identified by data base search using two peptides (NMPQADAMVLVAR and DLRDFR) from amino acid sequencing and peptide mass data from mass spectrophotometer analysis of a TIP30-interacting protein (65 kDa). The expressed sequence tag clones (IMAGE: 1185534 and 1335209), containing similar cDNA sequences, were identified and purchased from ATCC and sequenced. Primers were designed for 5′-RACE and 3′-RACE PCRs according to the sequence of the insert cDNA. The HeLa cDNA library (Clontech) was used as a template for 5′-RACE and 3′-RACE. The experiments were carried out according to the manufacturer's instruction (Clontech). The resulting DNA fragments were subcloned into a pCR2.1 vector by PCR kits (Invitrogen). Several cDNA fragments were amplified and sequenced by the core facility at the University of Nebraska Medical Center, and the resulting sequences were used for searching the expressed sequence tag clones and known genes in GenBank™. The 856-bp cDNA containing the translational start codon was amplified using PCR primers (primary primer, 5′-ATCTCTACTATGTGTGTG-GTCCCG; nest primer, 5′-CAAGTCTCGGGGGTCTCGAATGTC). The pCR2.1-CIA containing full-length CIA cDNA was constructed by subcloning a PCR-amplified cDNA from the HeLa cDNA library (Clontech) using specific primers (forward, 5′-GGAAGATCTATGAATACGGCTC-CATCAAGACCCAGC; reverse, 5′-GGAAGATCTCAGTAATGCCTCT-GGTAAGATCCCAT).

Plasmids and Antibodies—The pcDNA3.1-CIA plasmid was generated by inserting the CIA cDNA, excised from pCR2.1-CIA with BglII, into pcDNA3.1 at the BamHI site. For antibody production, the bacterial expression plasmid pREST-his-CIA was generated by inserting a BglII-DNA fragment released from pCR2.1-CIA into pRSET-B (Invitrogen). The recombinant His tag CIA protein was expressed in bacteria, purified as described previously, and used to generate rabbit anti-CIA antibodies (Covance Inc., Denver, PA). The pGL3-hu-Myc plasmid containing the human c-*myc* promoter was constructed by subcloning a 2540-bp HindIII-DNA fragment excised from pSV40CAT-hu-Myc plasmid (a gift from David Bentley, University of Colorado Health Science Center) into pGL3-basic vector (Promega) at the HindIII site. This DNA fragment extends 2.3 kb 5′ of the P1 start site to a NaeI site at +50 relative to the P2 start site. Antigen-purified anti-TIP30 (23) and anti-CIA antibodies were purified as described previously (30). Anti-ERα (HC-20, Santa Cruz Biotechnology), anti-CBP (A22, Santa Cruz Biotechnology), and anti-RNA polymerase II (8WG16) antibodies were used for ChIP assays.

Mice and MEFs—Generation of TIP30 null mice and MEFs was described previously (28). The genetic backgrounds of *Tip30*$^{+/+}$ and *Tip30*$^{-/-}$ mice were regarded to be identical because they were backcrossed 10 times with C57BL6J mice. MEF clones of each genotype were prepared from sibling embryos obtained by a heterozygous crossing. All animal experimentation was performed according to the National Institutes of Health guidelines.

Pull-down Assay—Pull-down assays were performed as described previously (22). [^{35}S]Methionine-labeled CIA and Bax proteins were generated by *in vitro* transcription and translation using the TnT-coupled reticulocyte lysate system (Promega). Fusion proteins were induced in DH5α *Escherichia coli* with 0.4 mM isopropyl-β-D-thiogalactopyranoside for 2 h. The cells were sonicated 10 times using 30-s pulses in 1× phosphate-buffered saline containing 1 mM phenylmethylsulfonyl fluoride and 1 mM dithiothreitol. The cleared lysates were bound to glutathione-Sepharose (Amersham Biosciences) for 15 min at 4 °C. The protein-saturated beads were washed three times in 1× phosphate-buffered saline with 1 M NaCl and stored in BC100 (20 mM Tris-HCl, pH 7.9, 1 mM EDTA, 1 mM dithiothreitol, 20% glycerol, 100 mM KCl, 0.1% Nonidet P-40). 20 μl of GST or GST-TIP30 beads were incubated with 10 μl of [^{35}S]methionine-labeled proteins in 10 μl of BC135 buffer (20 mM Tris-HCl, pH7.9, 1 mM EDTA, 1 mM dithiothreitol, 20% glycerol, 0.1% Nonidet P-40, 135 mM KCl) for 2 h at 4 °C. The binding reaction mixture was washed three times in BC135 buffer. The bound proteins were analyzed by SDS-PAGE followed by autoradiography of fixed and dried gels.

ChIP Assays—ChIP assays were performed as described previously (15). MCF-7 cells were treated with or without 10^{-8} M E2 for 45 min and with formaldehyde to cross-link proteins to DNA. Soluble chromatin was prepared and immunoprecipitated with preimmune serum and protein A-Sepharose and then immunoprecipitated with anti-CIA, anti-TIP30 serum, or control anti-ERα, anti-CBP, and anti-RNA polymerase II antibodies. The final DNA preparations were amplified using a pair of primers and analyzed in 1.5% agarose gel following ethidium bromide stain.

Transient Transfection—Transfection assays were performed as described previously (26). COS-1 cells in 24-well dishes or MEFs in 6-well dishes were transfected with plasmid DNA using LipofectAMINE according to the manufacturer's instruction (Invitrogen). In all experiments, a plasmid pRL-CMV for expressing *Renilla* luciferase was used as a control for transfection efficiency, and activities of firefly and *Renilla* luciferases were measured with Promega's dual luciferase reporter assay system, normalized, and expressed as relative luciferase light units. The vector pCMV-ERα for expressing human ERα and vector pNT7-TRα for human thyroid receptor α (TRα) were described previously (31). TRE-luciferase reporter was described previously (31). Gal-RXR expressing vector and Gal-luciferase reporter were described previously (19).

Histology and Immunohistochemistry—Mammary gland 4 was removed and fixed with 10% buffered-formalin and embedded in paraffin blocks. The sections were deparaffinized, rehydrated, and stained with hematoxilin and eosin. For immunohistochemistry staining, unstained sections were rehydrated and incubated overnight at 4 °C with anti-Myc antibody (Upstate Biotechnology, Inc.), and staining was developed using VECTASTAIN Elite ABC kit (Vector Laboratories) according to the manufacturer's instructions and then counter-stained with hematoxilin and eosin. The number of Myc nuclear positive epithelial cells was divided by the total number of epithelial cells counted.

RNA Isolation and RT-PCR—The abundance of c-*myc* mRNA in the tissue was studied by a semi-quantitative RT-PCR analysis using β-actin mRNA as control. Total RNA was isolated from mammary glands of 8-week-old virgin mice using Trizol reagent. 2 μg of DNA-free total RNA was reverse transcripted into cDNA using oligo(dT)$_{12-18}$ and SuperScript II RT (Invitrogen) following the manufacturer's instructions. The same amounts of resulting cDNA were used for PCR amplification. The primers used for PCR and their sequences are as follows: c-*myc*: sense, 5′-ATTGAGCCAAATCTTAAGTTGTGA, and antisense, 5′-TTTGGAG-TGAGCAGGGGACTGGCA; β-actin: sense, 5′-CACCCTGTGCTGCTC-ACCGAGGCC, and antisense, 5′-CCACACAGAGTACTTGCGCTC-AGG; and cyclin B1: sense, 5′-ACCTACAGGGTCGTGAAGTGACTGG-AAAC, and antisense, 5′-TGAGAATCTTCATCTCCATCTGTCTG. The PCR product was analyzed in 1.2% agarose gel following ethidium bromide stain.

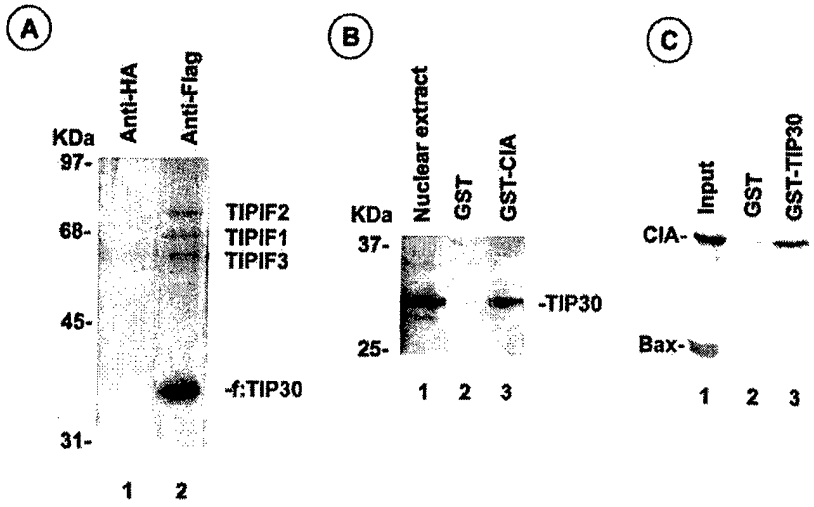

FIG. 1. **Purification of TIP30-interacting proteins.** *A*, TIP30-interacting proteins were purified from HeLa nuclear extracts as described under "Experimental Procedures." The final preparations were resolved in 10% SDS-PAGE and stained with silver (*lane 2*). These three proteins were not coimmunoprecipitated if anti-hemagglutinin epitope immunoaffinity matrix was used (*lane 1*). *B*, CIA binds to TIP30 from HeLa nuclear extracts. 300 μl of HeLa nuclear extracts was chromatographed on 30 μl of GST and GST-CIA columns. The columns were washed with BC100 extensively and eluted with 120 μl of BC1000. The proteins eluted from the columns were separated with SDS-PAGE and immunoblotted with anti-TIP30 antibodies. *C*, TIP30 interacts with *in vitro* synthesized CIA. Pull-down assays were performed as described under "Experimental Procedures." The bound proteins were analyzed by 12.5% SDS-PAGE and autoradiography. The input represents 17% of the [^{35}S]methionine-labeled CIA and [^{35}S]methionine-labeled BAX used in the assay (*lane 1*). CIA, but not a pro-apoptotic protein BAX, interacts with GST-TIP30 (*lane 3*) but not with GST (*lane 2*).

RESULTS

Identification of a TIP30-interacting Protein and Cloning Its Full-length Cognate cDNA—The discovery of roles of TIP30 in the control of expression of genes involved in apoptosis and angiogenesis indicates that TIP30 may interact with transcription factors to regulate gene expression. To identify and affinity purify cellular proteins that interact with TIP30, we first established HeLa cell lines that stably expressed FLAG-tagged wild type TIP30. After preparation of nuclei from these cells, nuclear proteins were cross-linked by mixing the nuclei with the water-soluble cross-linker sulfosuccinimidylpropionate. Sulfosuccinimidylpropionate-treated nuclear extracts were made and subjected to affinity purification with anti-FLAG M2 beads. The bound proteins were eluted with FLAG peptide and analyzed by SDS-polyacrylamide gel electrophoresis after cleaving the cross-linker. As shown in Fig. 1*A*, three proteins were coimmunopurified with TIP30 and designated TIP30-interacting proteins. These three proteins were not immunoprecipitated with control anti-hemagglutinin beads. Amino acid sequencing of one of these interacting proteins (65 kDa), designated TIP30-interacting protein 1 (TIPIF-1), yielded two peptide sequences (NMPQADAMVLVAR and DLRDFR). A HeLa cell-derived 2.2-kb cDNA encoding TIPIF-1 was cloned and sequenced (GenBank™ accession number AF470686). Sequence analysis revealed that it encodes a 587-amino acid protein with a tract of Arg-Asp residues in the amino-terminal region. The repeat Arg-Asp residues were previously identified in the splicing factor U1 70K and the RD protein, a component of the negative elongation factor NELF (32). TIPIF-1 also contains a receptor-binding motif known as the LXXLL motif (33, 34) and seven repeats of a short sequence motif (RDLRD(H/F)R) that is present in subunit 10 of mouse translation initiation factor 3. Following cloning of the TIPIF-1 cDNA, a data base search revealed identity with the estrogen receptor coactivator CIA (22). The reported CIA cDNA, which was isolated from a human fetal kidney cDNA library, contains a 620-residue open reading frame lacking a translational stop codon at the 5′ end. In contrast, the open reading frame in our TIFIF-1 cDNA starts at a methionine residue located immediately after two in-frame stop codons, indicating that it encodes a full-length CIA. The sequence discrepancy in the 5′-untranslated region between TIPIF-1 and CIA may be due to alternative splicing products in HeLa and kidney cells, because the cDNA encoding CIA was cloned from the human fetal kidney cDNA library (22). We now refer to TIPIF-1 as CIA. To ascertain whether CIA interacts with TIP30, we tested the binding of TIP30 from nuclear extracts to a GST-CIA fusion protein. As shown in Fig. 1*B*, TIP30 was detected in the eluate from the GST-CIA affinity column but not in the eluate from the control GST column. In addition, we also tested the binding of *in vitro* translated CIA to GST-TIP30 using a pull-down assay. As shown in Fig. 1*C*, CIA bound GST-TIP30 but not GST control protein. By contrast, BAX protein, a pro-apoptotic protein used as a negative control was not bound by GST-TIP30. Collectively, these results indicate that CIA interacts with TIP30.

Estrogen Regulates TIP30 and CIA Occupancy of the c-myc Gene in Breast Cancer MCF-7 Cells—Transcription of the c-*myc* gene is controlled by transcription factors that interact with numerous positive and negative regulatory elements in the c-*myc* promoter regions (35). ERα can stimulate c-*myc* transcription by interacting with an estrogen-responsive element of the c-*myc* promoter (8). Using ChIP assays, a previous study has established that a number of ERα-interacting coactivators are recruited to the promoters of endogenous estrogen-responsive target genes, including c-*myc*, following estrogen treatment (15). If CIA and TIP30 are specific cofactors for ERα, they might also be associated with ERα on endogenous estrogen-responsive target genes. To test this possibility, we used the same ChIP assay (15) to determine whether CIA and/or TIP30 is recruited to the promoter of the c-*myc* gene in the estrogen-dependent human breast cancer cell line MCF-7. Fig. 2*B* shows that, as previously reported, the anti-ERα antibody precipitated a c-*myc* promoter fragment containing P1 and P2 promoters in the presence (*lane 6*) but not in the absence (*lane 5*) of E2. In contrast, the c-*myc* promoter was precipitated by anti-TIP30 antibody (*lane 3*) but much less so by anti-CIA antibody (*lane 1*) in the absence of E2. E2 increased the asso-

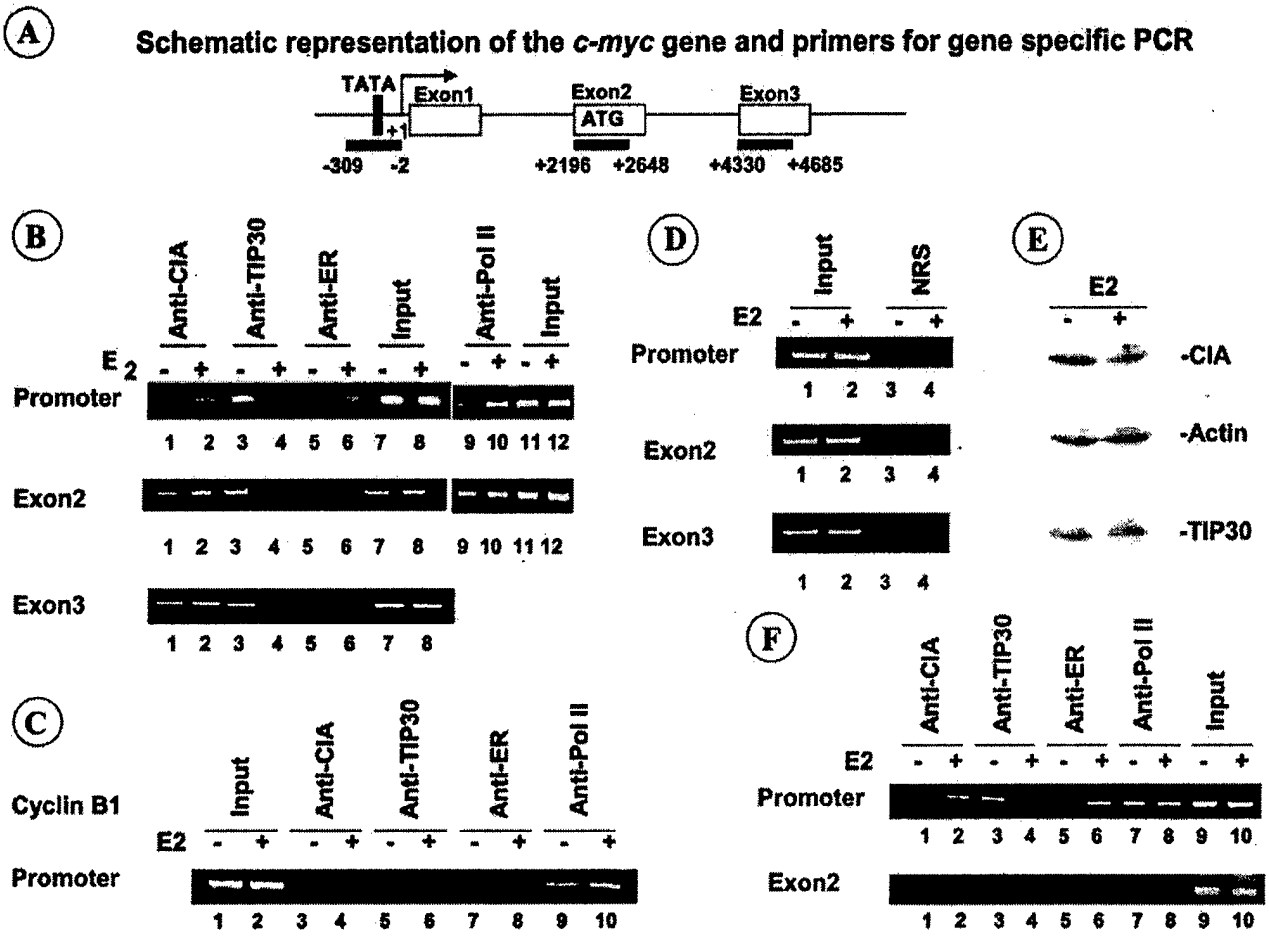

FIG. 2. **Recruitment of CIA and TIP30 to the endogenous c-*myc* gene.** *A*, schematic representation of the c-*myc* gene and primers for PCR. Transcription initiation site and start codon are indicated. The *solid bars* and *numbers* indicate the positions of the primers corresponding to the regions of the c-*myc* gene. The end of c-*myc* mRNA is at position 5190 or 5350 (7). *B*, assembly of CIA and TIP30 on the c-*myc* gene in the first transcription cycle upon E2 induction. MCF-7 cells were treated with 10^{-8} M E2 for 45 min. *Top panel*, recruitment of ERα and CIA to the promoter of the c-*myc* gene. The 307-bp amplified DNA fragment corresponds to the region of the promoter. *Middle panel*, association of CIA with exon 2 that is 2 kb downstream of the initiation site; *bottom panel*, or exon 3 that is 4 kb downstream of the initiation site. The 452- or 355-bp amplified DNA fragments correspond to the region of exon 2 or exon 3, respectively. *C*, ERα, TIP30, and CIA are not assembled on *Cyc B1* promoter. Primer pairs covering −75 to +185 region (33) were used for ChIP analysis. *Pol II*, polymerase II. *D*, ChIP analysis with a normal rabbit preimmune serum (*NRS*). *E*, CIA and TIP30 protein levels in MCF-7 cells in MCF-7 cells after E2 treatment. The cell lysates were prepared from MCF-7 cells treated with or without E2 for 45 min and then analyzed by Western blotting with anti-TIP30, anti-CIA, or anti-β-actin antibodies. *F*, occupancy of TIP30 and CIA on exon 2 is inhibited by α-amanatin. ChIP analysis was performed after cells were treated with 10 μg/ml of α-amanatin for 1 h before the addition of E2.

ciation of CIA (*lane 2*) but diminished the association of TIP30 (*lane 4*) with the same DNA region.

Because previous studies demonstrated that ERα and coactivators (AIB1, p300, CBP, pCAF, and TRAP220) are assembled on the promoter during preinitiation but subsequently released during elongation (15), we next determined whether CIA and TIP30 occupy the c-*myc* gene during elongation. Four pairs of primers covering a region (+2196 to +2628) in exon 2 and a region (+4330 to +4685) in exon 3 were used for PCR amplification of the final DNA preparations. Binding of both TIP30 and CIA to these regions was observed in the absence of E2 (Fig. 2*B*, *lanes 1* and *3*). E2 induction resulted in increased CIA binding (*lanes 1 versus* 2) but decreased TIP30 binding (*lanes 3 versus* 4) to these regions. As a positive control, binding of the largest subunit of RNA polymerase II to the regions upstream and downstream of the initiation site was also observed in both the absence and presence of E2 (Fig. 2*B*, *lanes 9* and *10*). These results suggest that estrogen increases association of CIA with the coding regions of c-*myc*.

To assess the specificity of association of TIP30 and CIA with the c-*myc* gene, we examined whether TIP30 and CIA were assembled on the promoter of the cyclin B1 gene that is not directly regulated by ERα (21). As expected, RNA polymerase II is associated with the promoter (Fig. 2*C*, *lanes 9* and *10*), but ERα is not (*Lanes 7* and 8). However, ERα, TIP30, and CIA were not associated with the promoter in either the presence or the absence of E2 (*Lanes 3*-6). In addition, nonspecific antibodies from a preimmune rabbit serum did not precipitate the DNA elements of the c-*myc* gene (Fig. 2*D*). The protein levels of TIP30 and CIA in MCF-7 cells are not significantly changed after E2 treatment (Fig. 2*E*), suggesting that E2-regulated association of TIP30 and CIA with the c-*myc* gene is not due to the influence of TIP30 and CIA expression by E2. Therefore, associations of these proteins with the c-*myc* gene are specific.

To determine whether the occupancy of the c-*myc* gene by TIP30 and CIA requires elongating RNA polymerase II in estrogen-dependent and -independent transcription, MCF-7 cells were treated with α-amanitin, which specifically inhibits RNA polymerase II elongation (15, 36), and then subjected to ChIP analysis. Consistent with the preceding observations, the occupancy of the c-*myc* promoter by TIP30 and CIA was not affected by α-amanitin (Fig. 2*F*). In contrast, the occupancy of

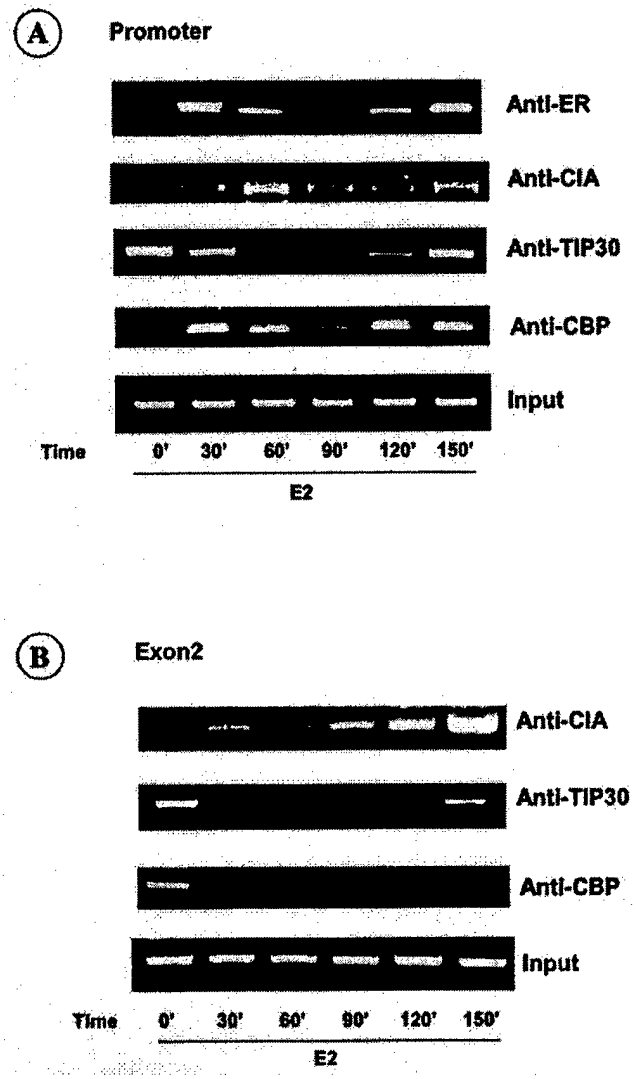

FIG. 3. **Occupancy of the c-*myc* gene by TIP30 and CIA in the second cycle transcription as measured by ChIP.** MCF-7 cells were treated with 10^{-8} M E2 and harvested at different time points. Antibodies used for immunoprecipitation are indicated. *A*, assembly of TIP30 and CIA on the promoter in the second transcription cycle. The 307-bp amplified DNA fragment corresponds to the region of the promoter. *B*, assembly of TIP30 and CIA on exon 2 in the second transcription cycle. The 452-bp amplified DNA fragment corresponds to the region of exon 2.

the coding region of the c-*myc* gene by TIP30 and CIA was inhibited by α-amanitin (Fig. 2*E*). This result suggests that association of TIP30 and CIA with the coding regions of the c-*myc* gene depends on elongating RNA polymerase II.

Estrogen Dynamically Regulates Occupancy of the c-myc Gene by TIP30 and CIA—Occupancy of ERα and RNA polymerase II on the promoter was previously shown to peak at 30–45 min in the first transcription cycle and at 120–150 min in the second cycle following the addition of E2 (15). We therefore sought to determine the timing of TIP30 and CIA occupancy on the promoter. As was shown previously, ERα and CBP occupancy on the promoter peaked at 30–60 min in the first transcription cycle and at 150 min in the second cycle upon E2 treatment (Fig. 3*A*). The results obtained with CIA were similar to those obtained with ERα and CBP. Interestingly, TIP30 was dissociated with the promoter at 60 min and reassociated with the promoter at 120–150 min in the second cycle (Fig. 3*A*). Increased binding of TIP30 and CIA to exon 2 was observed at 150 min following E2 treatment (Fig. 3*B*). In contrast, much less CBP was detected to associate with exon 2 upon E2 induction (Fig. 3*B*). Therefore, these results suggest that estrogen increases the recruitment of CIA to but decreases dissociation of TIP30 from the c-*myc* promoter region during the first transcription cycle. Unlike the other known ERα coactivators, which are released during elongation, CIA shows an increased association with the coding regions following E2 treatment. However, in the second cycle of estrogen-induced transcription, both CIA and TIP30 are associated with the promoter as was observed for ERα and CBP. Prolonged estrogen treatment even further increases association of CIA and TIP30 with the coding region of the c-*myc* gene (Fig. 3*B*).

Ectopic Expression of CIA and TIP30 Inhibits ERα-mediated Transcription—To test whether CIA and TIP30 function as coregulators of ERα in the transcription of the c-*myc* gene, we transfected COS-1 cells with vectors expressing ERα, CIA, TIP30, and a kinase-defective mutant TIP30 (30) with a construct containing a luciferase reporter gene controlled by the c-*myc* promoter (−2.3 kb 5′ of P1 start site to +50 relative to P2 start site). As shown in Fig. 4*A*, ectopic TIP30 inhibited the E2-dependent transcriptional activity of ERα in COS-1 cells, whereas ectopic CIA had no significant effect on transcription. The kinase-defective mutant TIP30 (30) did not significantly affect ERα-dependent transcription. Surprisingly and paradoxically, coexpression of ectopic CIA with ectopic TIP30 did not reverse but instead further potentiated the inhibitory effect of TIP30 (4-fold) in ERα-mediated transcription.

To determine whether TIP30 and CIA also regulate transcription from other promoters, we performed transient-transfection experiments using the luciferase reporter gene construct containing the artificial promoter either with estrogen receptor-binding sites (EREs) or with thyroid receptor (TR) α-binding sites (31). As expected, CIA potentiated ERα-mediated transcription from this promoter in the presence of E2 (Fig. 4*B*), but TIP30 inhibited the activity of ERα, whereas a kinase-defective mutant TIP30 (30) did not. Consistent with the observations for c-*myc* promoter, the activity of ERα on the ERE-binding promoter was inhibited by ectopic expression of both TIP30 and CIA. In contrast to ERα, the activity of TRα on the TRE-binding promoter was only slightly increased by cotransfection of TIP30 and/or CIA with TRα (Fig. 4*C*), suggesting that neither TIP30 nor CIA had a significant effect on TR-mediated transactivation.

Taken together, these data indicate that both CIA and TIP30 are important interacting factors in modulating the activity of ERα, and CIA can cooperate with TIP30 to repress ERα-mediated transcription when they are overexpressed. However, because Western blot analyses revealed that the levels of transiently expressed ectopic TIP30 and CIA were much higher than the levels of endogenous TIP30 and CIA in COS-1 cells (data not shown), it is possible that the effects of TIP30 and CIA on ERα-mediated transcription observed here may not represent their physiological functions.

Loss of TIP30 Increases ERα-mediated Transcription—To verify that the effect of TIP30 on ERα-mediated transcription is not limited by its overexpression, we next examined whether the loss of TIP30 expression affected ERα-mediated transcription by performing transient transfection assays in *Tip30*$^{+/+}$, *Tip30*$^{+/-}$, and *Tip30*$^{-/-}$ MEFs. Consistent with the preceding results, Fig. 5*A* shows that the loss of TIP30 results in an increased ERα-mediated transcription from the artificial ERE-binding promoter containing three EREs (*left panel*). Coexpression of either TIP30 alone or TIP30 and CIA in *Tip30*$^{-/-}$ MEFs results in inhibition of ERα-mediated transcription (*right panel*). In contrast, the loss of TIP30 had a minimal effect on

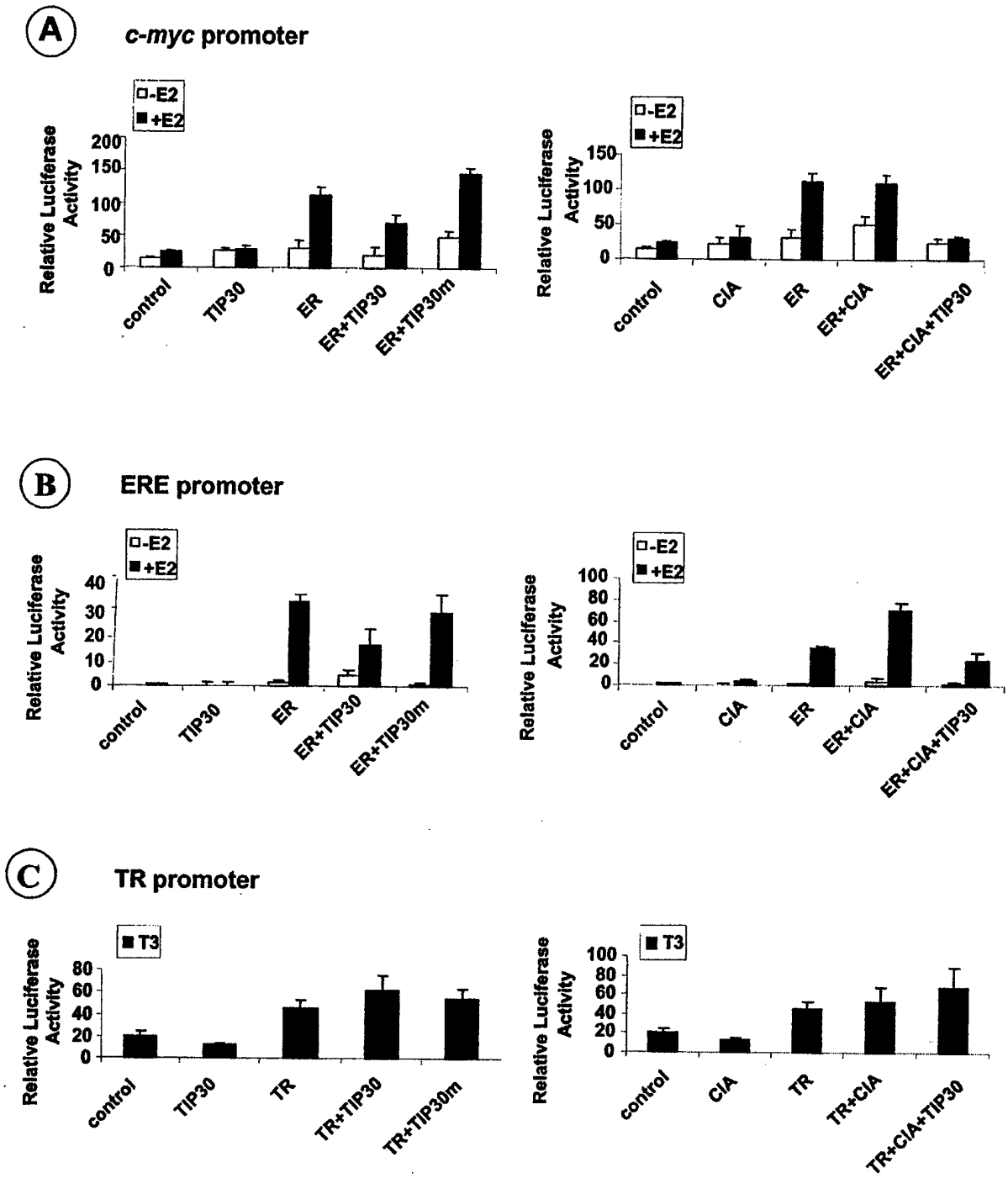

FIG. 4. **Effect on ERα-mediated transcription by overexpression of CIA and TIP30.** *A*, COS-1 cells were transfected with a Myc-luciferase reporter containing the human c-*myc* promoter (250 ng) and vectors for expressing ERα (25 ng), CIA (50 ng), TIP30 (50 ng), or a kinase defective TIP30 mutant (TIP30M, 50 ng) in the presence of 10^{-8} M E2. *B*, COS-1 cells were transfected with a reporter (250 ng) containing three copies of ERE-binding sites and vectors for expressing ERα (25 ng), CIA (50 ng), TIP30 (50 ng), or TIP30m (950 ng), a kinase-defective mutant (27) in the presence of 10^{-8} M E2 as indicated. *C*, COS-1 cells were transfected with a TRE_5-luciferase reporter (250 ng) containing five copies of TRE-binding sites and vectors for expressing human TRα (25 ng), CIA (50 ng), TIP30 (50 ng), or TIP30m (50 ng) as indicated in the presence of 10^{-7} M T3.

ligand-dependent transactivation by Gal4-RXRα (AF2 domain of retinoid X receptor) (19), implying that TIP30 may preferentially inhibit the transcriptional activity of ERα (Fig. 5*C*). Expression of TIP30 did not completely restore ERα activity in *Tip30*$^{-/-}$ MEFs. We reasoned that increased ERα-mediated transcription was partly due to TIP30 deficiency in *Tip30*$^{-/-}$ MEFs and partly due to other genetic changes that these cells may have undergone.

We also tested whether the complete absence of TIP30 in cells affects the transcriptional activity of ERα on the c-*myc* promoter. As expected, ERα showed a greater stimulation of the c-*myc* promoter in *Tip30*$^{-/-}$ MEFs than in *Tip30*$^{+/+}$ MEFs (16-fold; Fig. 5*B*, *left panel*) and *Tip30*$^{+/-}$ MEFs (3-fold lower) in the presence of E2. TIP30 loss also resulted in a 5-fold increase in estrogen-independent transcription from the c-*myc* prompter (Fig. 5*B*, *left panel*). This effect was due to the ab-

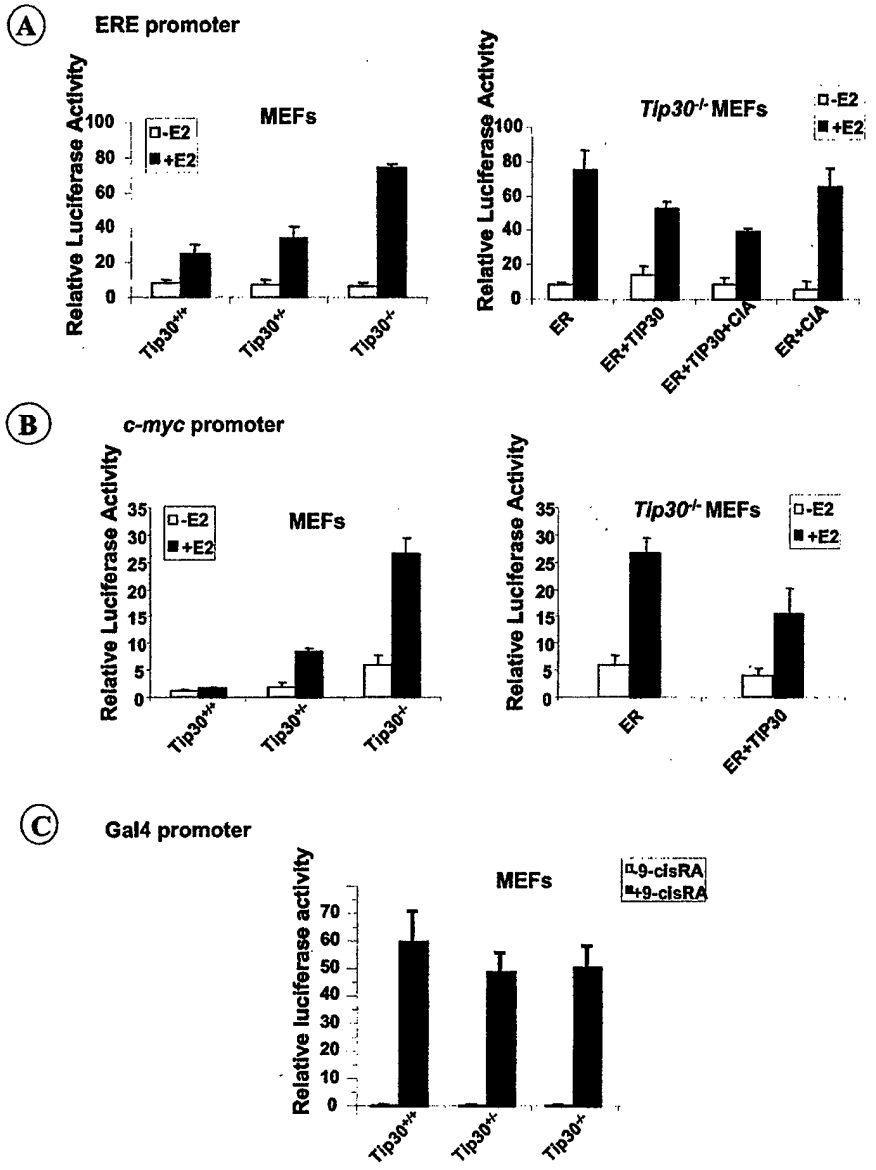

FIG. 5. **Effect on ERα-mediated transcription by loss of TIP30.** *A*, TIP30 loss affects the activity of ERα on an artificial promoter. *TIP30*$^{+/+}$, *TIP30*$^{+/-}$, and *TIP30*$^{-/-}$ MEFs were transfected with ERE-luciferase reporter plasmid and the expression vector for ERα in the presence of either 10^{-8} M E2 or ethanol carrier (*left panel*). TIP30$^{-/-}$ MEFs were cotransfected with ERα, TIP30, and CIA in the presence of either 10^{-8} M E2 or ethanol (*right panel*). *B*, deletion of the TIP30 gene affects the activity of ERα on c-*myc* promoter. *TIP30*$^{+/+}$, *TIP30*$^{+/-}$, and *TIP30*$^{-/-}$ MEFs were transfected with Myc-luciferase reporter and the expression vector for ERα in the presence of either 10^{-8} M E2 or ethanol carrier (*left panel*). TIP30$^{-/-}$ MEFs were cotransfected with ERα and TIP30 in the presence of either 10^{-8} M E2 or ethanol (*right panel*). *C*, Gal4-RXR-driven transcription is not affect by TIP30 loss. *TIP30*$^{+/+}$, *TIP30*$^{+/-}$, and *TIP30*$^{-/-}$ MEFs were transfected with a Gal-luciferase reporter and Gal4-RXR in the presence or absence of 9-*cis*-retinoic acid (*9-cisRA*, 10^{-6} M).

sence of TIP30, because expression of TIP30 in *Tip30*$^{-/-}$ cells resulted in a 42% inhibition in transcriptional activity of ERα (Fig. 5*B*, *right panel*). The finding that deletion of the *Tip30* gene elicits higher transcription from the c-*myc* promoter indicates that the function of TIP30 is to repress both estrogen-independent and estrogen-dependent ERα-mediated c-*myc* transcription.

Lack of TIP30 Increases c-myc Expression in the Mammary Gland—To demonstrate that TIP30 negatively regulates expression of the c-*myc* gene *in vivo*, we utilized a semi-quantitative RT-PCR analysis to examine the level of c-*myc* mRNA in the mammary gland from virgin *Tip30*$^{-/-}$ mice. As expected, a higher level of c-*myc* RNA was observed in mammary glands from *Tip30*$^{-/-}$ mice relative to age-matched *Tip30*$^{+/+}$ mice (Fig. 6*A*). In contrast, the level of cyclin B1 mRNA (Fig. 6*A*), whose promoter was not bound by ERα, CIA, or TIP30 (Fig. 2*C*), was relatively normal in these *Tip30*$^{-/-}$ mammary glands. We next used an immunohistochemical analysis to evaluate c-*myc* protein expression in the *Tip30*$^{-/-}$ mammary glands. Punctate staining for c-Myc protein was detected in both *Tip30*$^{+/+}$ and *Tip30*$^{-/-}$ mammary epithelial cells. However, 41% of the *Tip30*$^{-/-}$ mammary epithelial cells had nuclear staining for c-*myc*, whereas 27% of the *Tip30*$^{+/+}$ mammary epithelial cells had nuclear staining for c-*myc* (Fig. 6, *B* and *C*). We also examined ERα expression in these mammary glands using immunohistochemistry and Western blot analyses. The level of ERα and percentages of ERα nuclear staining in both *Tip30*$^{+/+}$ and *Tip30*$^{-/-}$ mammary epithelial cells were similar (data not shown), indicating that increased c-*myc* expression is not due to an increased expression of ERα in the mammary epithelium. These results demonstrate that a lack of TIP30 results in increased c-*myc* expression in mouse mammary glands. Taking these results together, we concluded that TIP30 is a repressor of ERα-mediated transcription of the c-*myc* gene.

DISCUSSION

ERα-mediated transcription requires coactivators that interact with ERα and enhance its transcriptional activity. Although most ER coactivators identified thus far associate with the AF-2 domain and enhance the transcriptional activity of many nuclear receptors, as well as nonreceptor activators (4, 14, 37), the unique coactivator CIA specifically enhances ERα activity independent of AF-2 function (22). In the present study, we have demonstrated the interaction between a puta-

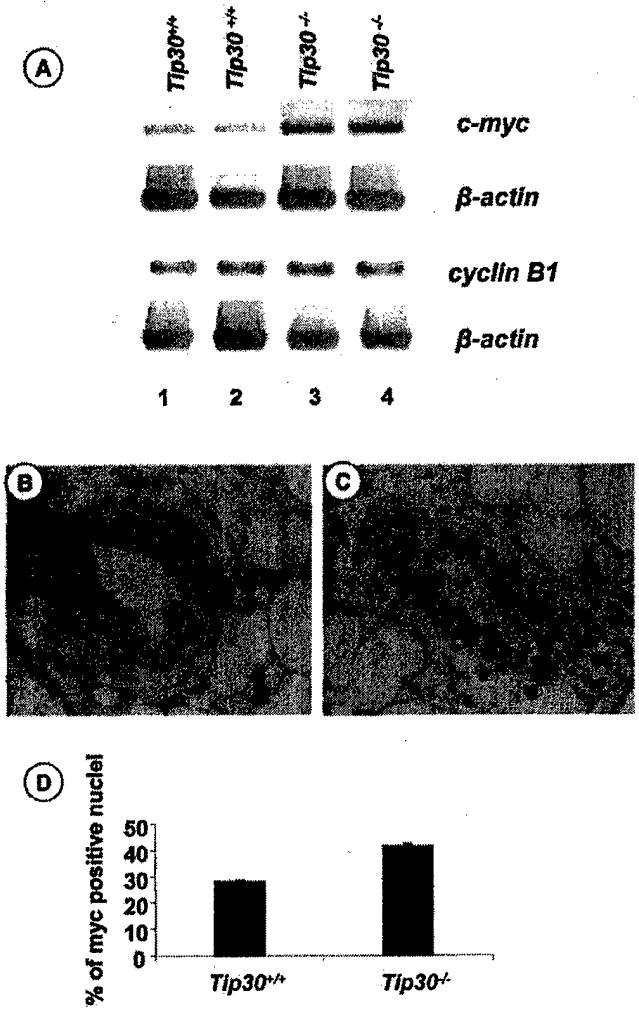

FIG. 6. **Loss of TIP30 increases c-*myc* expression in mammary glands.** *A*, loss of TIP30 increases the levels of c-*myc* mRNA in mammary glands. RNA was isolated from mammary glands of 8-week-old virgin *Tip30*$^{+/+}$ and *Tip30*$^{-/-}$ mice. RT-PCR analysis was used to monitor expression of the c-*myc*, cyclin B1, and β-actin genes. *B–D*, loss of TIP30 increases c-*myc*-stained epithelial cells in mammary glands. Representative immunostaining for c-*myc* on mammary gland sections from 8-week-old *Tip30*$^{+/+}$ (*B*) and *Tip30*$^{-/-}$ virgin mice (*C*) are shown. The *bar graph* indicates the percentage of c-*myc* nuclear-positive epithelial cells (*D*). The results represent two 8-week-old virgin mice for each genotype. About 500 epithelial cells were counted in the mammary gland section for each animal.

tive tumor suppressor TIP30 and CIA and subsequently cloned the full-length cDNA encoding CIA. Our biochemical and genetic data argue strongly that TIP30 is a repressor of ERα-mediated transcription of the c-*myc* gene. Specifically, TIP30 is coimmunoprecipitated with CIA from HeLa nuclear extracts and bound to CIA *in vitro* (Fig. 1). TIP30 and CIA are associated with the c-*myc* promoter in the absence of E2 and associated with the promoter and transcribed regions in the second transcription cycle in the presence of E2, suggesting that they are present in the same transcription complexes (Fig. 2). This is further supported by the results (Fig. 3*A*) that TIP30 and CIA cooperatively inhibit ERα-mediated transcription in transient transfection assays. The fact that TIP30 and CIA were copurified in the presence of protein cross-linkers also indicates that they do not form a stable complex but may transiently interact with each other during the second transcription cycle. Finally, involvement of TIP30 in ERα-mediated transcription is also supported by the observations that a lack of TIP30 results in enhanced ERα-mediated transcription in transient transfection assays (Fig. 3) and increased c-*myc* expression in mammary glands (Fig. 4). Therefore, we conclude that interaction between TIP30 and CIA is biologically relevant, and TIP30 is a repressor of ERα-mediated transcription of the c-*myc* gene.

Although CIA is not related to any known proteins, it contains a receptor-binding motif known as the LXXLL motif and a motif consisting of Arg-Asp repeats (22). Interestingly, the Arg-Asp repeats were previously found in a putative RNA-binding component (RD) of NELF (32) that interacts with RNA polymerase II and represses transcription. Because CIA, unlike other ER-interacting coactivators, is not released during elongation (Fig. 3), it may bind to RNA via the Arg-Asp repeats to regulate elongation. It is interesting in this regard that estrogen promotes occupancy of CIA on the promoter and the coding regions of the c-*myc* gene. The precedent for this type of assembly of transcription factors is observed in galactose activation of *GAL1* and heat shock activation of *HSP82* in yeast and *hsp70* in HeLa cells. Elongation factors such as Spt5 (38) and Sug1/Rpt6 (39, 40) are associated with both promoters and open reading frames of transcribed genes in yeast. Transcription activation induces occupancy of those factors on the *GAL1* promoter and the open reading frame. Therefore, we propose that CIA may be an elongation factor that is specifically involved in the transcription of ERα-targeted genes in mammalian cells. TIP30 and CIA may represent a novel class of coregulators for ERα.

The c-*myc* gene is controlled by numerous transcription factors through upstream sequences of its P1 and P2 start sites (7, 35). Previous studies have established that ERα increases c-*myc* transcription through a noncanonical ERE element (8). The experiments in the current study were designed to first determine the role of TIP30 and CIA in ERα-mediated c-*myc* transcription. Our data clearly demonstrate that TIP30 and CIA are involved in the regulation of c-*myc* transcription. It should be emphasized that the inhibition of ERα-mediated transcription by TIP30 is not caused by a nonspecific repression, because TIP30 overexpression or loss of expression failed to alter transactivation by other nuclear receptors under the same conditions. Overall, previous (22) and current studies have suggested complicated roles of TIP30 and CIA in ERα-mediated transcription, although it remains unclear precisely how TIP30 and CIA function in this process. However, based on our data, we hypothesize that TIP30 and CIA may act as repressors of c-*myc* transcription. In this scenario, the binding of TIP30 to the c-*myc* promoter in the absence of E2 might lead to phosphorylation of the CTD of RNA polymerase II (27) during the formation of preinitiation complexes. This in turn might destabilize the association of RNA polymerase II with coactivators such as AIB1, p300, pCAF, CBP, and TRAPs (15) at the initiation step. In this regard, an inhibitor of RNA polymerase II elongation, α-amanitin, (15, 36), which inhibited the association of RNA polymerase II with the coding region of the c-*myc* gene, also abolished the association of TIP30 and CIA (Fig. 2*F*), suggesting that association of TIP30 and CIA with the coding region is RNA polymerase II-dependent. In addition, TIP30 was previously shown to phosphorylate the CTD *in vitro* (27), and the kinase-defective TIP30 mutant failed to repress ERα-mediated transcription (Fig. 4*B*). In the first transcription cycle, CIA may facilitate displacement of TIP30 from the promoter, possibly through a transient interaction with TIP30, and subsequently associate with elongation complexes. Alternatively, ERα and ERα-recruited factors could also facilitate TIP30 displacement from the promoter, with the observed TIP30-CIA interactions being more relevant to their mutual presence in transcription elongation complexes in the absence

of estrogen as well as in the second cycle transcription complexes following estrogen treatment. In the second transcription cycle, CIA may cooperate with TIP30 to repress transcription. In support of this possibility, CIA was previously shown to inhibit transcription of a Gal-driven *TK* reporter when it was fused to a GAL4 DNA-binding domain, indicating that CIA may possess an intrinsic inhibitory function (22). Clearly, further studies will be required for testing this hypothesis.

Notwithstanding, we could not pinpoint the binding site for TIP30 on the c-*myc* promoter in the absence of estrogen because of the limitations in ChIP assays. Given the bewildering regulatory elements in the c-*myc* promoter and observations of RNA polymerase II holdback at the P2 promoter (35), future studies will focus on the effects of TIP30 and CIA on RNA polymerase II and the mechanism by which CIA and TIP30 regulate transcription.

The finding that TIP30 acts as a negative regulator in both unliganded and liganded ERα-mediated c-*myc* expression led us to predict that TIP30 may regulate tumorigenesis and tissue development of ERα-targeted organs (41, 42). As described in a recent report (28), we observed that a group of C57B6/129Svj hybrid mice deficient in TIP30 spontaneously developed tumors in ERα target organs including the ovary, uterus, and liver but not in the mammary gland. Recently, we have extended these studies by examining mammogenesis and tumorigenesis of cohorts of C57B6 mice deficient in TIP30 and control wild type mice. We have observed that virgin female mice lacking TIP30 exhibited ductal hyperplasia and spontaneously developed tumors in the mammary gland compared with control wild type mice.[2] Because mild hyperplasia was described previously in the mammary gland of transgenic mice overexpressing c-*myc* (9, 37, 43), the ductal hyperplasia in *Tip30*$^{-/-}$ mice could be partly due to elevated expression of the c-*myc* gene that was observed in their mammary glands (Fig. 6). This genetic evidence agrees well with a negative role of TIP30 in ERα-mediated c-*myc* transcription. However, we do not exclude the possibility that TIP30 may also regulate other ERα target genes that may also contribute to the ductal hyperplasia. Future studies should identify additional TIP30 target genes in the mammary epithelial cells and illuminate the molecular basis for TIP30 loss-facilitated tumorigenesis.

In summary, we have identified a TIP30-interacting protein as the ER-interacting coactivator CIA and revealed that TIP30 and CIA directly regulate the transcription of the c-*myc* gene. Like other ERα cofactors (14, 15), TIP30 and CIA are recruited by ERα on the c-*myc* promoter in a cyclic fashion. Concordant with its effect on ERα-mediated c-*myc* transcription, loss of TIP30 increases c-*myc* expression in the mammary gland of mice. Our studies suggest that TIP30 and CIA represent a novel class of coregulators for regulating gene expression during mammogenesis and tumorigenesis.

Acknowledgments—We thank the Core Facility of the Rockefeller University for the amino acid sequence of CIA protein and K.-U. Wagner, Z. X. Wang, C. M. Eischen, and A. Diehl for technical help and useful discussions and critical reading of the manuscript.

[2] J. Pecha, C. Jiang, and H. Xiao, manuscript in preparation.

REFERENCES

1. Couse, J. F., and Korach, K. S. (1999) *Ann. Endocrinol.* **60,** 143–148
2. Couse, J. F., and Korach, K. S. (1999) *Endocr. Rev.* **20,** 358–417
3. Mangelsdorf, D. J., Beato, M., Herrlich, P., Schutz, G., Umesono, K., Blumberg, B., Kastner, P., Mark, M., and Chambon, P. (1995) *Cell* **83,** 835–839
4. Mckenna, N. J., Xu, J., Nawaz Z., Tsai, S. Y., Tsai, M. J., and O'Malley, B. W. (1999) *J. Steroid Biochem. Mol. Biol.* **69,** 3–12
5. Nilsson, S., Makela, S., Treuter, E., Tujague, M., Thomsen, J., Andersson, G., Enmark, E., Pettersson, K., Warner, M., and Gustafsson, J. A. (2001) *Physiol. Rev.* **81,** 1535–1565
6. Planas-Silva, M. D., Shang, Y., Donaher, J. L., Brown, M., and Weinberg, R. A. (2001) *Cancer Res.* **61,** 3858–3862
7. Battey, J., Moulding, C., Taub, R., Murphy, W., Stewart, T., Potter, H., Lenoir, G., and Leder, P. (1983) *Cell* **34,** 779–787
8. Dubik, D., and Shiu, R. P. (1992) *Oncogene* **7,** 1587–1594
9. Leder, A., Pattengale, P. K., Kuo, A., Stewart, T. A., and Leder, P. (1986) *Cell* **45,** 485–495
10. Liao D. J, and Dickson, R. B. (2000) *Endocr. Relat. Cancer* **7,** 143–164
11. Tora, L., White, J., Brou, C., Tasset, D., Webster, N., Scheer, E., and Chambon, P. (1989) *Cell* **59,** 477–487
12. Tsai, M. J., and O'Malley, B. W. (1994) *Annu. Rev. Biochem.* **63,** 451–486
13. Burakov, D., Crofts, L. A., Chang, C. P., and Freedman, L. P. (2002) *J. Biol. Chem.* **27,** 14359–14362
14. Métivier, R., Penot, G., Hübner, M. R., Reid, G., Brand, H., Kos, M., and Gannon, F. (2003) *Cell* **115,** 751–763
15. Shang, Y., Hu, X., DiRenzo, J., Lazar, M. A., and Brown M. (2000) *Cell* **103,** 843–852
16. Shang, Y., and Brown, M. (2002) *Science* **295,** 2465–2468
17. Xu, L., Glass, C. K., and Rosenfeld, M. G. (1999) *Curr. Opin. Genet. Dev.* **9,** 140–147
18. Freedman, L. P. (1999) *Trends Endocrinol. Metab.* **10,** 403–407
19. Ito, M., Okano, H. J., Darnell, R. B., and Roeder, R. G. (2002) *EMBO J.* **21,** 3464–3475
20. Kang, Y. K., Guermah, M., Yuan, C. X., and Roeder, R. G. (2002) *Proc. Natl. Acad. Sci. U. S. A.* **99,** 2642–2647
21. Freedman, L. P. (1999) *Annu. Rev. Biochem.* **70,** 475–501
22. Sauve, F., McBroom, L. D., Gallant, J., Moraitis, A. N., Labrie, F., and Giguere, V. (2001) *Mol. Cell. Biol.* **21,** 343–353
23. Xiao, H., Tao, Y., Greenblatt, J., and Roeder, R. G. (1998) *Proc. Natl. Acad. Sci. U. S. A.* **95,** 2146–2151
24. Shtivelman, E. (1997) *Oncogene* **14,** 2167–2173
25. NicAmhlaoibh, R., and Shtivelman, E. (2001) *Oncogene* **20,** 270–275
26. Whitman, S., Wang, X., Shalaby, R., and Shtivelman, E. (2000) *Mol. Cell. Biol.* **20,** 583–593
27. Xiao, H., Palhan, V., Yang, Y., and Roeder, R. G. (2000) *EMBO J.* **19,** 956–963
28. Ito, M., Jiang, C., Krumm, K., Zhang, X., Pecha, J., Zhao, J., Guo Y., Roeder R. G., and Xiao, H. (2003) *Cancer Res.* **63,** 8763–8767
29. Dignam, J. D., Lebovitz, R. M., and Roeder, R. G. (1983) *Nucleic Acids Res.* **11,** 1475–1489
30. Xiao, H., Tao, Y., and Roeder, R. G. (1999) *J. Biol. Chem.* **274,** 3937–3940
31. Yuan, C. X., Ito, M., Fondell, J. D., Fu, Z. Y., and Roeder, R. G. (1998) *Proc. Natl. Acad. Sci. U. S. A.* **95,** 7939–7944
32. Yamaguchi, Y., Takagi, T., Wada, T., Yano, K., Furuya, A., Sugimoto, S., Hasegawa, J., and Handa, H. (1999) *Cell* **97,** 41–51
33. Heery, D. M., Kalkhoven, E., Hoare, S., and Parker, M. G. (1997) *Nature* **387,** 733–736
34. Le Douarin, B., Nielsen, A. L., Garnier, J. M., Ichinose, H., Jeanmougin, F., Losson, R., and Chambon, P. (1996) *EMBO J.* **15,** 6701–6715
35. Spencer, C. A., and Groudine M. (1990) *Ann. N. Y. Acad. Sci.* **599,** 12–28
36. Rudd, M. D., and Luse, D. S. (1996) *J. Biol. Chem.* **271,** 21549–21558
37. McCormack, S. J., Weaver, Z., Deming, S., Natarajan, G., Torri, J., Johnson, M. D., Liyanage, M., Ried, T., and Dickson, R. B. (1998) *Oncogene* **16,** 2755–2766
38. Pokholok, D. K., Hannett, N. M., and Young, R. A. (2002) *Mol. Cell* **9,** 799–809
39. Ferdous, A., Gonzalez, F., Sun, L., Kodadek, T., and Johnston, S. A. (2001) *Mol. Cell* **7,** 981–991
40. Gonzalez, F., Delahodde, A., Kodadek, T., and Johnston, S. A. (2002) *Science* **296,** 548–550
41. Cardiff, R. D., Anver, M. R., Gusterson, B. A., Hennighausen, L., Jensen, R. A., Merino, M. J., Rehm, S., Russo, J., Tavassoli, F. A., Wakefield, L. M., Ward, J. M., and Green, J. E. (2000) *Oncogene* **19,** 968–988
42. Cunha, G. R., Wiesen, J. F., Werb Z., Young, P., Hom, Y. K., Cooke, P. S., and Lubahn D. B. (2000) *Adv. Exp. Med. Biol.* **480,** 93–97
43. D'Cruz, C. M., Gunther, E. J., Boxer, R. B., Hartman, J. L., Sintasath, L., Moody, S. E., Cox, J. D., Ha, S. I., Belka, G. K., Golant, A., Cardiff, R. D., and Chodosh, L. A. (2001) *Nat. Med.* **7,** 235–239

JBC Papers in Press. Published on June 21, 2004 as Manuscript M400408200

Cell cycle arrest and cell death are controlled by p53-dependent and p53-independent mechanisms in Tsg101-deficient cells

Marissa J. Carstens[1], Andrea Krempler[1,3], Aleata A. Triplett[1], Maarten van Lohuizen[2], and Kay-Uwe Wagner[1,*]

[1] Eppley Institute for Research in Cancer and Allied Diseases, University of Nebraska Medical Center, 986805 Nebraska Medical Center, Omaha, Nebraska 68198-6805, USA

[2] The Netherlands Cancer Institute, Department of Molecular Genetics, H5, Plesmanlaan 121, 1066 CX Amsterdam, The Netherlands

[3] Present address: University of the Saarland, Medical Biochemistry and Molecular Biology, Building 44, Homburg, 66424, Germany

Running title: Tsg101 deficiency and cell cycle progression

* Correspondence to:

Kay-Uwe Wagner, Ph.D.
Eppley Institute for Research in Cancer and Allied Diseases, University of Nebraska Medical Center, 986805 Nebraska Medical Center, Rm. 8009, Omaha, NE 68198-6805
Tel: (402) 559-3288, Fax: (402) 559-4651, E-mail: kuwagner@unmc.edu

Summary

Our previous studies have shown that cells conditionally deficient in Tsg101 arrested at the G1/S cell cycle checkpoint and died. We created a series of Tsg101 conditional knockout cell lines that lack p53, $p21^{Cip1}$, or $p19^{Arf}$ to determine the involvement of the Mdm2-p53 circuit as a regulator for G1/S progression and cell death. In this new report, we show that the cell cycle arrest in Tsg101-deficient cells is p53-dependent, but a null mutation of the *p53* gene is unable to maintain cell survival. The deletion of the *Cdkn1a* gene in Tsg101 conditional knockout cells resulted in G1/S progression suggesting that the p53-dependent G1 arrest in the *Tsg101* knockout is mediated by $p21^{Cip1}$. The Cre-mediated excision of *Tsg101* in immortalized fibroblasts that lack $p19^{Arf}$ seemed not alter the ability of Mdm2 to sequester p53, and the p21-mediated G1 arrest was not restored. Based on these findings, we propose that the p21-dependent cell cycle arrest in Tsg101-deficient cells is an indirect consequence of cellular stress and not caused by a direct effect of Tsg101 on Mdm2 function as previously suggested. Finally, the deletion of *Tsg101* from primary tumor cells that express mutant p53 and that lack $p21^{Cip1}$ expression results in cell death suggesting that additional transforming mutations during tumorigenesis do not affect the important role of Tsg101 for cell survival.

Keywords: Cell Growth / Cell Survival / Cre Recombinase / Gene Targeting / Tsg101 / Knockout / mouse embryonic fibroblasts / mammary development

Introduction

The tumor susceptibility gene 101 (*Tsg101*) encodes a multi-domain protein that mediates a variety of biological functions. Some of these functions have been postulated from the predicted protein structure, its intracellular localization, the identification of Tsg101 binding proteins, and very recently, the generation of Tsg101-deficient mouse models. These functions include a role in ubiquitination (1, 2), transcriptional regulation (3, 4), endosomal trafficking (5-8), proliferation (9-12), and cell survival (12, 13). The C-terminal coiled-coil domain of Tsg101, formally known as CC2, was isolated first in a yeast-two-hybrid screen with the cell growth regulating protein Stathmin (14). This region is a potential co-repressor, which is able to modulate the transcriptional activity of steroid receptors (3, 4, 15). Furthermore, Tsg101 possesses a proline-rich sequence known to exist in activation domains of transcription factors (16). The N-terminal region of Tsg101 (UEV domain) is similar to the catalytic domain of ubiquitin-conjugating (E2) enzymes. Since Tsg101 lacks a key cysteine residue found in authentic E2 enzymes, it has been postulated that this protein might serve as a negative regulator for the ubiquitin-mediated degradation of other proteins (1, 2). Suggested targets of important factors for cell cycle regulation, whose stability and function were affected by Tsg101, are Mdm2 and $p21^{Cip1}$ (17, 18).

New insights about the biological role of Tsg101 *in vivo* were obtained from genetically engineered mice that lack Tsg101 completely (11, 13) or in selected cell types (12, 13). The deletion of the promoter and the first coding exon of *Tsg101* resulted in embryonic lethality around implantation (13). Tsg101-deficient embryos lacking exons 8 and 9 die around day 6.5 of gestation due to a defect in cell proliferation and mesoderm formation (11). The WAP-Cre[1]-

mediated deletion of Tsg101 from differentiating mammary epithelial cells (conditional knockout) in adult females resulted in increased cell death, impaired mammary development, and a lactation-deficient phenotype (13). The excision of the *Tsg101* gene in primary cultures of mouse embryonic fibroblasts (MEFs) or mammary epithelial cells (MECs) revealed that Tsg101-deficient cells arrested at the G1/S transitional phase of the cell cycle before they underwent cell death (12, 13). In contrast to previous reports (16, 19), neither haploinsufficiency of *Tsg101* nor the deletion of both *Tsg101* alleles in the conditional knockout models (*in vitro* and *in vivo*) resulted in neoplastic transformation suggesting that a null mutation of *Tsg101* is not an initiating event for tumorigenesis (11-13).

Cell cycle arrest at the G1/S checkpoint and cell death were two major phenomena that we observed in the Tsg101 conditional knockout model (12, 13). The analysis of crucial regulators of the cell cycle revealed that Tsg101 deficiency resulted in growth arrest through the inactivation of cyclin-dependent kinase 2 (Cdk2). Consequently, DNA replication was not initiated in Tsg101-deficient cells before they died (12). A crucial regulatory mechanism, which is commonly associated with G1 arrest and cell death, is the $p19^{Arf}$-Mdm2-p53 tumor-surveillance or stress-response pathway (20). The goal of this study was to further discriminate the p53-dependent and p53-independent mechanisms that lead to either cell cycle arrest or cell death as a consequence of Tsg101 deficiency. We now show that the G1 arrest in Tsg101-deficient cells is dependent upon the presence of functional p53 and its downstream mediator $p21^{Cip1}$. Our findings suggest that, in contrast to keratinocytes (18), Tsg101 is not required for $p21^{Cip1}$ protein stability and function in proliferating fibroblasts. The absence of either p53 (and therefore p21) or $p21^{Cip1}$ alone is, however, unable to sustain cell survival. In addition to these

findings *in vitro*, a null mutation of the *p53* gene does not restore normal mammogenesis and lactation in Tsg101 mammary-specific knockout mice (WAP-Cre $Tsg101^{fl/fl}$ $p53^{-/-}$). To address the proposed role of Tsg101 as a crucial regulator for Mdm2 function (17), we have generated a conditional double-knockout of *Tsg101* and *Cdkn2a*. The deletion of Tsg101 in immortalized fibroblasts that lack expression of $p19^{Arf}$ does not alter Mdm2 function and does not restore the p21-mediated G1 arrest. In summary, our data does not support a biologically relevant function of Tsg101 as a stabilizer for Mdm2. Therefore, we propose that the p21-mediated induction of the G1 arrest might be an indirect consequence of Tsg101 deficiency due to cellular dysfunction and stress. Finally, we show that the deletion of Tsg101 from tumorigenic cells that express mutant p53 and that lack $p21^{Cip1}$ expression results in cell death. This observation suggests that additional, transforming mutations during tumorigenesis do not affect the important role of Tsg101 for cell survival.

Experimental Procedures

Mouse models, genotyping protocols, and whole mount analysis of mammary glands. The PCR protocol for genotyping the Whey-Acidic-Protein-(WAP)-Cre mice [TgN(Wap-cre)11738Mam], as well as the generation and phenotypic characterization of *Tsg101* conditional knockout mice [$Tsg101^{tm1Kuw}$], have been described earlier (13, 21). Mutant mice with a targeted deletion of the *p53* gene [$Trp53^{tm1Brd}$] (22) were purchased from Taconic Farms, Inc. *Cdkn1a* (23) and *Cdkn2a* (24) knockout mice [$Cdkn1a^{tm1Tyj}$ and $Cdkn2a^{tm1Rdp}$, respectively] were obtained from the Jackson Laboratory and the repository of the Mouse Model for Human Cancer Consortium (MMHCC). Athymic nude mice (NCr strain, NCI) were used for transplantation studies. The preparation and staining of mammary gland whole mounts were described

previously (13, 25). All animals used in the studies were treated humanely and in accordance with federal guidelines and institutional policies.

Primary cell cultures and retroviral expression vectors. Mouse embryonic fibroblasts (MEFs) from 13.5 or 14.5-day-old *Tsg101*$^{fl/fl}$, *Tsg101*$^{fl/fl}$ *p53*$^{-/-}$, *Tsg101*$^{fl/fl}$ *Cdkn1a*$^{-/-}$, or *Tsg101*$^{fl/fl}$ *Cdkn2a*$^{-/-}$ embryos and their littermate controls were explanted and maintained in DMEM supplemented with 10% fetal bovine serum, 2 mM glutamine, 0.1 mM nonessential amino acids, 10 μg/ml gentamycin, 100 U/ml penicillin and 100 μg/ml streptomycin (Invitrogen). Cells at passages two through four were plated at a density of 4 x 10^5 cells per 10 cm culture dish and infected with the pBabe and pBabe-Cre constructs. The generation of these retroviral vectors was published previously (12, 13). Forty-eight hours after infection, cells were selected in complete medium containing 7 μg/ml puromycin (Sigma) or 200 μg/ml hygromycin B (Invitrogen).

Cell cycle analysis and MTT assay. Approximately 10^6 MEFs were harvested four days after puromycin selection to determine cell cycle progression using a flow cytometric analysis. Cells were washed in 1xPBS and fixed in ice-cold 70% ethanol for 30 minutes. After an additional washing step, cells were stained overnight with propidium iodide as described previously (26). The stained MEFs were analyzed in a FACScalibur (Beckton-Dickinson) flow cytometer. The software packages CELLquest (Beckton-Dickinson) and Modfit LT (Verity) were used for data acquisition. The cell cycle analysis was repeated three or four times for each experimental setting, and a t-test was performed to validate statistically significant differences between the various double knockout cell lines and their controls. An MTT growth assay was performed as described earlier (27) to determine the growth properties of *Tsg101/p53* double knockout cells.

The 3-(4,5-dimethylthiazol-2-yl)-2,5-diphenyltetrazolium bromide (MTT) was obtained from Sigma. Two times 10^4 cells of each genotype were seeded in triplicates in a 96-well microtiter plate. Absorbance was measured at 570 nm with an Elx 808 (Bio-Tek Instruments) ELISA reader.

Western blot analysis and Cdk2 kinase assay. MEFs were pelleted and lysed on wet ice for 30 minutes in 1x PBS, 1 % NP-40, 0.5 % Na-deoxycholate, 0.1 % SDS, 1 mM PMSF, 0.4 U/ml aprotinin, 1 mM NaF, 0.1 mM Na-Orthovandate. Protein was quantified using a Bradford assay (PIERCE) according to the manufacture's protocol. Approximately fifty to one hundred micrograms of protein per lane was resolved on a 4-20% SDS-PAGE gradient gel and blotted onto PVDF membranes (Invitrogen). The membranes were blocked for one hour in 1x TBS, 0.1% Tween-20, and 5% dry milk. Subsequently, membranes were incubated with primary antibodies in blocking buffer at 4°C overnight, washed three times for 15 minutes in washing buffer (1x TBS / 0.1 % Tween-20), and incubated for one hour at room temperature with horseradish-peroxidase-(HRP)-conjugated secondary antibodies in blocking buffer. Membranes were washed again three times in washing buffer and once for 15 minutes in 1x TBS without Tween-20. Protein bands were detected using the ECL chemiluminescence kit for western blot analysis (Amersham) according to the manufacture's protocol. Membranes were stripped using 0.2 M NaOH for consecutive detection of various proteins. The following antibodies were used in this study: α- Tsg101 (C-2), α-cyclin B1 (M-20), α-cyclin A2 (C-19), α-$p16^{Ink4a}$ (M-156), and α-ActB (I-19) from Santa Cruz Biotechnology as well as α-$p21^{Cip1}$ (SX118) from PharMingen and α-$p19^{Arf}$ (Ab-1) from Oncogene at a 1:1000 dilution. HRP-conjugated secondary antibodies were purchased from Santa Cruz Biotechnology and used at a 1:1000 dilution. A Cdk2 kinase

assay was performed using the α-Cdk2 (M-2) antibody from Santa Cruz Biotechnology and Histone H1 (1 μg/μl) from Sigma.

Results

A null mutation of *p53* does not rescue the deleterious phenotype caused by Tsg101 deficiency *in vitro* and *in vivo*.

The Cre-mediated excision of both *Tsg101* floxed alleles from proliferating primary fibroblasts (MEFs) and mammary epithelial cells (MECs) resulted in cell cycle arrest and cell death (12, 13). The activation of the $p19^{Arf}$-Mdm2-p53 stress-response pathway is frequently associated with both phenomena. To further discriminate the p53-dependent and p53-independent mechanisms that lead to either cell cycle arrest or cell death as a consequence of Tsg101 deficiency, we derived mouse embryonic fibroblasts (MEFs) from Tsg101 conditional knockout mice ($Tsg101^{fl/fl}$) that carry a targeted null mutation of the *p53* gene (22). Cells treated with a control virus (pBabe) or a retrovirus expressing Cre recombinase (pBabe-Cre) were grown for seven days after infection to quantitatively examine the growth of Tsg101 knockout cells in the presence or absence of p53. The multiplication of Tsg101-deficient MEFs and their controls were determined using an MTT assay between days four through seven post-infection when optimal puromycin selection, expression of Cre, and excision of *Tsg101* had been achieved (Fig. 1A). The Cre-mediated deletion of *Tsg101* resulted in a severe growth inhibition and reduction in the number of viable cells. More importantly, we did not observe a significant modification of growth properties or prolonged cell survival in the presence or absence of one or both copies of the *p53* gene. Our data suggested that a *p53* null mutation was neither able to rescue growth inhibition nor significantly modify the rate of cell death of Tsg101-deficient primary fibroblasts.

We have shown in a control experiment that the expression of Cre recombinase can be excluded as a cause or possible modifier of this phenotype. Tsg101 wildtype cells (*Tsg101*$^{+/+}$) infected with the retroviral pBabe-Cre vector did not exhibit growth retardation in an MTT assay. In addition, we were able to rescue the deleterious phenotype of *Tsg101*$^{-/-}$ cells through the expression of exogenous, HA-tagged Tsg101 from a retroviral vector (12).

To verify these initial findings in a different cell type and *in vivo*, we bred two mutant *p53* alleles into mammary-specific Tsg101 conditional knockout mice (WAP-Cre *Tsg101*$^{fl/fl}$ *p53*$^{-/-}$). The expression of Cre under the whey acidic protein (WAP) promoter is largely confined to differentiating mammary epithelial cells in late-pregnant and lactating females (21, 25). In contrast to littermate controls (*Tsg101*$^{fl/fl}$ *p53*$^{+/+}$), the WAP-Cre-mediated deletion of *Tsg101* in a *p53* wildtype background (WAP-Cre *Tsg101*$^{fl/fl}$ *p53*$^{+/+}$) resulted in impaired mammogenesis at the onset of lactation (Fig 1B). The introduction of two mutant copies of the *p53* gene into the Tsg101 conditional knockout (WAP-Cre *Tsg101*$^{fl/fl}$ *p53*$^{-/-}$) was unable to rescue impaired mammogenesis caused by the WAP-Cre-mediated excision of the two floxed *Tsg101* alleles. Therefore, our observations in mutant female mice were consistent with the cell culture studies on *Tsg101/p53* double mutant MEFs. Taken together, the outcome of both studies (*in vitro* and *in vivo*) suggests that the inability of a *p53* null mutation to rescue a Tsg101-deficient phenotype is neither a cell culture phenomenon nor caused by a possible difference in p53 function between different cell types of mesodermal and ectodermal origin (i.e. fibroblasts and mammary epithelial cells).

Deletion of p53 in Tsg101-deficient cells restores the activity of Cdk2 and progression into the S phase.

Despite p53-independent mechanisms that trigger the dominant phenotype (i.e. lethality) of *Tsg101*$^{-/-}$ cells, we postulated that deficiency of p53 might modify or even eliminate the cell cycle arrest in Tsg101-deficient cells before they die. To address this hypothesis, we analyzed the cell cycle progression of Tsg101 null cells lacking one or two copies of the *p53* gene. The Cre-mediated deletion of *Tsg101* in MEFs with a heterozygous null mutation of *p53* (*Tsg101*$^{fl/fl}$ *p53*$^{+/-}$ pBabe-Cre) leads to a significant reduction in the number of cells in S-phase (Fig. 2A) ($P<0.01$; t-Test), a decrease of the cyclin A2 protein level (Fig. 2B, lane 3), and the inactivation of the cyclin dependent kinase 2, Cdk2 (Fig. 2C). Consequently, the inhibition of only one *p53* allele had no effect on impaired G1/S progression of *Tsg101*$^{-/-}$ cells, and the consequences of Tsg101 deficiency were identical to cells with two functional copies of *p53* (12). In contrast, the deletion of both *p53* alleles in Tsg101 conditional knockout MEFs (*Tsg101*$^{fl/fl}$ *p53*$^{-/-}$ pBabe-Cre) re-established a normal G1/S progression (Fig. 2A) ($P<0.02$; t-Test), increased the expression of cyclins A2 (Fig. 2B), and restored the activation of Cdk2 (Fig. 2C). In summary, these observations confirm our previously stated hypothesis that p53 deficiency is able to lift the G1 cell cycle arrest and to revert part of the complex phenotype of Tsg101 knockout cells despite its inability to sustain cell survival.

P21^{Cip1} is a mediator of the G1 cell cycle arrest in Tsg101 conditional knockout cells.

The activity of Cdk2 in complex with cyclin E is negatively regulated by the cell cycle inhibitor p21^{Cip1} whose expression level is dependent upon the transcriptional activation of p53 (28-30). Therefore, we hypothesized that p21^{Cip1} might be a component of the p53-dependent cell cycle

arrest in response to Tsg101 deficiency. To address this issue, we bred *Cdkn1a*$^{-/-}$ mice (23) into the *Tsg101* floxed background (*Tsg101*$^{fl/fl}$ *p21*$^{-/-}$) to generate MEFs that lack expression of p21 and Tsg101 after infection with pBabe-Cre and selection with puromycin (Fig. 3A). The infection of p21^{Cip1}-deficient cells with the control vector pBabe and selection with puromycin had little or no consequences on the viability and multiplication of primary cells. The Cre-mediated excision of only one floxed allele of *Tsg101* (*Tsg101*$^{fl/+}$ *p21*$^{-/-}$ pBabe-Cre) also did not affect the survival and G1/S progression of p21^{Cip1}-deficient MEFs as determined by flow cytometry (Fig. 3B). The deletion of two floxed alleles of *Tsg101* (*Tsg101*$^{fl/fl}$ *p21*$^{-/-}$ pBabe-Cre) progressively led to the death of Tsg101-deficient MEFs within seven days after infection with the retroviral Cre vector (data not shown). Like the deletion or functional inhibition of p53, a null mutation of the *Cdkn1a* gene was, however, able to restore the G1/S progression in cells lacking Tsg101 (Fig. 3B). The average number of cells in S-phase was not significantly different between the double knockout cells and their controls ($P>0.05$). The relative increase in a subset of cells at the G2/M phase is probably caused by the puromycin selection since we observed the same phenomenon when these cells where infected with the pBabe vector control. Collectively our findings confirmed the working hypothesis, which predicted that p21^{Cip1} is a mediator of the G1 cell cycle arrest in Tsg101-deficient cells.

The deletion of *Tsg101* in immortalized fibroblasts that lack p19^{Arf} does not alter the ability of Mdm2 to sequester p53.

Several reports propose a potential role for Tsg101 as an important negative regulator for the ubiquitn-mediated turnover of Mdm2 and p21^{Cip1} in various cells lines and in differentiating primary keratinocytes (11, 17, 18). In addition, Oh et al. (2002) suggested that Tsg101 is critical

for the p21-mediated inhibition of cyclin/Cdk complexes in proliferating keratinocytes (18). The cell cycle analysis in double knockout MEFs lacking *Tsg101* and *Cdkn1a* revealed that $p21^{Cip1}$ is important for the G1 arrest (see previous paragraph). This observation suggests that a knockout of *Tsg101* does not impair the stability, ubiquitin-mediated proteolysis, or function of $p21^{Cip1}$ in proliferating fibroblasts. To address the proposed function of Tsg101 as a stabilizer for Mdm2, we designed a new set of experiments illustrated in figure 4. Thus far, we determined the role of p53 and $p21^{Cip1}$ as regulators for the G1/S progression in Tsg101-deficient cells. Both proteins act *downstream* of Mdm2 (20). In this new experimental design we planned to immortalize primary MEFs *upstream* of Mdm2 through deletion of the *Cdkn2a* gene (Fig. 4A, left). The *Cdkn2a* locus encodes $p19^{Arf}$, which is known to negatively regulate Mdm2 (20). Therefore, $p19^{Arf}$-deficient immortalized cells also lack expression of p53 and $p21^{Cip1}$. The level of unrestrained Mdm2 protein for the sequestration of p53 is crucial in immortal $p19^{Arf}$-null cells.[2] This causal relationship is probably best illustrated by the fact that the deletion of $p19^{Arf}$ alone has no influence on the survival of *Mdm2* mutant mice, whereas *p53/Mdm2* double knockouts (31, 32) or $p19^{Arf}$*/Mdm2/p53* triple mutant mice are viable (33). According to this mechanism, the destabilization and downregulation of Mdm2 as a consequence of Tsg101 deficiency (Fig. 4A, right) should result in an accumulation of p53 and $p21^{Cip1}$. In turn, the upregulation of p53 and $p21^{Cip1}$ should inhibit cell cycle progression in *Cdkn2a* mutant cells. In conclusion, if Tsg101 is essential for the stability and function of Mdm2 as previously suggested (17), then its deletion in immortalized MEFs lacking $p19^{Arf}$ should impair G1/S progression in a very similar fashion as in Tsg101-deficient nonimmortalized cells with normal p53 and $p21^{Cip1}$ levels.

To generate a conditional double-knockout of *Tsg101* and *Cdkn2a,* we decided to cross *Tsg101* floxed animals with *Cdkn2a* knockout mice (24) that lack both tumor susceptibility proteins ($p19^{Arf}$ and $p16^{Ink4a}$) encoded by this locus. Our decision was based on the fact that Tsg101 and its proposed biological functions were first described in murine 3T3 fibroblasts and their derived tumorigenic SL6 cells (16). These cell lines lack $p16^{Ink4a}$ in addition to $p19^{Arf}$ as determined in a preliminary study (Fig. 5A). To generate primary *Tsg101/p19*^{Arf} double knockout cells, we infected MEFs carrying two floxed alleles of *Tsg101* in addition to two null alleles of *Cdkn2a* (*Tsg101*$^{fl/fl}$ *Cdkn2a* $^{-/-}$) with the pBabe-Cre virus (Fig. 5B). *Tsg101* knockout cells in a *Cdkn2a* heterozygous background (*Tsg101*$^{fl/fl}$ *Cdkn2a*$^{+/-}$) or *Tsg101* heterozygous mutants carrying two *Cdkn2a* null alleles (*Tsg101*$^{fl/+}$ *Cdkn2a* $^{-/-}$) were used as controls. The infection of these control cell lines with the pBabe retroviral control vector and puromycin selection had also no influence on cell survival (data not shown). As expected, the expression of Cre also had no effect on cell proliferation and cell survival of MEFs with a *Tsg101* floxed heterozygous mutation whether cells express $p19^{Arf}$ or not. However, the ablation of Tsg101 in $p19^{Arf}$-deficient cells using the pBabe-Cre construct (*Tsg101*$^{fl/fl}$ *Cdkn2a* $^{-/-}$ pBabe-Cre) resulted in cell death shortly after excision of *Tsg101*, and the phenotype was comparable to those observed in *Tsg101/p53* and *Tsg101/p21* double mutants (data not shown). This observation suggested that none of the genes of the $p19^{Arf}$-Mdm2-p53-$p21^{Cip1}$ circuit alone or in combination with $p16^{Ink4a}$ seem to be required for the initiation of cell death of Tsg101-deficient MEFs.

Our previous studies showed that the conditional deletion of the *Tsg101* gene did not negatively affect the steady-state level of Mdm2 in primary fibroblasts (12). Similarly, the steady-state level of Mdm2 was not reduced but slightly elevated in *Cdkn2a*$^{+/-}$ or *Cdkn2*$^{-/-}$ MEFs lacking Tsg101

expression (Fig. 5B). We performed a flow cytometric analysis to study whether the loss of Tsg101 function was able to restore the G1 arrest in $p19^{Arf}$-deficient cells before they died (Fig. 5C). In addition, we used $p19^{Arf}$-deficient cells (*Tsg101*$^{fl/fl}$ *Cdkn2a* $^{-/-}$) deprived of essential growth factors (0.1% FBS) as a positive control to monitor the accumulation of cells at G1 and the relative decrease in the number of cells at the S phase of the cell cycle. Cells deficient in Tsg101 and $p19^{Arf}$ did not arrest at G1 and had approximately the same relative number of cells in S phase as MEFs lacking Tsg101 in addition to p53, and/or $p21^{Cip1}$ (see Fig. 2A and 3B; $P>0.05$).

To verify these findings in a different experimental setting, we immortalized *Tsg101*$^{fl/fl}$ MEFs and their wildtype controls by inhibiting the expression of $p19^{Arf}$ through overexpression of the T-box protein 2 (data not shown). Tbx2 is a known transcriptional repressor for the mouse and human *CDKN2A(ARF)* promoters (34). MEFs expressing Tbx2 exhibited reduced levels of $p19^{Arf}$ and $p21^{Cip1}$ at passages seven and eight. After Cre-mediated recombination of the floxed *Tsg101* locus, these immortalized cells died within seven days post-infection. The steady-state levels of Mdm2 did not decrease and $p21^{Cip1}$ protein expression levels remained low and unchanged in the Tsg101 knockout cells lacking functional $p19^{Arf}$ (data not shown). In summary, these results are consistent with our findings in Tsg101 knockout cells with a targeted deletion of the entire *Cdkn2a* locus. Therefore, Tsg101 deficiency seemed to not alter Mdm2 function in a biologically relevant manner that would influence the Mdm2/p53 negative feedback loop.

Transforming mutations during neoplastic transformation do not affect the important role of Tsg101 for cell survival

Li and Cohen (1996) reported that a functional knockout of *Tsg101* using a conventional antisense approach and inducible overexpression of *Tsg101* resulted in reversible neoplastic transformation of mouse 3T3 fibroblasts (16). Our published observations using a site-directed, targeted knockout in animal models and derived cell lines suggested that a loss-of-function of *Tsg101* is insufficient to trigger neoplastic transformation *in vitro* and *in vivo* (12, 13). Since *Tsg101* seems not to be a primary tumor suppressor, we hypothesized that this gene might function as a modifier for neoplastic transformation (12). Null or inactivating mutations in $p19^{Arf}$, p53, or $p21^{Cip1}$ are able to partially rescue the complex phenotype caused by Tsg101 deficiency (i.e. the G1/S progression), and it is therefore logical to test whether additional mutations during neoplastic transformation have an impact on the crucial role of Tsg101 as a survival factor in tumorigenic cells. Figure 6A illustrates our experimental design to address this issue. We previously described the generation of immortalized $Tsg101^{fl/fl}$ MEFs using a standard 3T3 protocol (12). These cells carry an E255D mutation in the DNA binding domain of p53, and consequently, the $p21^{Cip1}$ protein is not expressed. The deletion of *Tsg101* in this immortalized cell line resulted in instant cell death (12). The G1/S transition is, however, restored due to the lack of $p21^{Cip1}$. Hence, the phenotype of these cells relating to cell cycle regulation and cell death is equivalent to double-mutant MEFs with targeted deletions of *p53* and *Tsg101*.[4] Immortal $Tsg101^{fl/fl}$ 3T3 cells were passaged numerous times, infected with a pBabe-hygro retrovirus, and selected for hygromycin resistance. Next, $8x10^5$ cells were injected subcutaneously into Athymic nude mice (NCr strain) to select mutants that were able to grow *in vivo* and to form solid tumors. Tumorigenesis was observed in all animals after a medium latency of three to five weeks (Fig.

6B). Histopathologically, these lesions were well vascularized, and neoplastic cells invaded into adjacent normal tissues such as the fat pad of the thoracic mammary gland (Fig. 6C). Tumor cells were explanted and grown in culture in hygromycin-containing media to remove all nontumorigenic cell types such as endothelial cells, epithelial cells, and tumor-associated fibroblasts of the host. Next, neoplastic cells were infected with pBabe-Cre to excise both floxed copies of *Tsg101*. Infection of these cells with the control vector pBabe and selection with puromycin had little effect on their viability, whereas the deletion of *Tsg101* resulted in growth arrest and cell death (Fig. 6D and 6E). These data suggested that additional transforming mutations during neoplastic transformation did not rescue the lethal phenotype caused by Tsg101 deficiency, and therefore, Tsg101 might be important for the survival of both normal and neoplastic cells.

Discussion

Tsg101 deficiency and cellular stress response

We previously reported that Tsg101 is indispensable for the survival of cells *in vitro* and *in vivo* (12, 13). The collective data presented in this new report demonstrated that targeted mutations to abolish the function of $p19^{Arf}$, $p16^{Ink4a}$, p53, and $p21^{Cip1}$ were insufficient to maintain the survival of Tsg101 knockout cells. These observations suggest that the $p19^{Arf}$-Mdm2-p53 tumor surveillance or stress response pathway does not control cellular mechanisms that lead to the death of Tsg101-deficient cells. These results are in full agreement with our previous studies, in which we have demonstrated that the functional inhibition of p53, through expression of E6 or a spontaneous mutation within the DNA binding domain of p53, had no effect on the viability of Tsg101 knockout cells (12). By analyzing conventional knockout mice that die very early *in*

utero, Ruland et al. (11) established that Tsg101 is required for cell proliferation and that p53 is a crucial player for the replication defect of Tsg101-deficient cells. Using our conditional knockout model, we established that the deletion of *Tsg101* resulted in a sustained cell cycle arrest at the G1 checkpoint before these cells died (12). Based on the findings by Ruland et al. and due to the fact that Tsg101 conditional knockout cells lacked active Cdk2, we hypothesized that the p53 and its downstream mediator $p21^{Cip1}$ may, at least in part, contribute to the complex phenotype. We proposed that cell cycle arrest and cell death were controlled by separate, p53-dependent and p53-independent, pathways (13). In this report we show that, in contrast to mechanisms leading to cell death, the G1 arrest in Tsg101-deficient cells is dependent upon expression of functional p53. We also determined that $p21^{Cip1}$ is an integral part of this phenotype. Recent reports suggested a potential role for Tsg101 as a dominant-negative regulator for Mdm2 and $p21^{Cip1}$ protein turnover (17, 18). Evidently, Tsg101 cannot serve simultaneously as a stabilizer for both regulators of the cell cycle. According to the model by Li et al. (17) and Ruland et al. (11), functional levels of $p21^{Cip1}$ were required to mediate the cell cycle arrest. Tsg101 deficiency leads to destabilization of Mdm2, accumulation of active p53, and subsequently, the transcriptional activation of $p21^{Cip1}$. If Tsg101 is required for p21 stability or the recruitment of p21 to the Cyclin/Cdk2 complex as proposed by Oh and coworkers (18), then the combined effects of a Tsg101 knockout on Mdm2 and $p21^{Cip1}$ should nullify each other.

The overexpression of Tsg101 or its conditional deletion results in a G1 arrest and cell death, suggesting that the level of Tsg101 protein in a given cell is tightly regulated and that a high or low amount of Tsg101 outside a narrow range cannot be tolerated (9, 10, 12, 13, 35, 36). Interestingly, $p21^{Cip1}$ seems to be a key player for the G1 arrests not only in the overexpression

model (18) but also the conditional knockout. As demonstrated in this report, a knockout of the *Cdkn1a* gene ($p21^{Cip1}$) eliminated the G1 arrest and restored the G1/S progression of Tsg101-deficient cells. Based on the fact that $p21^{Cip1}$ levels did not change in the Tsg101 conditional knockout [(12), and Fig. 2B, lanes 2 and 3 and Fig. 3A, lanes 5 and 6 in this article], we presume that Tsg101 deficiency leads directly to cellular conditions where p21's ability to bind to the Cdk2 is elevated. The pathways that link the function of Tsg101 and $p21^{Cip1}$ need to be identified. There is increasing evidence in the recent literature that Tsg101 is essential for endosomal trafficking and other cellular processes in addition to the regulation of ubiquitination (5-8). It is, therefore, very likely that Tsg101 deficiency or its overexpression will cause a severe negative impact on a number of biological processes. Those might subsequently trigger the activation of cellular stress responses such as the recruitment of $p21^{Cip1}$ to the Cdk2 complex to arrest cells in the G1 phase. Ruland et al. (11) suggested that p53 is the upstream regulator of $p21^{Cip1}$, which mediates the cell cycle arrest in Tsg101 deficient cells. Based on data by Li et al (17), the authors proposed a direct interaction of Tsg101 with members of the p53 stress response pathway, in particular Mdm2. In the conditional knockout model we were, however, unable to detect higher levels of p53 or changes in the p53 transcriptional activation of $p21^{Cip1}$ (12). Moreover, we questioned the suggested role of Tsg101 as a positive regulator for Mdm2 function based on the evidence that *Tsg101/p53* double mutant mice still die early *in utero* (11), whereas p53 deficiency results in a complete rescue of embryonic lethality in *Mdm2* knockout mice (31, 32). To rigorously examine the proposed function of Tsg101 as a stabilizer for Mdm2, we generated cells lacking Tsg101 and $p19^{Arf}$. The functional inhibition of $p19^{Arf}$ leads to increased Mdm2-mediated sequestration of p53 and immortalization (20). We utilized the complete deletion of the *Cdkn2a* locus and the Tbx2-mediated transcriptional repression of

$p19^{Arf}$ as two alternative approaches to immortalize MEFs carrying two conditional *Tsg101* knockout alleles. In both model systems, the deletion of *Tsg101* had no effect on Mdm2 steady-state levels and function. In particular, the p53-mediated transcriptional activation of $p21^{Cip1}$ and induction of a G1 arrest was not restored. In addition, we were unable to co-precipitate Mdm2 with endogenous Tsg101 or transgenic HA-tagged Tsg101 expressed at near physiological levels[5] suggesting that under normal conditions these proteins show weak or no interaction. In summary, results obtained from three double knockout models (*Tsg101/p53*, *Tsg101/p21*, and *Tsg101/*$p19^{Arf}$) suggest that a direct interaction of Tsg101 with members of the Mdm2-p53 circuit is unlikely. We propose that the activation of a $p21^{Cip1}$-mediated G1 arrest might be an indirect effect of Tsg101 deficiency on other cellular processes that subsequently trigger stress response pathways.

Normal Tsg101 function is crucial for the survival of primary, immortalized, and neoplastic cells.

The role of the *TSG101* gene as a tumor suppressor or oncogene in human malignancies is still controversial. After cloning the mouse *Tsg101* locus and revising the human *TSG101* gene structure, we found that many of the previously described aberrant splice variants in human malignancies represent alternative splice forms that originate solely from exon skipping (35, 37). While the transforming capability of *Tsg101* as an oncogene has not been examined in an animal model to date, we and others could show that neither haploinsufficiency of *Tsg101* (11, 13) nor the deletion of both *Tsg101* alleles in selected cell types of conditional knockout mice resulted in tumorigenesis (12, 13). In contrast to a previous report (16), we demonstrated that a null mutation of *Tsg101* is not an initiating event for neoplastic transformation of primary cells (12,

13). Therefore, we hypothesized that this gene might function as a modifier for tumorigenesis (12). This earlier assumption was based on the fact that the role of Tsg101 in neoplastic transformation was initially established in immortalized 3T3 cells (16). In preliminary studies, we could show that these cells lacked expression of other important tumor suppressor proteins, in particular $p19^{Arf}$ and $p16^{Ink4a}$ (see Fig. 5 in this report). As discussed above, Tsg101 was also suggested to be a crucial regulator of the Mdm2-p53 circuit and $p21^{Cip1}$. In contrast to our earlier working hypothesis, we can demonstrate in this study that none of the immortalizing mutations (i.e. knockout of $p19^{Arf}$, $p16^{Ink4a}$, p53, and/or $p21^{Cip1}$) or additional sporadic mutations causing neoplastic transformation and tumorigenesis had an impact on the important role of Tsg101 for cell survival. In agreement with these findings in primary cell cultures, the deletion of the *p53* gene in *Tsg101* mammary-specific knockout mice (WAP-Cre $Tsg101^{fl/fl}$ $p53^{-/-}$) did not rescue the survival of Tsg101-deficient epithelial cells. More importantly, haploinsufficiency of *p53* in the Tsg101 somatic knockout model did not cause mammary tumorigenesis in 12-month-old animals. Unlike in our *Brca1* mammary-specific knockout mice (38), the deletion of *Tsg101* in *p53* heterozygous mutants (WAP-Cre $Tsg101^{fl/fl}$ $p53^{+/-}$) seemed not to cause genomic alterations that lead to the loss-of-heterozygosity of the wildtype *p53* allele and neoplastic transformation.[6] Mammary tumors were also not observed in females carrying two mutant *p53* alleles (WAP-Cre $Tsg101^{fl/fl}$ $p53^{-/-}$). Like *p53* single knockout mice, they succumbed to lymphoma after a latency period of approximately six months. Finally, we have confirmed the importance of Tsg101 as a survival factor for tumorigenic cells in a murine cancer model that carries an MMTV-driven Her2/neu oncogene (39) in addition to the somatic knockout of *Tsg101* (MMTV-neu WAP-Cre $Tsg101^{fl/fl}$). In this animal model, the deletion of *Tsg101* did not accelerate but delayed neoplastic transformation.[7] In conclusion to the data presented in this study, we propose that Tsg101 is an

important factor for cell survival in normal, immortalized, and neoplastic cells. Since Tsg101 is essential for cell survival, being able to target tumor cells and inhibit Tsg101 function should result in the death of neoplastic cells regardless of the functional inactivation of the Mdm2-p53 circuit or sporadic mutations in the p53, $p19^{Arf}$, or $p16^{Ink4a}$ tumor susceptibility loci.

Acknowledgements

The authors thank MaLinda D. Henry for technical assistance and animal husbandry. We also thank Charles Kuszynski and Linda Wilkie of the UNMC Flow Cytometry Facility for the cell cycle analysis and Joerg Rahnenfuehrer (UC Berkeley) for his help in the evaluation of the MTT assay. We are grateful to Dr. Alan Diehl (University of Pennsylvania) for reading this manuscript and his valuable suggestions. This work was supported by a Public Health Service grant CA93797 from the National Cancer Institute to K.U.W.. M.J.C. receives a stipend from the Department of Defense (DAMD17-00-1-0361). A.K. was supported by the Deutsche Forschungsgemeinschaft (DFG, KR 2107/1-1).

References

1. Koonin, E. V. and Abagyan, R. A. (1997) *Nat.Genet.* **16,** 330-331
2. Ponting, C. P., Cai, Y. D., and Bork, P. (1997) *J.Mol.Med.* **75,** 467-469
3. Watanabe, M., Yanagi, Y., Masuhiro, Y., Yano, T., Yoshikawa, H., Yanagisawa, J., and Kato, S. (1998) *Biochem.Biophys.Res.Commun.* **245,** 900-905
4. Hittelman, A. B., Burakov, D., Iniguez-Lluhi, J. A., Freedman, L. P., and Garabedian, M. J. (1999) *EMBO J.* **18,** 5380-5388
5. Babst, M., Odorizzi, G., Estepa, E. J., and Emr, S. D. (2000) *Traffic* **1,** 248-258

6. Garrus, J. E., von Schwedler, U. K., Pornillos, O. W., Morham, S. G., Zavitz, K. H., Wang, H. E., Wettstein, D. A., Stray, K. M., Cote, M., Rich, R. L., Myszka, D. G., and Sundquist, W. I. (2001) *Cell* **107,** 55-65

7. Lu, Q., Hope, L. W., Brasch, M., Reinhard, C., and Cohen, S. N. (2003) *Proc.Natl.Acad.Sci.U.S.A* **100,** 7626-7631

8. Bache, K. G., Brech, A., Mehlum, A., and Stenmark, H. (2003) *J.Cell Biol.* **162,** 435-442

9. Zhong, Q., Chen, Y., Jones, D., and Lee, W. H. (1998) *Cancer Res.* **58,** 2699-2702

10. Xie, W., Li, L., and Cohen, S. N. (1998) *Proc.Natl.Acad.Sci.U.S.A.* **95,** 1595-1600

11. Ruland, J., Sirard, C., Elia, A., MacPherson, D., Wakeham, A., Li, L., Luis, D. L. P., Cohen, S. N., and Mak, T. W. (2001) *Proc.Natl.Acad.Sci.U.S.A* **98,** 1859-1864

12. Krempler, A., Henry, M. D., Triplett, A. A., and Wagner, K. U. (2002) *J.Biol.Chem.* **277,** 43216-43223

13. Wagner, K. U., Krempler, A., Qi, Y., Park, K., Henry, M. D., Triplett, A. A., Riedlinger, G., Rucker III, E. B., and Hennighausen, L. (2003) *Mol.Cell Biol.* **23,** 150-162

14. Maucuer, A., Camonis, J. H., and Sobel, A. (1995) *Proc.Natl.Acad.Sci.U.S.A.* **92,** 3100-3104

15. Sun, Z., Pan, J., Hope, W. X., Cohen, S. N., and Balk, S. P. (1999) *Cancer* **86,** 689-696

16. Li, L. and Cohen, S. N. (1996) *Cell* **85,** 319-329

17. Li, L., Liao, J., Ruland, J., Mak, T. W., and Cohen, S. N. (2001) *Proc.Natl.Acad.Sci.U.S.A* **98,** 1619-1624

18. Oh, H., Mammucari, C., Nenci, A., Cabodi, S., Cohen, S. N., and Dotto, G. P. (2002) *Proc.Natl.Acad.Sci.U.S.A* **99,** 5430-5435

19. Li, L., Li, X., Francke, U., and Cohen, S. N. (1997) *Cell* **88,** 143-154

20. Sherr, C. J. (1998) *Genes Dev.* **12,** 2984-2991

21. Wagner, K. U., Wall, R. J., St-Onge, L., Gruss, P., Wynshaw-Boris, A., Garrett, L., Li, M., Furth, P. A., and Hennighausen, L. (1997) *Nucleic.Acids.Res.* **25,** 4323-4330

22. Donehower, L. A., Harvey, M., Slagle, B. L., McArthur, M. J., Montgomery, C. A., Jr., Butel, J. S., and Bradley, A. (1992) *Nature* **356,** 215-221

23. Brugarolas, J., Chandrasekaran, C., Gordon, J. I., Beach, D., Jacks, T., and Hannon, G. J. (1995) *Nature* **377,** 552-557

24. Serrano, M., Lee, H., Chin, L., Cordon-Cardo, C., Beach, D., and DePinho, R. A. (1996) *Cell* **85,** 27-37

25. Wagner, K. U., Boulanger, C. A., Henry, M. D., Sgagias, M., Hennighausen, L., and Smith, G. H. (2002) *Development* **129,** 1377-1386

26. Telford, W. G., King, L. E., and Fraker, P. J. (1991) *Cell Prolif.* **24,** 447-459

27. van de Loosdrecht, A. A., Beelen, R. H., Ossenkoppele, G. J., Broekhoven, M. G., and Langenhuijsen, M. M. (1994) *J.Immunol.Methods* **174,** 311-320

28. el Deiry, W. S., Tokino, T., Velculescu, V. E., Levy, D. B., Parsons, R., Trent, J. M., Lin, D., Mercer, W. E., Kinzler, K. W., and Vogelstein, B. (1993) *Cell* **75,** 817-825

29. Xiong, Y., Hannon, G. J., Zhang, H., Casso, D., Kobayashi, R., and Beach, D. (1993) *Nature* **366,** 701-704

30. Sherr, C. J. and Roberts, J. M. (1999) *Genes Dev.* **13,** 1501-1512

31. Jones, S. N., Roe, A. E., Donehower, L. A., and Bradley, A. (1995) *Nature* **378,** 206-208

32. Montes de Oca, L. R., Wagner, D. S., and Lozano, G. (1995) *Nature* **378,** 203-206

33. Weber, J. D., Jeffers, J. R., Rehg, J. E., Randle, D. H., Lozano, G., Roussel, M. F., Sherr, C. J., and Zambetti, G. P. (2000) *Genes Dev.* **14,** 2358-2365

34. Jacobs, J. J., Keblusek, P., Robanus-Maandag, E., Kristel, P., Lingbeek, M., Nederlof, P. M., van Welsem, T., van de Vijver, M. J., Koh, E. Y., Daley, G. Q., and van Lohuizen, M. (2000) *Nat.Genet.* **26,** 291-299

35. Wagner, K. U., Dierisseau, P., Rucker, E. B., Robinson, G. W., and Hennighausen, L. (1998) *Oncogene* **17,** 2761-2770

36. Feng, G. H., Lih, C. J., and Cohen, S. N. (2000) *Cancer Res.* **60,** 1736-1741

37. Wagner, K. U., Dierisseau, P., and Hennighausen, L. (1999) *Cytogenet.Cell Genet.* **84,** 87-88

38. Xu, X., Wagner, K. U., Larson, D., Weaver, Z., Li, C., Ried, T., Hennighausen, L., Wynshaw-Boris, A., and Deng, C. X. (1999) *Nat.Genet.* **22,** 37-43

39. Guy, C. T., Webster, M. A., Schaller, M., Parsons, T. J., Cardiff, R. D., and Muller, W. J. (1992) *Proc.Natl.Acad.Sci.U.S.A* **89,** 10578-10582

Footnotes:

[1] The following abbreviations were used: WAP, whey acidic protein; Cre, site-specific recombinase in bacteriophage P1 (catalyses recombination between *lox*P sites); loxP, locus of X-ing over; PGK-neo, phosphogylcerine kinase–neomycin;Tbx2, T-box protein 2; Mdm2, transformed mouse 3T3 double minute 2 protein; PCR, polymerase chain reaction; MEF, mouse embryonic fibroblasts; MTT, 3-(4,5-dimethylthiazol-2-yl)-2,5-diphenyltetrazolium bromide; Cdk2, cyclin-dependent kinase 2; DMEM, Dulbecco's modified Eagle's medium; PBS, phosphate buffered saline; PMSF, phenylmethylsulfonyl fluoride; SDS, sodium dodecyl sulfate; EDTA, ethylenediaminetetraacetic acid; PAGE, polyacrylamide gel electrophoresis; PVDF, polyvinylidene fluoride; TBS, tris buffered saline; HRP, horse raddish peroxidase; ECL, enhanced chemiluminescence; FBS, fetal bovine serum; MEC, mammary epithelial cells; HA, heamagglutinin; MOI, multiplicity of infection; AdCre, adenoviral vector expressing Cre recombinase, FACS, fluorescene activated cell sorting; HPV-E6, human papilloma virus E6; Her2/neu; Erbb2, member of the epidermal growth factor receptor family; MMTV, mouse mammary tumor virus; GFP, green fluorescent protein

[2] personal communications with C. Eischen (University of Nebraska Medical Center), J. Weber (Washington University), and G. Zambetti (St. Judes Children's Research Hospital)

[3] J Jacobs and M. van Lohuizen (The Netherlands Cancer Institute), personal communication

[4] A. Krempler and K.-U. Wagner, unpublished

[5] A. Krempler, A. A. Triplett and K.-U.Wagner, unpublished

[6] A. Krempler, A. A. Triplett and K.-U.Wagner, unpublished

[7] manuscript in preparation

Figure Legends

Fig. 1: p53 deficiency does not rescue cell death in the Tsg101 conditional knockout. A. *In vitro* analysis: MTT color assay to determine growth rates of pBabe and pBabe-Cre infected *Tsg101*$^{fl/fl}$ MEFs that lack one or two alleles of the *p53* gene (p53$^{+/-}$ and p53$^{-/-}$) and their wildtype controls (p53$^{+/+}$). The OD_{570nm} values that correspond to total cell numbers decrease in the Tsg101 knockout (*Tsg101*$^{fl/fl}$ pBabe-Cre) between four and seven days after retroviral Cre infection regardless of the *p53* mutation status. In contrast, the number of cells in the pBabe infected controls increase steadily. Error bars correspond to standard deviations. **B.** *In vivo* analysis: Whole mounts of carmine alum-stained mammary glands from tissue-specific Tsg101 knockout mice (WAP-Cre *Tsg101*$^{fl/fl}$ *p53*$^{+/+}$), females that are conditionally deficient in both, Tsg101 and p53 (WAP-Cre *Tsg101*$^{fl/fl}$ *p53*$^{-/-}$), and their controls (*Tsg101*$^{fl/fl}$ *p53*$^{+/+}$). Mammary glands were taken, fixed, and stained several hours *post-partum* (magnification 40x). Note that alveolargenesis is severely impaired in the Tsg101 conditional knockouts, regardless of whether p53 is expressed or not.

Fig. 2: A p53 null mutation restores G1/S progression and the activity of Cdk2 in Tsg101-deficient cells. A. Flow cytometric analysis of the DNA content of viable Tsg101-deficient MEFs (*Tsg101*$^{fl/fl}$, pBabe-Cre) that lack one or two alleles of the *p53* gene (p53$^{+/-}$ and p53$^{-/-}$) and their uninfected controls (*Tsg101*$^{fl/fl}$ *p53*$^{-/-}$). The sub-G1 population of apoptotic cells was gated out in this assay. Note that the relative number of cells in S-phase is reduced only in p53 heterozygous knockout cells lacking Tsg101 but not in Tsg101-deficient MEFs carrying two mutant p53 alleles. **B.** Western blot analysis of cyclin A (S-phase cyclin) and regulators of G1/S progression (p19^{Arf} and p21^{Cip}) in Tsg101-deficient MEFs that lack one or two

copies of *p53* and their uninfected controls. Note that cyclin A2 was markedly downregulated in Tsg101-deficient MEFs that carry at least one functional allele of *p53*. Immortal p53/p21^{Cip1}-deficient MEFs express high levels of cyclin A2 and p19^{Arf} regardless of the *Tsg101* mutation status. **C.** Cyclin dependent kinase 2 (Cdk2) activity assay using Histone H1 as a substrate for phosphorylation. Only *Tsg101* knockout MEFs that carry at least one functional p53 allele exhibit a reduced activity of Cdk2. The complete deletion of *p53* and, subsequently, the absence of the Cdk2 inhibitor p21^{Cip1} restore a normal activity of Cdk2 in Tsg101-deficient cells.

Fig. 3: p21^{Cip1} is a mediator of the cell cycle block at the G1 checkpoint in Tsg101 conditional knockout cells. **A.** Western blot analysis of Tsg101 and p21^{Cip1} to monitor effective Cre-mediated excision and downregulation of Tsg101 in MEFs lacking one or two copies of *the Cdkn1a* gene and their controls. **B.** Flow cytometric analysis of the DNA content in cells doubly deficient in Tsg101 and p21^{Cip1} (*Tsg101$^{fl/fl}$ p21$^{-/-}$* pBabe-Cre) and their controls. The sub-G1 population of apoptotic cells was gated out in this assay. Note that the relative number of cells in S-phase is normal in Tsg101-deficient MEFs carrying two mutant *Cdkn1a* alleles compared to their controls ($P>0.05$).

Fig. 4: The p19^{Arf}-p53 tumor surveillance and stress response pathway and its proposed interaction with Tsg101. **A.** Mdm2 is negatively regulated by p19^{Arf}. As a ubiquitin ligase, Mdm2 regulates the ubiquitin-mediated degradation of the tumor suppressor protein p53. Therefore, p19^{Arf}-deficient cells are immortal and lack expression of p53 and p21^{Cip1}. In normal cells, p21^{Cip1} is transcriptionally regulated by p53. It has been suggested recently that

Tsg101 is a positive regulator for Mdm2 protein levels and function. Therefore, the deletion of the *Tsg101* gene (right panel) should destabilize Mdm2 and induce a p53/p21^{Cip1}-mediated G1 arrest in cells lacking p19^{Arf}. **B.** Experimental design to study the proposed interaction of Tsg101 with Mdm2/p53 in immortalized cells lacking p19^{Arf}. The Cre-mediated deletion of *Tsg101* in *Cdkn2a*$^{-/-}$ immortalized cells should have a biologically relevant effect on Mdm2 and p53 protein levels and restore the cell cycle arrest.

Fig. 5: Cell cycle regulation in immortal cells that lack *Cdkn2a* and *Tsg101*. **A.** The tumorigenic, Tsg101-antisense-expressing SL6 cell line and its parental mouse 3T3 fibroblast cell line lack expression of p19^{Arf} and p16^{Ink4a}. *Cdkn2a*-deficient cells were used as negative controls, and immortal *p53*$^{-/-}$ MEFs served as positive controls for p19^{Arf} and p16^{Ink4a} protein expression. **B.** Western blot analysis of Tsg101 and Cdkn2a to monitor effective Cre-mediated downregulation of Tsg101 in MEFs lacking one or two copies of *the Cdkn2a* gene and their controls. The steady-state levels of Mdm2 did not decrease and where slightly elevated in cells lacking Tsg101. **C.** Flow cytometric analysis of the DNA content in cells doubly deficient in Tsg101 and p19^{Arf} (*Tsg101*$^{fl/fl}$ *Cdkn2a*$^{-/-}$ pBabe-Cre) and their controls. The sub-G1 population of apoptotic cells was gated out in this assay. P19^{Arf}-deficient cells deprived of essential growth factors (*Tsg101*$^{fl/fl}$ *Cdkn2a* $^{-/-}$ 0.1% FBS) served as an additional positive control to monitor the accumulation of cells at G1 and the relative decrease in the number of cells at the S-phase of the cell cycle. Note that the deletion of *Tsg101* in a p19^{Arf}-deficient background does not cause a cell cycle arrest, whereas growth factor withdrawal from these cells results in a sharp reduction of cells in S phase.

Fig. 6: Tsg101 deficiency causes cell death of tumorigenic cells. **A.** Experimental design to address whether *Tsg101* is dispensable or essential for the survival of neoplastic cells. **B.** The subcutaneous injection of immortal $Tsg101^{fl/fl}$ 3T3 fibroblasts expressing mutant p53 into $whn^{-/-}$ nude mice (NCr strain) form solid tumors. **C.** H&E staining of histological sections from solid tumors (magnification 100x). Note that these lesions are highly vascularized, and tumor cells invade into adjacent normal tissues. V vasculature; NT necrotic tumor tissue; MG mammary gland, M muscle. **D.** Explanted tumor cells carrying two floxed alleles of Tsg101 ($Tsg101^{fl/fl}$) infected with pBabe (control) or the pBabe-Cre retroviral vector to excise both copies of *Tsg101* (magnification 200x). Note that additional, transforming mutations during neoplastic transformation are incapable of rescuing lethality caused by Tsg101 deficiency. **E.** MTT color assay to quantify the lack of cell growth of tumor cells lacking *Tsg101* compared to their controls. Error bars correspond to standard deviations.

Fig. 1 Carstens et al.

A

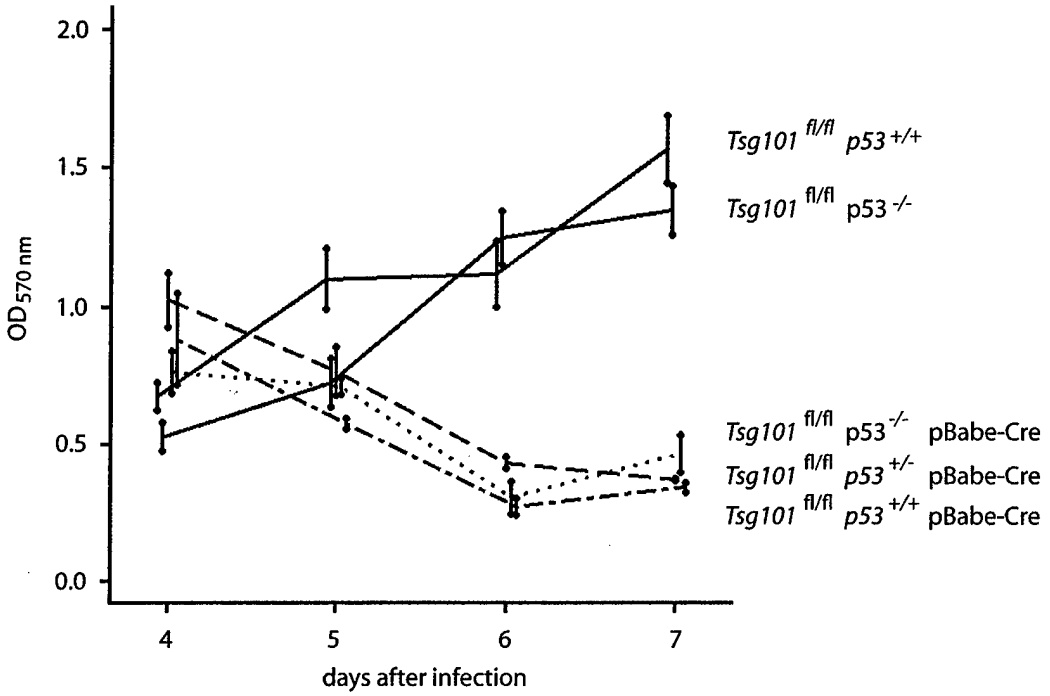

B

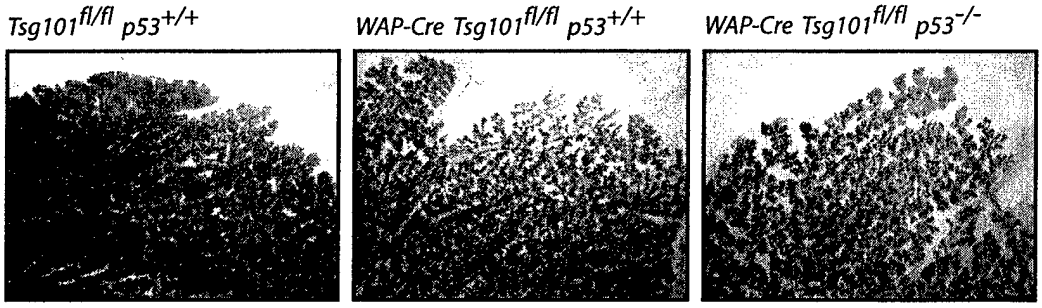

Fig. 2 Carstens et al.

A

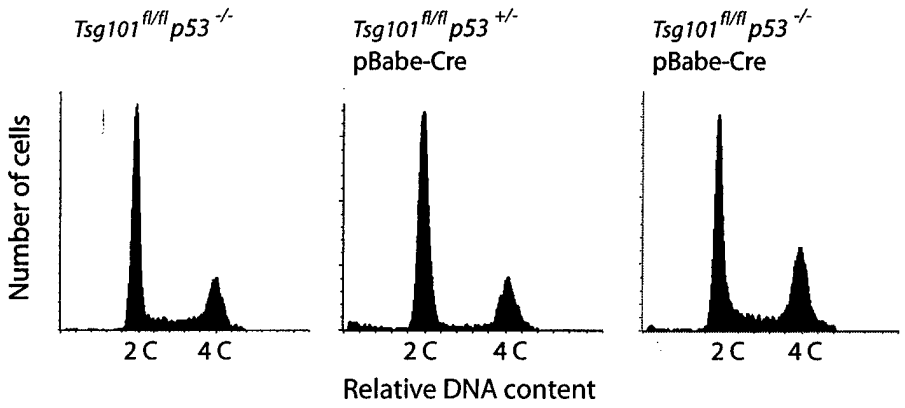

Genotype	G0/G1	S-Phase	G2/M
Tsg101$^{fl/fl}$ *p53*$^{-/-}$ no virus	60.8 (±5.0) %	18.5 (±3.4) %	20.7 (±3.0) %
Tsg101$^{fl/fl}$ *p53*$^{+/-}$ pBabe-Cre	63.8 (±9.9) %	6.8 (±1.5) %*	29.4 (±9.8) %
Tsg101$^{fl/fl}$ *p53*$^{-/-}$ pBabe-Cre	53.2 (±5.8) %	16.6 (±6.6) %*	30.2 (±3.5) %

* P<0.02

B

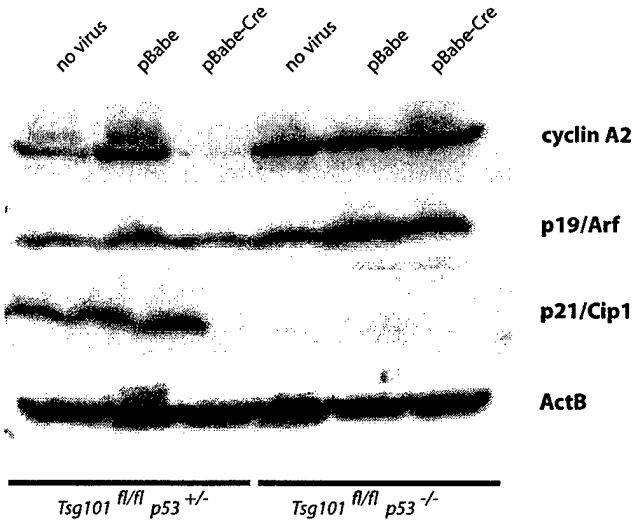

C

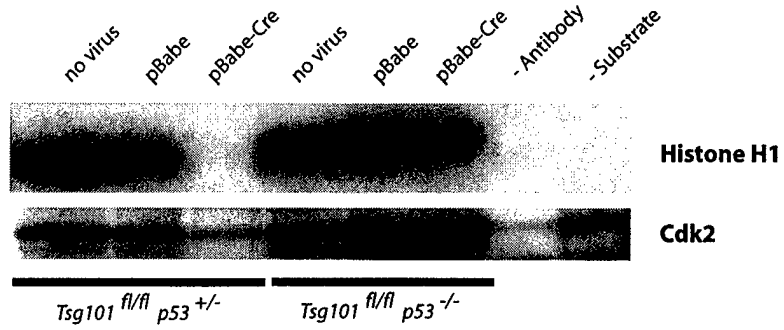

Fig. 3 Carstens et al.

A

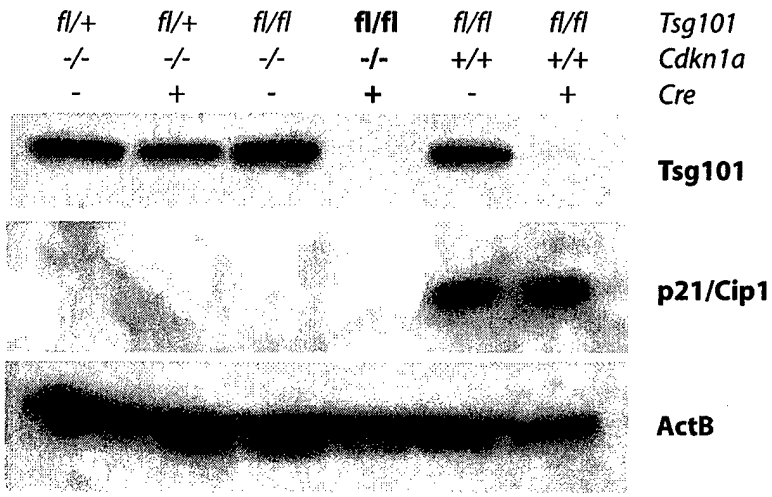

B

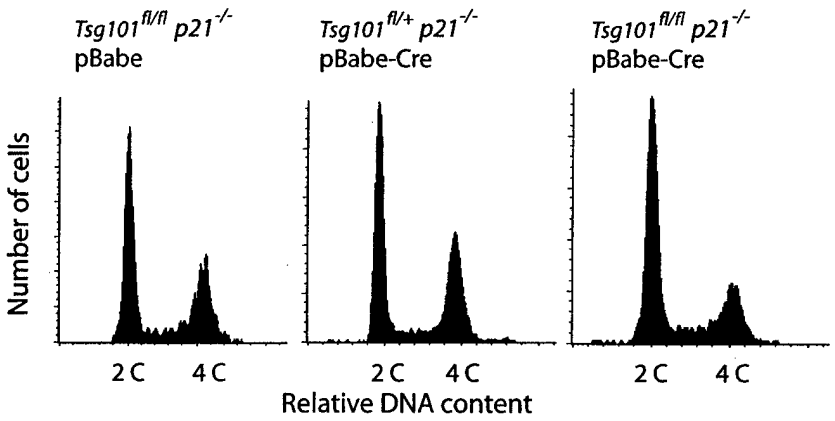

Genotype	G0/G1	S-Phase	G2/M
Tsg101$^{fl/fl}$ *p21*$^{-/-}$ pBabe	39.7 (±6.7) %	20.8 (±2.4) %	39.5 (±5.2) %
Tsg101$^{fl/+}$ *p21*$^{-/-}$ pBabe-Cre	59.6 (±9.1) %	18.4 (±3.5) %	22.0 (±9.5) %
Tsg101$^{fl/fl}$ *p21*$^{-/-}$ pBabe-Cre	45.7 (±7.9) %	22.4(±3.0) %	31.9 (±7.1) %

Fig. 4 Carstens et al.

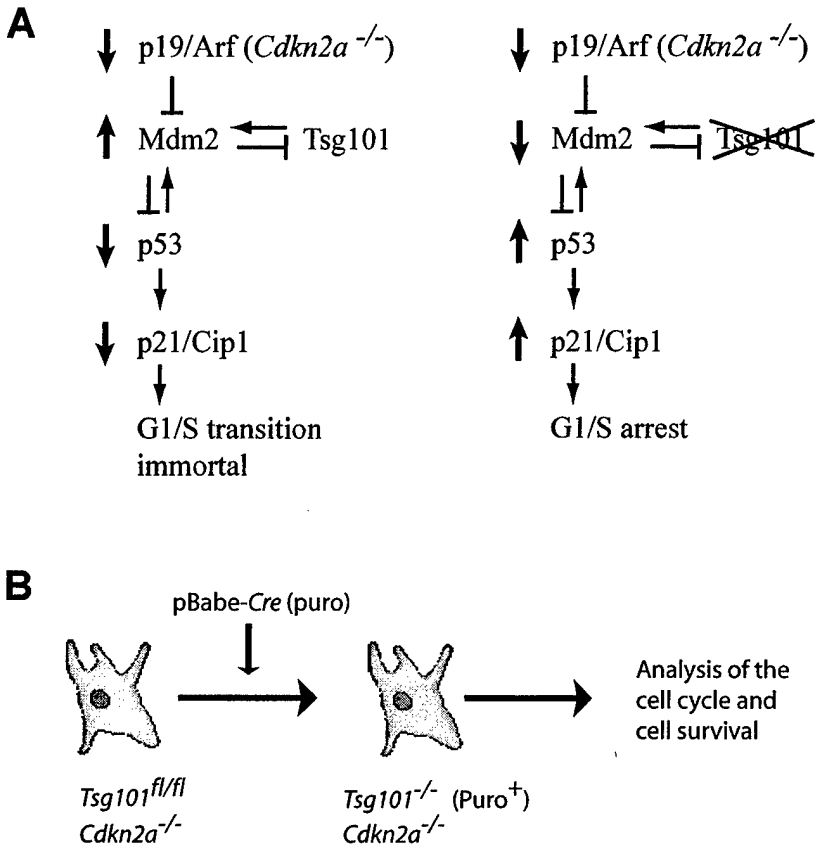

Fig. 5 Carstens et al.

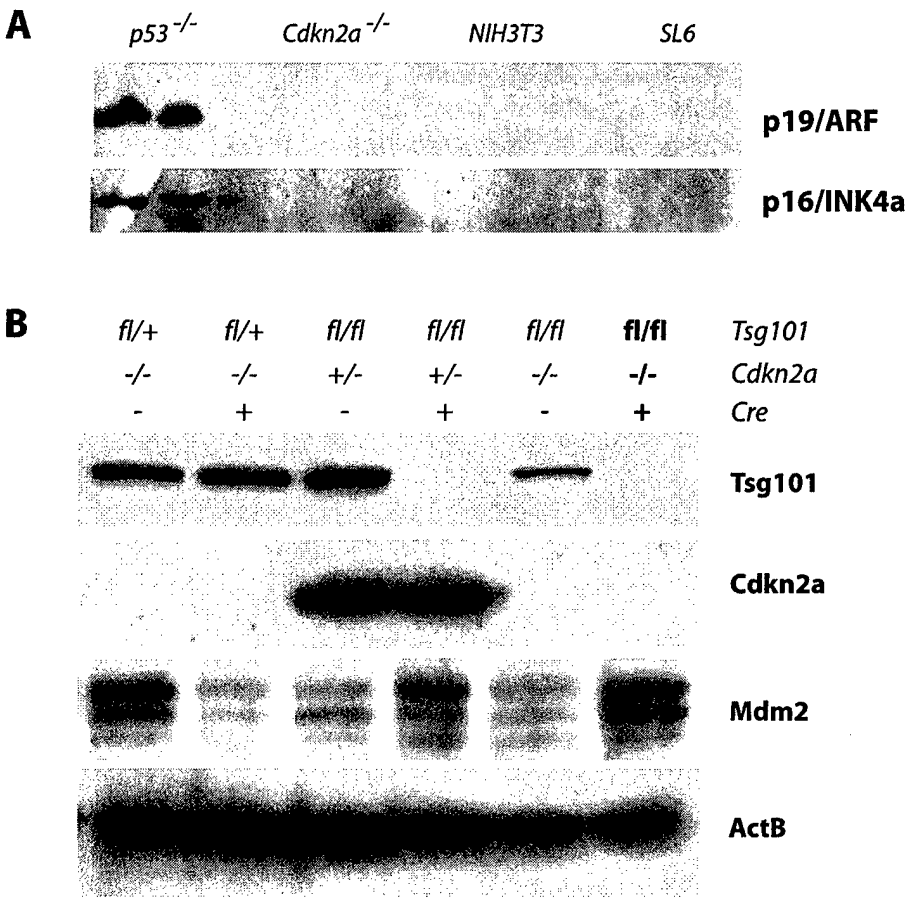

Genotype	G0/G1	S-Phase	G2/M
Tsg101 $^{fl/fl}$ *Cdkn2a* $^{-/-}$ pBabe	56.2 (±8.4) %	26.9 (±2.7) %*	16.9 (±7.3) %
Tsg101 $^{fl/fl}$ *Cdkn2a* $^{-/-}$ pBabe-Cre	56.7 (±7.6) %	20.6 (±3.2) %*	22.7 (±9.5) %
Tsg101 $^{fl/fl}$ *Cdkn2a* $^{-/-}$ 0.1% FBS	85.6 (±1.6) %	6.1 (±1.2) %	8.3 (±2.6) %

* P>0.05

Fig. 6 Carstens et al.

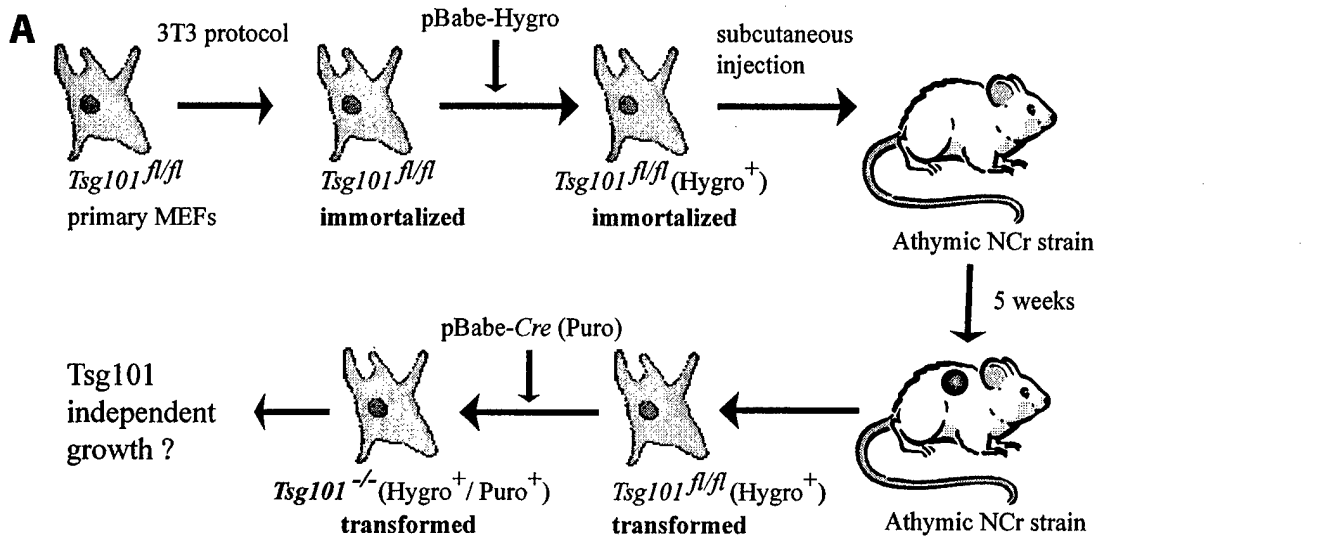

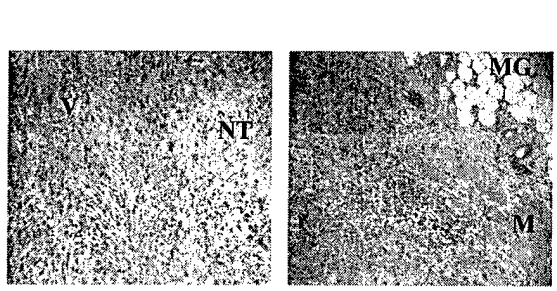

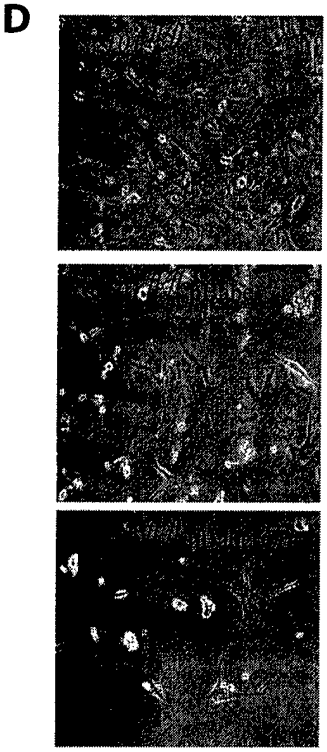

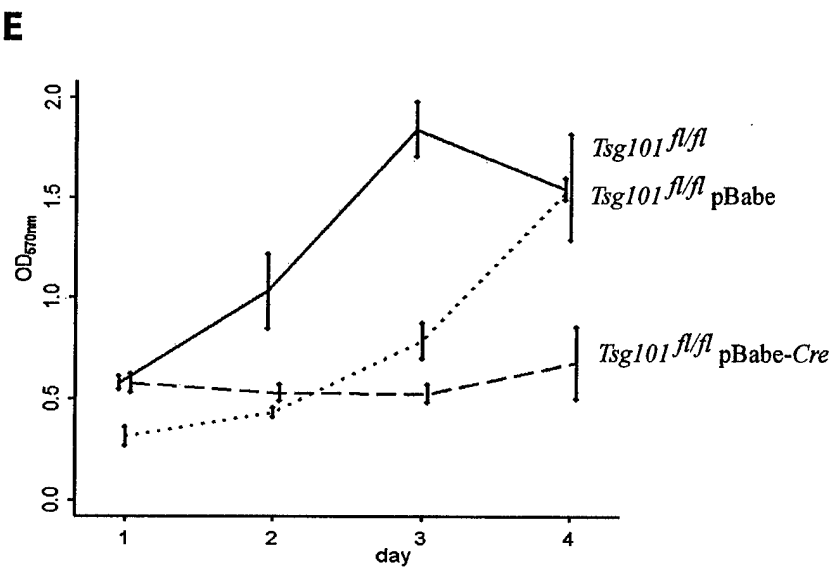

Genetic Bases of Estrogen-Induced Pituitary Tumorigenesis: Identification of Genetic Loci Determining Estrogen-Induced Pituitary Growth in Reciprocal Crosses between the ACI and Copenhagen Rat Strains

Tracy E. Strecker*,†, Thomas J. Spady*,†, Amy E. Kaufman*, Fangchen Shen*, Mac T. McLaughlin*, Karen L. Pennington*,**, Jane L. Meza‡, Beverly S. Schaffer*,**, Karen A. Gould*,**, and James D. Shull*,†,§,**

*Eppley Institute for Research in Cancer, †Department of Biochemistry and Molecular Biology, ‡Department of Preventive and Societal Medicine, §Department of Pathology and Microbiology, ** Department of Genetics, Cell Biology and Anatomy, University of Nebraska Medical Center, Omaha, Nebraska 58198-5805.

Running Title: Genetics of Pituitary Tumorigenesis

Key words: ACI rat, Copenhagen rat, estrogen, diethylstilbestrol, pituitary, lactotroph

Address correspondence to: Dr. James D. Shull, Department of Genetics, Cell Biology and Anatomy, 6005 Durham Research Center, 985805 Nebraska Medical Center, Omaha, NE 68198-5805. Phone: (402) 559-4633. Fax: (402) 559-7328. Email: jshull@unmc.edu.

ABSTRACT

Estrogens stimulate proliferation and enhance survival of the prolactin (PRL)-producing lactotroph of the anterior pituitary gland and induce development of PRL-producing pituitary tumors in certain inbred rat strains but not others. The goal of this study was to elucidate the genetic bases of estrogen-induced pituitary tumorigenesis in reciprocal intercrosses between the genetically related ACI and Copenhagen (COP) rat strains. Following 12 weeks of treatment with the synthetic estrogen diethylstilbestrol (DES), pituitary mass, an accurate surrogate marker of absolute lactotroph number, was increased 10.6-fold in ACI rats and 4.5-fold in COP rats. Linkage analysis of phenotypically defined F_2 progeny from reciprocal crosses between the ACI and COP strains identified six loci that determine the pituitary growth response to DES. These loci reside on chromosome 6, *Ept1* (*Estrogen-induced pituitary tumor*); chromosome 3, *Ept2* and *Ept6*; chromosome 10, *Ept9*; and chromosome 1, *Ept10* and *Ept13*. Together, these loci and two additional suggestive loci on chromosomes 4 and 5, account for approximately 48% of the phenotypic variance exhibited by the F_2 population, while 34% of the phenotypic variance was estimated to result from environmental factors. These data indicate that DES-induced pituitary mass behaves as a quantitative genetic trait and provide information that will facilitate identification of genes that determine the tumorigenic response of the pituitary gland to estrogens.

INTRODUCTION

Estrogens play a central role in the regulation of cell proliferation and survival in numerous mammalian tissues and are implicated in the etiology of several types of cancer (SHULL 2002). The prolactin (PRL)-producing lactotroph of the anterior pituitary gland provides a well-defined cell model for studying estrogen action. It is well established that estrogens enhance transcription of the PRL gene, stimulate lactotroph proliferation and promote lactotroph survival (SPADY *et al.* 1999b). Continuous treatment with either naturally occurring or synthetic estrogens induces rapid and sustained growth of the anterior pituitary gland in male or female rats of the Fischer 344 (F344) (SEGALOFF and DUNNING 1945; WIKLUND *et al.* 1981a; WIKLUND *et al.* 1981b; WIKLUND and GORSKI 1982), ACI (SEGALOFF and DUNNING 1945; HOLTZMAN *et al.* 1979; SHULL *et al.* 1997; SPADY *et al.* 1999c; SPADY *et al.* 1999d), Copenhagen (COP) (SPADY *et al.* 1998a; SPADY *et al.* 1999d) and several other inbred rat strains (NOBLE *et al.* 1940; FURTH *et al.* 1973; SPADY *et al.* 1999b). The grossly enlarged pituitary glands, commonly referred to as pituitary tumors, exhibit diffuse lactotroph hyperplasia histologically and result in marked hyperprolactinemia (SPADY *et al.* 1998b; SPADY *et al.* 1999b; SPADY *et al.* 1999c). In contrast, continuous estrogen treatment induces very little pituitary growth in other rat strains, such as the outbred Holtzman strain (WIKLUND *et al.* 1981b; WIKLUND and GORSKI 1982) or the inbred Brown Norway (BN) strain (WENDELL *et al.* 1996; WENDELL and GORSKI 1997; SPADY *et al.* 1999d).

The genetic bases of sensitivity of the F344 rat strain to estrogen-induced pituitary tumors have been investigated in crosses to the insensitive Holtzman and BN strains. Following 8 weeks of treatment with the synthetic estrogen diethylstilbestrol (DES), average pituitary mass

was increased 7.8-fold in female F344 rats but was unaffected in female Holtzman rats (WIKLUND *et al.* 1981a). Average pituitary mass was increased 1.8- and 2.2-fold in DES treated (Holtzman x F344)F_1 and (F344 x Holtzman)F_1 rats, respectively, suggesting that sensitivity to DES-induced pituitary growth is recessive or incompletely dominant in these crosses. More recently, Wendell and colleagues (WENDELL *et al.* 1996; WENDELL and GORSKI 1997; WENDELL *et al.* 2000) have evaluated DES-induced pituitary growth in crosses between the F344 and BN strains and have mapped six genetic loci, each of which harbors one or more genes that control the pituitary growth response to DES in these crosses. Together, these studies indicate that estrogen stimulated pituitary growth behaves as a quantitative genetic trait. The effects of two of these loci have now been evaluated using congenic rat lines (SCLAFANI and WENDELL 2001; WENDELL *et al.* 2002).

Our laboratory is studying the genetically related ACI and COP rat strains to define the genetic bases of the differing sensitivities of these strains to estrogen-induced pituitary growth (SPADY *et al.* 1999d) as well as susceptibility to estrogen-induced mammary cancer (SHULL *et al.* 1997; SPADY *et al.* 1998a; HARVELL *et al.* 2000; SHULL *et al.* 2001). The goals of this study were to characterize the phenotypes of F_1, F_2 and backcross (BC) progeny from reciprocal crosses between the ACI and COP rat strains with respect to DES-induced pituitary growth and to map the genetic loci that determine the differing pituitary growth responses of the ACI and COP rat strains to DES. We demonstrate that sensitivity to DES-induced pituitary growth behaves as a complex genetic trait determined by at least six quantitative trait loci (QTL). For the most part, these loci are distinct from those mapped previously by Wendell *et al.* in crosses between the F344 and BN rat strains (WENDELL *et al.* 1996; WENDELL and GORSKI 1997; WENDELL *et al.* 2000). Moreover, the majority of these loci are distinct from loci mapped by

us that determine susceptibility to estrogen-induced mammary cancer (GOULD *et al.*, submitted as accompanying manuscript). These data indicate that the genes that determine the tumorigenic potential of estrogens act in a rat strain- and tissue-specific manner.

MATERIALS AND METHODS

Care and Treatment of Animals: The Institutional Animal Care and Use Committee of the University of Nebraska Medical Center approved all procedures involving live animals. ACI rats were obtained from Harlan Sprague Dawley, Inc. (Indianapolis, IN). COP rats were obtained from the breeding program of the National Cancer Institute. Animals were housed in a barrier facility under controlled temperature, humidity, and 12h light/12h dark lighting conditions. This facility was accredited by the American Association for Accreditation of Laboratory Animal Care and operated in accordance with the standards outlined in *Guide for the Care and Use of Laboratory Animals* (DHHS Publication 85-23). The animals were caged and fed as described previously (SPADY *et al.* 1999d). Female COP rats were mated to male ACI rats to produce (COP x ACI)F_1 progeny, F_1 siblings were mated to generate (COP x ACI)F_2 progeny and ACI females were mated to F_1 males to produce (COP x ACI)BC progeny. Pups were weaned at 20-24 days of age. Implants, either empty or containing 5 mg of DES (Sigma, St. Louis, MO), were made from Silastic™ brand tubing and medical adhesive (DOW Corning Corp., Midland, MI) and were inserted subcutaneously in the interscapular region as described previously (SPADY *et al.* 1998a). Treatment with DES was initiated when the animals were 63 ± 4 days of age. Small populations of male rats of each genetic type received empty implants. The rats were sacrificed by decapitation after 12 weeks of DES or sham treatment. The pituitary gland was immediately

removed and weighed. Pituitary mass is an accurate indicator of estrogen-induced pituitary growth because it correlates highly with pituitary DNA content (WIKLUND *et al.* 1981b) and circulating PRL (SPADY *et al.* 1999d). The spleen was collected as a source of DNA and stored at −80 C.

Analysis of Linkage: The phenotypically defined (COP x ACI)F_2 population described herein and the (ACI x COP)F_2 population described by us previously (SPADY *et al.* 1999d) were subjected to linkage analyses. DNA was isolated from the spleen of each animal using DNeasy columns (Qiagen Inc., Valencia, CA). For one rats from each cross, tissue was not available for isolation of DNA. Therefore, these animals were not used in the linkage analysis. Each rat for which tissue was available was genotyped at simple sequence length polymorphism (SSLP) markers that were selected at approximately 20 cM intervals, where available, from those distributed across the rat genome (Rat Genome Database, http://rgd.mcw.edu). Oligonucleotide primers specific to each SSLP were obtained from Invitrogen Corporation (Carlsbad, CA). Each DNA sample was amplified in a 10 μl reaction containing 30 ng of DNA; 1.25 U Taq polymerase (Invitrogen Corporation, Carlsbad, CA); 20 mM Tris (pH 8.4); 1.5 mM $MgCl_2$; 50 mM KCl; 198 nM of each of the forward and reverse primers; 200 μM each of dATP, dGTP, dCTP, dTTP; and 1.0 μCi [α-^{32}P] dATP (Amersham, Arlington Heights, IL). The reaction mixtures were incubated at 94°C for 5 minutes and subjected to 30 cycles of PCR as follows: 1) 94°C for 30 seconds; 2) 55°C for 30 seconds; 3) 72°C for 1.5 minutes, with the final cycle followed by incubation at 72°C for 3 minutes. The DNA products were denatured, resolved on 5, 6, or 8% polyacrylamide gels and visualized using a PhosphorImager and ImageQuant 5.0 for Windows NT software (Molecular Dynamics, Sunnyvale, CA).

Genotypes were initially determined for the subpopulation of rats that were selected from each of the F_2 populations because of their extreme phenotypes (LANDER and BOTSTEIN 1989). Prior to linkage analyses, the pituitary masses were $\log_{10}$ transformed to normalize the population distribution relative to the population mean as described by Wendell et al. (WENDELL and GORSKI 1997; WENDELL *et al.* 2000). Genetic maps were generated using MAPMAKER/EXP version 3.0 (LANDER *et al.* 1987). The likelihood ratio statistic (LRS) values estimating the correlation between genotype and phenotype were generated using MAPMANAGER QTX version 0.29 (MANLY et al. 2001). For initial linkage analysis of autosomes, the phenotypically extreme F_2 populations, experimentwise threshold values were obtained from 1000 permutations conducted at 2 cM intervals (CHURCHILL and DOERGE 1994). When the correlation of phenotype to genotype in these populations yielded an LRS value suggestive of linkage, the remaining F_2 animals were genotyped across that chromosome. The genetic maps, LRS values and permutation-derived threshold values were subsequently recalculated for the (COP x ACI)F_2 population, the (ACI x COP)F_2 population, and the combined F_2 population. Estimation of the phenotypic contribution of each locus and potential interaction between individual markers for the combined F_2 population were determined using MAPMANAGER QTX version 0.29 software (MANLY et al. 2001). Linkage of markers on the X chromosome to a locus modulating pituitary tumorigenesis was assessed using the Wilcoxon rank sum test.

The analysis of potential interactions was performed using MAPMANAGER QTX version 0.29 (MANLY et al. 2001). Specifically, potential interactions were evaluated between markers on the six chromosomes for which the all of the F_2 rats had been genotyped, those for

which suggestive or significant evidence of linkage had been obtained. Interaction testing was performed with the probability of a type I error = 10^{-5} as recommended (MANLY et al. 2001). Evidence of an interaction was considered significant if both the interaction value was above the permutation derived threshold of significant evidence for linkage used in the linkage analysis in which the free regression model is used and the LRS value for the interaction exceeded the permutation derived threshold obtained for evidence of linkage in which the free model with interaction is used.

Statistical Analysis of Data: A two-tailed Student's T-test allowing for unequal variances was run and an ANOVA T-test with Bonferroni adjustment was used to evaluate differences between individual populations. A one-way ANOVA for linear trend was used to evaluate the association between the total number of growth conferring alleles and pituitary mass. Linear regression was used to evaluate the association of ACI and COP alleles in the interaction between SSLP markers *D1Rat75* and *D10Mit7*. SPSS software (release 10.1.3, SPSS Inc., Chicago, IL) was used for these analyses.

RESULTS

Phenotypic characterization of progeny from a COP x ACI intercross: Treatment with the synthetic estrogen DES for 12 weeks resulted in significant increases in pituitary mass in each of the experimental groups evaluated in the context of the COP x ACI intercross (Figure 1). DES increased pituitary mass in male ACI rats 10.6-fold, from 7.7 mg (standard deviation (SD) = 0.9) in untreated male ACI rats to 81.7 mg (SD = 10.3). In contrast, DES increased pituitary mass 4.4-fold in male COP rats, from 7.6 mg (SD = 1.0) to 34.2 mg (SD = 5.9). Male (COP x ACI)F_1

rats treated with DES displayed a 6.9-fold increase in average pituitary mass, from 8.2 mg (SD = 1.2) to 56.6 mg (SD = 13.2). The pituitary growth response of the (COP x ACI)F_1 progeny was intermediate to that exhibited by the parental ACI ($P = 0.01$) and COP strains ($P = 0.01$). Male (COP x ACI)F_2 rats displayed a 7.8-fold increase in pituitary mass, whereas male (COP x ACI)BC rats displayed a 9.2-fold increase in pituitary mass. Average pituitary mass in the DES treated (COP x ACI)BC progeny did not differ significantly from that observed in DES-treated ACI rats ($P = 0.94$). The relatively large standard deviations exhibited by the F_2 and BC populations are suggestive of the segregation of multiple loci within these populations.

The pituitary growth responses exhibited by the male ACI, COP, F_1, F_2 and BC rats evaluated in association with this COP x ACI intercross were compared to the responses exhibited by rats generated in the cross originating with ACI females and COP males and described by us previously (SPADY *et al.* 1999d). DES induced pituitary growth in the two groups of F_1 progeny did not differ significantly ($P > 0.05$), indicating no discernable affect of mating order on the phenotype in these groups. Similarly, the phenotypes of the two groups of F_2 and BC progeny from the two reciprocal intercrosses did not differ as a function of mating order ($P > 0.05$). The pituitary growth response of the combined F_1 population to DES was intermediate to and significantly different from the responses exhibited by the parental ACI and COP strains (Table 1). The growth response of the combined BC population to DES did not differ significantly from that exhibited by male ACI rats ($P = 1.00$).

Mapping of genetic determinants of estrogen-induced pituitary tumorigenesis: Because the phenotype of the F_2 populations from the COP x ACI and ACI x COP crosses did not differ, these populations were combined for linkage analyses. A genome-wide linkage scan was

performed using 181 SSLP markers. Genotypes were initially determined for the subpopulations of 45 (COP x ACI)F_2 and 44 (ACI x COP)F_2 progeny that exhibited the phenotypic extremes with respect to pituitary mass following 12 weeks of DES treatment. Initial analysis of linkage revealed eight loci on six chromosomes with LRS values greater than the permutation derived threshold of 10.6 for suggestive evidence of linkage. Genotypes were subsequently determined over these six chromosomes for the remaining 117 (COP x ACI)F_2 progeny and the remaining 58 (ACI x COP)F_2 progeny. Permutation-derived threshold values were subsequently recalculated using data from the 264 rats from the combined F_2 population on the six chromosomes of interest. Linkage analysis using the 264 rats from the combined F_2 population identified one locus on chromosome 3 (RNO3) with a peak LRS value that exceeded 20.9, the permutation derived threshold for highly significant evidence of linkage (Figure 2). Four additional loci exhibited peak LRS values that exceeded 14.0, the permutation derived threshold for significant evidence of linkage (Figure 2). Three other loci exhibited LRS values above 7.9, the permutation derived threshold for suggestive evidence of linkage. To determine if the locus on RNO3 interfered with the ability to detect evidence of linkage at other loci, composite interval mapping (CIM) was employed. For this analysis, marker regression was performed with *D3Rat26*, the marker closest to the LRS peak on RNO3, fixed as background. This analysis confirmed the linkage of the four previously identified significant loci on RNO1, RNO3, RNO6, and RNO10. Furthermore, using CIM, a second locus on RNO1, which had previously been identified by marker regression analysis as just below the significant threshold of 14.0 (LRS 13.8), crossed the threshold for significant evidence of linkage with an LRS value of 14.2. Bootstrap analysis was performed to provide an estimate of the confidence intervals for the six significant loci. The six significant loci have been designated as *Estrogen-induced pituitary*

tumor loci: *Ept1*, *Ept2*, *Ept6*, *Ept9*, *Ept10* and *Ept13*. The numbering of these loci is not continuous because other *Ept* loci not described here have been mapped in crosses between the ACI and Brown Norway strains (unpublished data).

Ept1 mapped to rat RNO6 (Figure 2A). The peak LRS value of 16.5 was observed between markers *D6Rat150* and *D6Rat80* with the confidence interval between *D6Rat108* and *D6Rat146* encompassing approximately 26 cM. *Ept2* and *Ept6* mapped to two distinct regions on RNO3 (Figure 2B). *Ept2*, with an LRS value of 31.3, was observed between markers *D3Rat37* and *D3Rat26*. The confidence interval, between markers *D3Rat37* and *D3Rat150*, spanned approximately 58 cM. A second LRS peak, with a value of 18.5, was located between markers *D3MGH16* and *D3MGH9*. The confidence interval for this locus, designated *Ept6*, was located between markers *D3MGH16* and *D3Rat277* and spanned approximately 17 cM (Figure 2B; solid tracing). When *D3Rat26*, the marker with the greatest LRS value within the *Ept2* interval, was fixed as background, CIM analysis yielded an LRS value of 20.4 within the *Ept6* interval, providing significant evidence of that *Ept6* was genetically distinct from *Ept2* (Figure 2B; dashed tracing). Likewise, when *D3MGH9*, the marker with the greatest LRS value within the *Ept6* interval, was designated as background, evidence for *Ept2* remained significant, with an LRS value of 31.7 (not shown). *Ept9* mapped to RNO10 (Figure 2C). The peak LRS value of 17.7 was observed between markers *D10Rat21* and *D10Mit7* with a confidence interval of approximately 58 cM between markers *D10Rat32* and *D10Rat11*. *Ept10* and *Ept13* mapped to two distinct regions on RNO1 (Figure 2D). *Ept10*, with a peak LRS value of 15.2 was observed between *D1Rat119* and *D1Rat81*. The confidence interval for *Ept10*, between markers *D1Rat104* and *D1Rat87*, spanned approximately 89 cM. A second locus on RNO1, *Ept13*, with a suggestive LRS value of 13.8, was located between marker *D1Rat192* and *D1Rat121* (Figure

2D; solid tracing). CIM was performed after fixing *D3Rat26*, the marker with the greatest LRS value within *Ept2*, as background. This analysis yielded a peak LRS value within the *Ept13* interval of 14.2, which crossed the threshold for significant evidence of linkage. Furthermore, when *D1Rat119*, the marker most closely associated with *Ept10*, was fixed as background, CIM analysis yielded a peak LRS value of 14.6 within *Ept13*, providing significant evidence that this locus was genetically distinct from *Ept10* (Figure 2D; dashed tracing). The confidence interval for this locus was located between markers *D1Rat192* and *D1Rat259* and spanned approximately 17 cM. Likewise, when *D1Rat192* was fixed as background, significant evidence of the *Ept10* locus was obtained with CIM analysis (not shown).

The genome-wide linkage scan suggested that two additional regions of the rat genome may harbor genetic determinants of estrogen-induced pituitary tumorigenesis. A peak LRS value of 11.1 was observed between RNO4 markers *D4Rat196* and *D4Mgh7* (not shown). The second locus was suggested by a peak LRS value of 8.1 between RNO5 markers *D5Rat28* and *D5Rat95* (not shown). Following CIM analysis in which the peak markers within the five loci with the highest LRS values (*Ept1*, *Ept2*, *Ept6*, *Ept10*, *Ept13*) were all fixed as background, the LRS values associated with these 2 additional loci still exceeded the permutation-derived threshold of suggestive evidence of linkage but failed to cross the threshold of 14.0 for significant evidence of linkage.

These mapping data indicate that DES-induced pituitary growth behaves as a quantitative trait for which multiple, independently segregating, genes act to determine the phenotype of individuals within the F_2 population. To determine the effect of each of the six significant *Ept* loci on pituitary mass, the combined F_2 population from the two crosses was divided into subpopulations depending upon genotype at the marker most closely associated with the peak

LRS value within each *Ept* locus. Homozygosity for ACI alleles at *Ept1*, *Ept2*, *Ept9* and *Ept13* was associated with 16.8 mg, 24.2 mg, 13.6 mg and 14.6, mg respectively, of additional pituitary mass relative to rats homozygous for COP alleles at these loci (Figure 3A-D). In contrast, homozygosity for COP alleles at *Ept6* and *Ept10* was associated with 19.6 mg and 15.8 mg, respectively, of additional pituitary mass relative to rats homozygous for ACI alleles (Figure 3E-F). The ACI allele of *Ept2* and the COP allele of *Ept6* appear to act in an incompletely dominant manner to enhance DES-induced pituitary growth. For both *Ept2* and *Ept6*, the average pituitary mass in heterozygous rats was significantly different than that in both of the homozygous populations ($P < 0.05$; Figure 3B and 3E). For *Ept1*, average pituitary mass in rats homozygous for the ACI allele was significantly greater than that in rats either heterozygous or homozygous for the COP allele ($P < 0.01$; Figure 3A). Although the average pituitary mass in rats heterozygous at *Ept1* did not differ significantly than those rats homozygous for the COP allele at *Ept1* ($P = 0.6$; Figure 3A), the power to detect a difference between these two populations was limited (24%). In contrast, for *Ept10*, average pituitary mass in rats homozygous for the COP allele was significantly greater than that in rats either heterozygous or homozygous for the ACI allele ($P < 0.05$; Figure 3F). Here again, although the average pituitary mass in rats heterozygous at *Ept10* did not differ significantly from rats homozygous for the ACI allele at *Ept10* ($P = 0.2$; Figure 3F), the power to detect a difference between these two populations was limited (39%). Thus, either a recessive or incompletely dominant mode of action is consistent with the data for *Ept1* and *Ept10*. For *Ept9* and *Ept13*, the mean pituitary mass in rats homozygous for the ACI allele differed significantly from that in rats homozygous for the COP allele ($P < 0.01$; Figure 3C and 3D). However, for each locus the mean pituitary mass in the heterozygous population did not differ significantly from that in either homozygous population

($P > 0.06$; Figure 3C and 3D), most likely due to the limited power to detect differences between the heterozygous population and either of the homozygous populations (< 48%). Thus, for these two loci, the mode of action could not be clearly determined from these analyses.

MAPMANAGER QTX provides estimates of the fraction of the phenotypic variance exhibited by the F_2 population that is determined by each of the *Ept* loci (Table 2). These data indicate that of the six *Ept* loci, *Ept2* exerts the greatest effect on DES-induced pituitary growth and that together these six significant and two suggestive loci determine approximately 48% of the phenotypic variance exhibited by the combined F_2 population. Using the method of Wright (WRIGHT 1968), we estimated from the variances exhibited by the DES treated ACI, COP, and F_1 populations that environmental factors determined approximately 34% of the variance exhibited by the genetically heterogeneous F_2 population. Thus, only 18% of the F_2 phenotypic variance remains undetermined.

Evidence for an interaction between *Ept9* and *Ept10*: To determine if the six *Ept* loci acted independently, MapManager QTX was used to evaluate potential pair-wise interactions between markers on the chromosomes for which all 264 F2 rats were genotyped. A single, statistically significant interaction, between markers *D10Mit7* and *D1Rat75* within the *Ept9* and *Ept10* loci, respectively, was detected. The interaction value for this association was 14.1, just above the 14.0 threshold for significant evidence of linkage in the mapping study. The LRS value associated with this interaction, 44.1, was greater than both the permutation-derived threshold of 34.6 for evidence of significance and 42.0 for evidence at the highly significant level. To understand the nature of the interaction between *D10Mit7* and *D1Rat75*, the F_2 population was subdivided initially based on genotype at the *Ept10* marker *D10Mit7* and then subsequently

classified by genotype at the *Ept9* marker *D1Rat75* (Figure 4). Genotype at *D1Rat75* had no significant effect on estrogen-induced pituitary growth in rats homozygous for either the ACI or COP allele at *D10Mit7* ($P > 0.05$; Figure 4A and 4C). However, in rats heterozygous at *D10Mit7*, homozygosity for the COP allele at *D1Rat75* was associated with a significantly greater estrogen-induced pituitary growth response than that in either rats heterozygous at *D1Rat75* ($P < 0.01$; Figure 4B) or homozygous for the ACI allele ($P < 0.001$; Figure 4B). The potential significance of this interaction is unclear.

DISCUSSION

It has been known for over 60 years that chronic treatment with estrogens, either naturally occurring or synthetic, leads to development of pituitary tumors in rats (MCEUEN *et al.* 1936; SEGALOFF and DUNNING 1945; CLIFTON and MEYER 1956) and mice (GARDNER and STRONG 1940; GARDNER 1941). Moreover, substantial evidence suggests that estrogens may contribute to development of pituitary tumors in humans (LANDOLT *et al.* 1984; MIYAI *et al.* 1986; HOLMGREN *et al.* 1986; GOOREN *et al.* 1988; PANTEON *et al.* 1988; BEVAN *et al.* 1989; KOVACS *et al.* 1994). However, the mechanisms through which estrogens induce pituitary tumor development remain poorly defined. Elucidation of the genetic bases of the differing sensitivities of the genetically related ACI and COP rat strains to DES-induced pituitary growth will likely provide novel insights into the mechanisms through which estrogens regulate pituitary lactotroph homeostasis and induce pituitary tumor development.

The data presented in this manuscript indicate that estrogen-induced pituitary growth behaves as a quantitative genetic trait in reciprocal crosses between the ACI and COP rat strains.

Six genetic loci that determine sensitivity to DES-induced pituitary growth have been mapped through analysis of the F_2 populations generated in these crosses. Thus, the genetic bases of estrogen-induced pituitary tumor development in these crosses are more complex than proposed by us previously (SPADY *et al.* 1999d). We have estimated that these six *Ept* loci, together with two suggestive loci, account for 48% of the phenotypic variance exhibited by the combined F_2 population from the two crosses. Environmental factors were estimated to account for an additional 34% of phenotypic variance. These data suggest that one or more unmapped *Ept* locus accounts for the estimated 18% of the phenotypic variance that remains unexplained. It is possible that an unmapped *Ept* locus may reside within a region of the rat genome too distant from the nearest polymorphic marker to allow the locus to be detected. Seven segments of the rat genome exist where an additional *Ept* locus, were it to reside there, would be 20-28 cM from the nearest polymorphic marker. These segments are located on chromosomes 1, 2, 5, 6, 7, 10 and 17. In addition, only a small portion of the X chromosome has been analyzed in these crosses because of a paucity of polymorphic markers for this chromosome. Alternatively, the remaining 18% of the phenotypic variance could result from the actions of multiple unmapped *Ept* loci, each of which would exert an effect on pituitary mass that was too small to be detected in our analyses (VAN OOIJEN 1992; MURANTY and GOFFINET 1997). Because the two F_1 populations from the reciprocal crosses exhibited similar phenotypes, it is unlikely that either the X or the Y chromosome harbors genes that act as strong determinants of DES-induced pituitary growth in these crosses between the ACI and COP rat strains.

The six *Ept* loci mapped in this study segregate and appear, for the most part, to function independently. ACI alleles at *Ept1*, *Ept2*, *Ept9*, and *Ept13* are associated with increased DES-induced pituitary growth, relative to COP alleles at these loci. In contrast, COP alleles at *Ept6*

and *Ept10* are associated with increased pituitary growth. Thus, the sensitivity of the COP strain to DES-induced pituitary tumorigenesis is not simply due to the action of growth conferring alleles shared with the genetically related ACI strain. Rather, the sensitivity of the COP strain to DES-induced pituitary tumorigenesis is due, at least in part, to the action of growth conferring alleles not carried in the ACI strain. This hypothesis is consistent with our previous observation that a 40% restriction of dietary energy consumption inhibits development of estrogen-induced pituitary tumors in COP, but not ACI, rats (SPADY *et al.* 1999a; SPADY *et al.* 1999c; HARVELL *et al.* 2001; HARVELL *et al.* 2002; HARVELL *et al.* 2003).

Wendell *et al.* have mapped to RNO2, RNO3, RNO5 and RNO9 a total of six QTL that impact DES-induced pituitary growth in female F_2 and BC progeny derived from crosses between the F344 and BN rat strains (WENDELL and GORSKI 1997; WENDELL *et al.* 2000). Data from the current study of male F_2 progeny from crosses between the ACI and COP rat strains specifically exclude pituitary growth controlling loci from the regions of RNO2 and RNO9 to which Wendell *et al.* mapped four of the six loci that control DES-induced pituitary growth in F344 x BN crosses. Although there are gaps in our genetic map of RNO2, the peaks of *Edpm2.1* and *Edpm2.2* lie outside of these gaps. The *Ept2* locus mapped by us to RNO3 overlaps with the *Edpm3* locus mapped by Wendell *et al.* In addition, the suggestive locus that we have mapped to RNO5 is encompassed by the confidence interval of *Edpm5*. Thus, the majority of the loci mapped in the ACI x COP crosses are distinct from those mapped by Wendell *et al.* in crosses between the F344 and BN strains. We hypothesize that the dissimilarities in the QTLs mapped in our study compared to those of Wendell *et al.* result from differences in the inbred strains being evaluated. However, we cannot exclude the possibility

that the differences in the QTLs identified in the two studies are due to variation in experimental design, such as the gender of rats used for linkage analysis.

We observed highly significant evidence of an epistatic interaction between *Ept9* and *Ept10*. These data suggest that the effect of *Ept10* (*D1Rat175*) is only detectable in rats heterozygous at *Ept9* (*D10Mit7*). The potential interaction between *Ept9* and *Ept10* is particularly intriguing because *Jak2* is tightly linked to *D1Rat75* and *Stat5a* and *Stat5b*, which are phosphorylated by *Jak2*, are linked to *D10Mit7*. Together, Jak2 and Stat5a/5b, mediate PRL signaling through the PRL receptor to regulate lactotroph function and number (SCHUFF *et al.* 2002; BOLE-FEYSOT *et al.* 1998). The known role of Jak2 and both Stat5a and Stat5b in mediating the effects of prolactin signaling make these genes attractive candidates for *Ept10* and *Ept9*, respectively.

In studies performed in parallel to those presented herein, analysis of female F_2 progeny from reciprocal crosses between the ACI and COP strains localized to RNO5 a locus, referred to as *Emca1*, that determines susceptibility to 17β-estradiol (E2)-induced mammary cancer (GOULD *et al.*, submitted as accompanying manuscript). A second suggestive determinant of susceptibility to E2-induced mammary cancer, *Emca2*, was mapped to RNO18. Although the genetic analyses described herein indicate that RNO18 does not harbor a genetic determinant of DES-induced pituitary growth, we obtained suggestive evidence of linkage with a region on RNO5 that overlaps the *Emca1* locus. Whereas, *Emca1* is a strong modifier of E2-induced mammary cancer, the locus mapped to RNO5 in this study is only a weak modifier of DES-induced pituitary growth. Moreover, the regions of the genome in which *Ept* loci reside do not determine susceptibility to estrogen-induced mammary carcinogenesis in the E2 treated female F_2 progeny (GOULD *et al.*, submitted as accompanying manuscript). Thus, the majority of the

loci that determine sensitivity to DES-induced pituitary tumorigenesis are distinct from those that determine susceptibility to E2-induced mammary carcinogenesis.

In summary, the data presented herein indicate that multiple genetic loci control sensitivity to DES-induced pituitary growth in F2 progeny produced in crosses between the ACI and COP rat strains. Congenic rat lines are under development that will allow the impact of each *Ept* locus on estrogen-induced pituitary tumorigenesis to be assessed both qualitatively and quantitatively. These congenic lines will also allow each *Ept* locus to be mapped with greater precision. The recent assembly of the draft sequence of the rat genome will facilitate the identification of those genes residing within each *Ept* locus, and this, in turn, should significantly enhance our understanding of how estrogens regulate lactotroph homeostasis and contribute to tumorigenesis.

ACKNOWLEDGMENTS

We thank the staff of the Eppley Institute Animal Care Facility for their excellent care of the research animals. We thank Dr. Douglas Wendell for many helpful suggestions on data analysis. Finally, we thank Ms. Cindy Lachel for her assistance and critical evaluation of this manuscript. This work was supported by National Institutes of Health grants R01-CA68529 and R01-CA77876. National Institutes of Health Cancer Center Support Grant P30-CA36727 supported shared resources within the UNMC Eppley Cancer Center. T.E.S. was supported in part by National Institutes of Health training grant T32-CA09476. T.E.S. and B.S.S. were supported in part by training grant DAMD17-00-1-0361 from the U.S. Army Breast Cancer Training Program. B.S.S. was supported in part by DAMD17-03-1-0477 from the U.S. Army Breast Cancer Training Program. T.J.S. was supported in part by a Bukey Presidential Fellowship from the Graduate College of the University of Nebraska.

LITERATURE CITED

BEVAN, J. S., J. SUSSMAN, A. ROBERTS, M. HOURIHAN and J. R. PETERS, 1989 Development of an invasive macroprolactinoma: a possible consequence of prolonged oestrogen replacement. Case report. Br. J. Obstet. Gynecol. **96**: 1440-1444.

BOLE-FEYSOT, C., V. GOFFIN, M. EDERY, N. BINART and P.A.KELLY, 1998 Prolactin (PRL) and its receptor: actions, signal transduction pathways and phenotypes observed in PRL receptor knockout mice. Endocr. Rev. **19**: 225-268.

CLIFTON, K. H. and R. K. MEYER, 1956 Mechanism of anterior pituitary tumor induction by estrogen. Anat. Rec. **125**: 65-81.

CHURCHILL,G. A. and R. W. DOERGE, 1994 Empirical threshold values for quantitative trait mapping. Genetics **138**: 963-971.

FURTH, J., G. UEDA and K. H. CLIFTON, 1973 The pathophysiology of pituitaries and their tumors: metholological advances. Methods Cancer Res. **10**: 201-277.

GARDNER, W. U., 1941 The effect of estrogen on the incidence of mammary and pituitary tumors in hybrid mice. Cancer Res. **1**: 345-358.

GARDNER, W. U. and L. C. STRONG, 1940 Strain-limited development of tumors of the pituitary gland in mice receiving estrogens. Yale J. Biol. Med. **12**: 543-548.

GOOREN, L. J. G., J. ASSIES, H. ASSCHEMAN, R. DE SLEGTE and H. VAN KESSEL, 1988 Estrogen-induced prolactinoma in a man. J. Clin. Endocrinol. Metab. **66**: 444-446.

HARVELL, D. M. E., L. K. BUCKLES, K. A. GOULD, K. L. PENNINGTON, R. D. MCCOMB *et al.*, 2003 Rat strain specific attenuation of estrogen action in the anterior pituitary gland by dietary energy restriction. Endocrine **21**: 175-183.

HARVELL, D. M. E., T. J. SPADY, T. E. STRECKER, A. M. LEMUS-WILSON, K. L. PENNINGTON *et al.*, 2001 Dietary energy restriction inhibits estrogen induced pituitary tumorigenesis in a rat strain specific manner. In: *Hormonal Carcinogenesis III*, Li, J. J., Li., S. A. and Daling, J. R., editors, Springer, New York, pages 496-501.

HARVELL, D. M. E., T. E. STRECKER, M. TOCHACEK, B. XIE, K. L. PENNINGTON *et al.*, 2000 Rat strain specific actions of 17β-estradiol in the mammary gland: correlation between estrogen-induced lobuloalveolar hyperplasia and susceptibility to estrogen-induced mammary cancers. Proc. Natl. Acad. Sci. **97**: 2779-2784.

HARVELL, D. M. E., T. E. STRECKER, B. XIE, K. L. PENNINGTON, R. D. MCCOMB *et al.*, 2002 Dietary energy restriction inhibits estrogen-induced mammary, but not pituitary, tumorigenesis in the ACI rat. Carcinogenesis **23**: 161-169.

HOLMGREN, U., G. BERGSTRAND, K. HAGENFELDT and S. WERNER, 1986 Women with prolactinoma--effect of pregnancy and lactation on serum prolactin and on tumour growth. Acta Endocrinol. (Copenh) **111**: 452-459.

HOLTZMAN, S., J. P. STONE and C. J. SHELLABARGER, 1979 Influence of diethylstilbestrol treatment on prolactin cells of female ACI and Sprague-Dawley rats. Cancer Res. **39**: 779-784.

KOVACS, K., L. STEFANEANU, S. EZZAT and H. S. SMYTH, 1994 Prolactin-producing pituitary adenoma in a male-to-female transsexual patient with protracted estrogen administration: A morphologic study. Arch. Pathol. Lab. Med. **118**: 562-565.

LANDER, E. and L. KRUGLYAK, 1995 Genetic dissection of complex traits: guidelines for interpreting and reporting linkage results. Nat. Genet. **11**: 241-247.

LANDER, E. S. and D. BOTSTEIN, 1989 Mapping Mendelian factors underlying quantitative traits using RFLP linkage maps. Genetics **121**: 185-199.

LANDER, E. S., P. GREEN, J. ABRAHAMSON, A. BARLOW, M. J. DALY *et al.*, 1987 MAPMAKER: An interactive computer package for constructing primary genetic linkage maps of experimental and natural populations. Genomics **1**: 174-181.

LANDOLT, A. M., E. DEL POZO and J. HAYEK, 1984 Injectable bromocriptine to treat acute, oestrogen-induced swelling of invasive prolactinoma. Lancet **2**: 111

MCEUEN, C. S., H. SELYE and J. B. COLLIP, 1936 Prolonged administration of oestrin in rats. Lancet **1**: 775-776.

MIYAI, K., K. ICHIHARA, K. KONDO and S. MORI, 1986 Asymptomatic hyperprolactinaemia and prolactinoma in the general population-mass screening by paired assays of serum prolactin. Clin. Endocrinol. **25**: 549-554.

MURANTY, H. and B. GOFFINET, 1997 Selective genotyping for location and estimation of the effect of a quantitative trait locus. Biometrics **53**: 629-643.

NOBLE, R. L., C. S. MCEUEN and J. B. COLLIP, 1940 Mammary tumours produced in rats by the action of oestrone pellets. Canad. Med. Assoc. J. **42**: 413-417.

VAN OOIJEN JW 1992 Accuracy of mapping quantitative trait loci in autogamous species. Theor. Appl. Genet. **84**: 803-811.

PANTEON, E., E. LOUMAYE, M. MAES and P. MALVAUX, 1988 Occurence of prolactinoma after estrogen treatment in a girl with constitutional tall stature. J. Pediatr. **113**: 337-339.

SCLAFANI, R. V. and D. L. WENDELL, 2001 Suppression of estrogen-dependent MMP-9 expression by *Edpm5*, a genetic locus for pituitary tumor growth in rat. Mol. Cell. Endocrinol. **176**: 145-153.

SCHUFF, K.G., S.T. HENTGES, M.A. KELLY, N. BINART, P.A. KELLY, P.M. IUVONE, S.L. ASA, and M.J. LOW, 2002 Lack of prolactin receptor signaling in mice results in lactotroph proliferation and prolactinomas by dopamine-dependent and -independent mechanisms. J. Clin. Invest. **110**: 973-981.

SEGALOFF, A. and W. F. DUNNING, 1945 The effect of strain, estrogen, and dosage on the reaction of the rat's pituitary and adrenal to estrogenic stimulation. Endocrinology **36**: 238-240.

SHULL, J. D., 2002 Hormonal Carcinogenesis. In: *Encyclopedia of Cancer*, Second Edition, edited by J. R. Bertino. Academic Press, San Diego, CA. Second Volume: 417-428.

SHULL, J. D., K. L. PENNINGTON, T. M. REINDL, M. C. SNYDER, T. E. STRECKER *et al.*, 2001 Susceptibility to estrogen-induced mammary cancer segregates as an incompletely dominant phenotype in reciprocal crosses between the ACI and Copenhagen rat strains. Endocrinology **142**: 5124-5130.

SHULL, J. D., T. J. SPADY, M. C. SNYDER, S. L. JOHANSSON and K. L. PENNINGTON, 1997 Ovary intact, but not ovariectomized female ACI rats treated with 17β-estradiol rapidly develop mammary carcinoma. Carcinogenesis **18**: 1595-1601.

SPADY, T. J., D. M. E. HARVELL, A. LEMUS-WILSON, T. E. STRECKER, K. L. PENNINGTON *et al.*, 1999a Modulation of estrogen action in the pituitary and mammary glands by dietary energy consumption. J. Nutr. **129**: 587S-590S.

SPADY, T. J., D. M. E. HARVELL, M. C. SNYDER, K. L. PENNINGTON, R. D. MCCOMB *et al.*, 1998a Estrogen-induced tumorigenesis in the Copenhagen rat: disparate susceptibilities to development of prolactin-producing pituitary tumors and mammary carcinomas. Can. Lett. **124**: 95-103.

SPADY, T. J., A. M. LEMUS-WILSON, K. L. PENNINGTON, D. J. BLACKWOOD, T. M. PASCHALL *et al.*, 1998b Dietary energy restriction abolishes development of prolactin-producing pituitary tumors in Fischer 344 rats treated with 17β-estradiol. Mol. Carcinog. **23**: 86-95.

SPADY, T. J., R. D. MCCOMB and J. D. SHULL, 1999b Estrogen action in the regulation of cell proliferation, cell survival, and tumorigenesis in the rat anterior pituitary gland. Endocrine **11**: 217-233.

SPADY, T. J., K. L. PENNINGTON, R. D. MCCOMB, D. F. BIRT and J. D. SHULL, 1999c Estrogen-induced pituitary tumor development in the ACI rat is not inhibited by dietary energy restriction. Mol. Carcinog. **26**: 239-253.

SPADY, T. J., K. L. PENNINGTON, R. D. MCCOMB and J. D. SHULL, 1999d Genetic bases of estrogen-induced pituitary growth in an intercross between the ACI and Copenhagen rat strains: dominant Mendelian inheritance of the ACI phenotype. Endocrinology **140**: 2828-2835.

WENDELL, D. L., S. B. DAUN, M. B. STRATTON and J. GORSKI, 2000 Different functions of QTL for estrogen-dependent tumor growth of the rat pituitary. Mamm. Genome **11**: 855-861.

WENDELL, D. L. and J. GORSKI, 1997 Quantitative trait loci for estrogen-dependent pituitary tumor growth in the rat. Mamm. Genome **8**: 823-829.

WENDELL, D. L., A. HERMAN and J. GORSKI, 1996 Genetic separation of tumor growth and hemorrhagic phenotypes in an estrogen-induced tumor. Proc. Natl. Acad. Sci. USA **93**: 8112-8116.

WENDELL, D. L., J. PANDEY and P. KELLEY, 2002 A congenic strain of rat for investigation of control of estrogen-induced growth. Mamm. Genome **13**: 664-666.

WIKLUND, J., J. RUTLEDGE and J. GORSKI, 1981a A genetic model for the inheritance of pituitary tumor susceptibility in F344 rats. Endocrinology **109**: 1708-1714.

WIKLUND, J., N. WERTZ and J. GORSKI, 1981b A comparison of estrogen effects on uterine and pituitary growth and prolactin synthesis in F344 and Holtzman rats. Endocrinology **109**: 1700-1707.

WIKLUND, J. A. and J. GORSKI, 1982 Genetic differences in estrogen-induced deoxyribonucleic acid synthesis in the rat pituitary: Correlations with pituitary tumor susceptibility. Endocrinology **111**: 1140-1149.

WRIGHT, S., 1968 The Genetics of Quantitative Variability. In *Evolution and the Genetics of Populations. Genetics and Biometrical Foundations*. University of Chicago Press, Chicago, vol. 1: 373-420.

Figure 1. Sensitivity to DES-induced pituitary growth in progeny from a COP x ACI cross is genetically determined. Male F_1, F_2 and BC rats from a cross originating with COP females and ACI males were generated and treated with DES for 12 weeks beginning at 9 weeks of age as described in Materials and Methods. Each data bar represents the mean mass of the anterior pituitary gland (mg ± SD). Each of the untreated control groups consisted of 5-6 rats. The numbers of DES treated rats were: ACI, 14; COP, 14; F_1, 18; F_2, 163; BC, 49. 1 indicates a statistically significant difference ($P \leq 0.05$) between a DES treated population and its corresponding control population. 2, indicates a significant difference between the indicated population and the treatment matched ACI population ($P \leq 0.05$). 3, indicates a significant difference between the indicated population and the treatment matched COP population ($P \leq 0.05$).

Figure 2. Six quantitative trait loci determine sensitivity to DES-induced pituitary growth in F_2 progeny from reciprocal crosses between the ACI and COP rat stains. Genotypes were determined at the indicated polymorphic SSLP markers for a total of 264 phenotypically defined F_2 progeny from reciprocal crosses between the ACI and COP strains. Each horizontal axis represents the indicated rat chromosome in genetic distance (Haldane cM). Each vertical axis represents the LRS level of correlation between phenotype ($\log_{10}$ transformed pituitary mass) and genotype along each chromosomal interval. Each black box represents the confidence interval identified by bootstrapping. LRS values for each of the six QTLs exceed the permutation derived threshold for significant evidence of linkage of 14.0. **A.** LRS values for RNO6 depicts the location of *Eptl*. Four markers used in the linkage analysis on this chromosome are not

shown here because of their close proximity to other markers depicted in this picture. A gap in our genetic map exists between *D6Rat146* and *D6Rat153*. **B**. LRS values for RNO3 depicts the locations of *Ept2* and *Ept6*. Solid tracing represents LRS values in the absence of fixing any marker as background. Dashed tracing represents LRS values with *D3Rat26* designated as background. Three markers used in the linkage analysis on this chromosome are not shown here because of their close proximity to other markers depicted in this picture. **C**. LRS values for RNO10 depicts the location of *Ept9*. Two markers used in the linkage analysis on this chromosome are not shown here because of their close proximity to other markers depicted in this picture. A gap in our genetic map exists between *D10Rat45* and *D10Rat32*. **D**. LRS values for RNO1 depicts the location of *Ept10* and *Ept13*. Solid tracing represents LRS values in the absence of fixing any marker as background. Dashed tracing represents LRS values with *D1Rat119* designated as background. A gap in our genetic map exists between *D1Rat104* and *D1Rat133*.

Figure 3. Impact of genotype at each *Ept* locus on DES-induced pituitary growth. Each of the 264 phenotypically defined F_2 rats from reciprocal crosses between the ACI and COP rat strains was classified as a function of its genotype at the indicated polymorphic marker most closely associated with the peak LRS value within each *Ept* locus: A/A, indicates homozygosity for ACI alleles; A/C indicates heterozygosity; C/C indicates homozygosity for COP alleles. Each data bar indicates mean pituitary mass (mg ± SEM) within each genotypically defined subpopulation. Statistically significant ($P \leq 0.05$) differences between subpopulations are indicated by different numerals above the data bars. 1 indicates that the distribution of pituitary mass in the population is significantly different from that in the A/A population. 2 indicates that the distribution of

pituitary mass in the population is significantly different from that in the C/C population. A-D. Impact of genotype of at loci for which the ACI allele is the growth conferring allele on DES-induced pituitary growth. E-F. Impact of genotype of at loci for which the COP allele is the growth conferring allele on DES-induced pituitary growth.

Figure 4. Characterization of the interaction between *Ept9* and *Ept10*. Each of the 264 phenotypically defined F_2 rats from the reciprocal crosses between the ACI and COP rat strains was classified by genotype at *D10Mit7* and then further classified by genotype at *D1Rat75*. Each data bar represents the mean pituitary mass (mg ± SEM) within the subpopulations of each genotype at *D1Rat75*. Statistically significant ($P \leq 0.05$) differences between subpopulations are indicated by different numerals above the data bars. 1 indicates that the distribution of pituitary mass in the population is significantly different from that in the A/A population. 2 indicates that the distribution of pituitary mass in the population is significantly different from that in the C/C population.

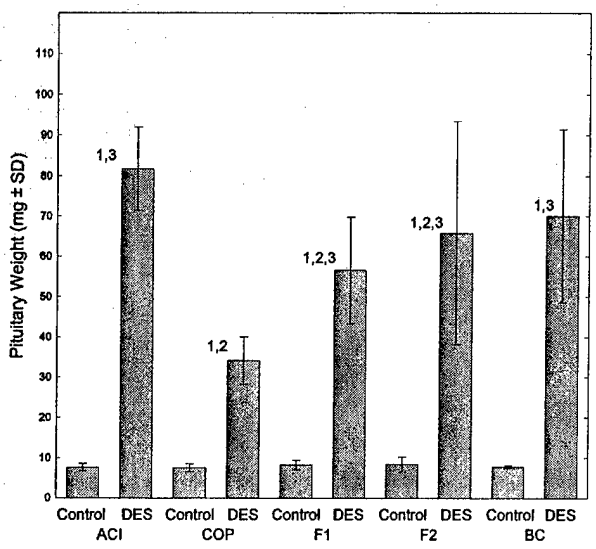
Pituitary Weight (mg ± SD)
0
10
20
30
40
50
60
70
80
90
100
110
1,3
1,2
1,2,3
1,2,3
1,3
Control
DES
ACI
COP
F1
F2
BC

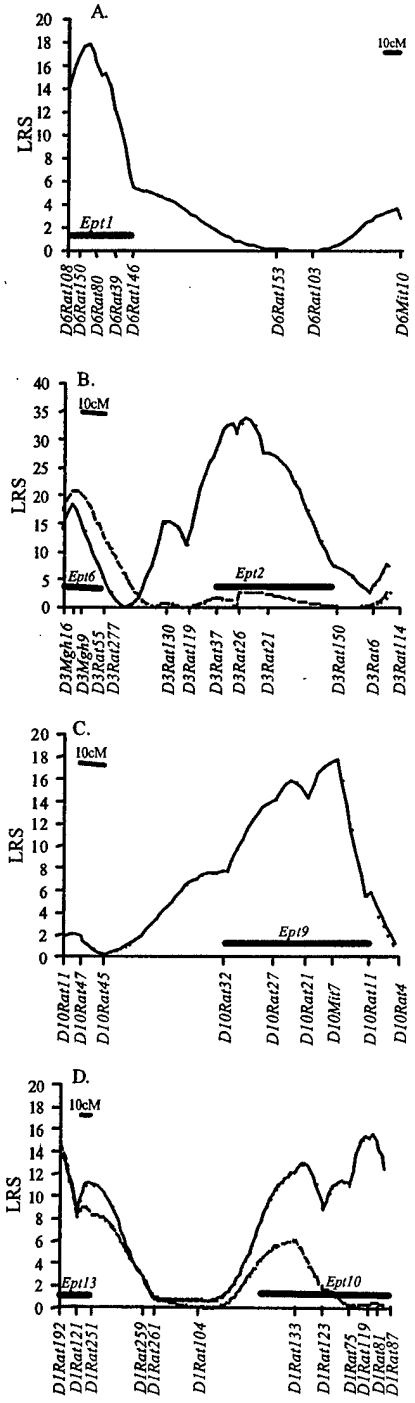
A.
10cM
LRS
Ept1
D6Rat108
D6Rat150
D6Rat80
D6Rat39
D6Rat146
D6Rat153
D6Rat103
D6Mit10
B.
10cM
LRS
Ept6
Ept2
D3Mgh16
D3Mgh9
D3Rat55
D3Rat277
D3Rat130
D3Rat119
D3Rat37
D3Rat26
D3Rat21
D3Rat150
D3Rat6
D3Rat114
C.
10cM
LRS
Ept9
D10Rat11
D10Rat47
D10Rat45
D10Rat32
D10Rat27
D10Rat21
D10Mit7
D10Rat11
D10Rat4
D.
10cM
LRS
Ept13
Ept10
D1Rat192
D1Rat121
D1Rat251
D1Rat259
D1Rat261
D1Rat104
D1Rat133
D1Rat123
D1Rat75
D1Rat119
D1Rat81
D1Rat87

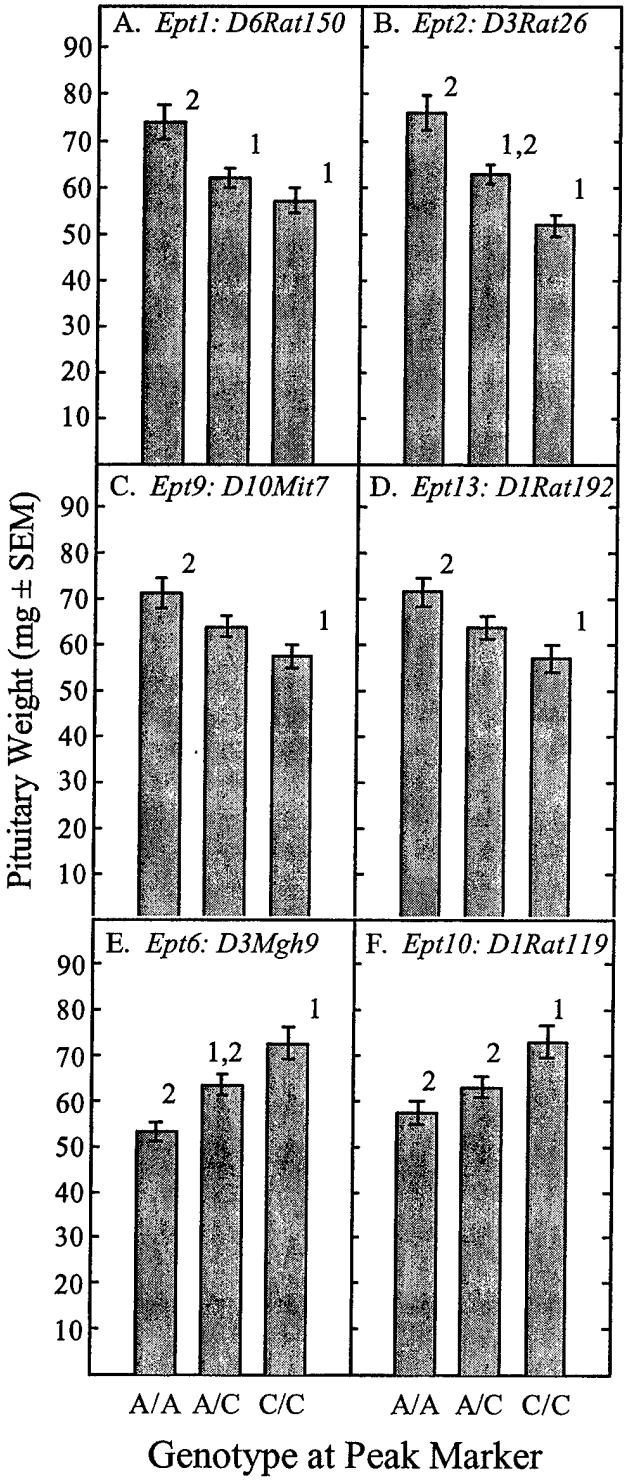
A. Ept1: D6Rat150
B. Ept2: D3Rat26
C. Ept9: D10Mit7
D. Ept13: D1Rat192
E. Ept6: D3Mgh9
F. Ept10: D1Rat119
Pituitary Weight (mg ± SEM)
90
80
70
60
50
40
30
20
10
2
1
1,2
A/A A/C C/C
Genotype at Peak Marker

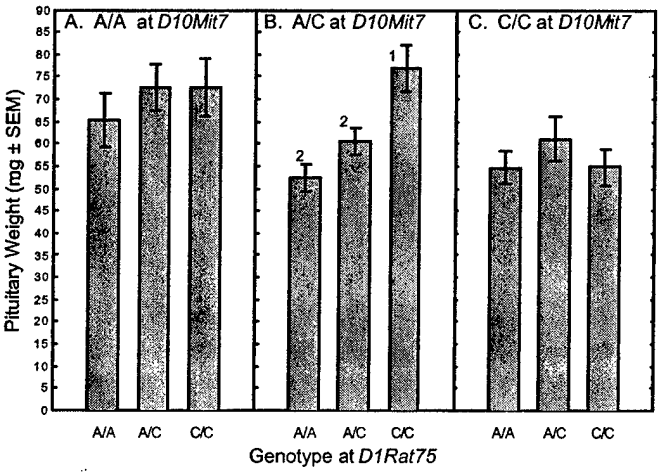
A. A/A at D10Mit7
B. A/C at D10Mit7
C. C/C at D10Mit7
Pituitary Weight (mg ± SEM)
90
85
80
75
70
65
60
55
50
45
40
35
30
25
20
15
10
5
0
2
2
1
A/A
A/C
C/C
A/A
A/C
C/C
A/A
A/C
C/C
Genotype at D1Rat75

Table 1. Analysis of Pituitary Mass Data for Rats from Reciprocal Crosses Between the ACI and COP Rat Strains.

Group	Untreated[a]	DES Treated[a]	*P* value vs ACI[b]	*P* value vs COP[c]
ACI	8.1 ± 1.1 (7)	72.7 ± 14.6 (28)	---	<0.001
COP	9.5 ± 2.7 (8)	36.2 ± 7.4 (28)	<0.001	---
F_1	8.4 ± 1.1 (8)	58.0 ± 10.0 (48)	0.038	<0.001
F_2	8.9 ± 1.7 (8)	63.6 ± 25.6 (266)	0.046	<0.001
BC	7.8 ± 0.4 (5)	70.7 ± 22.2 (68)	1.000	<0.001

[a] Pituitary wet weights (mg ± SD) in each group.
[b] Pituitary wet weights from the DES Treated F_1, F_2, and BC populations were compared to those exhibited by the ACI strain using a one-way ANOVA ($P = 0.05$ is significant).
[c] Pituitary wet weights from the DES Treated F_1, F_2, and BC populations were compared to those exhibited by the COP strain using a one-way ANOVA ($P = 0.05$ is significant).

The number of animals in each group is indicated in parentheses.

Table 2. Estimated Fraction of Phenotypic Variance Determined by each *Ept* Locus, Environmental Factors and Unknown Genetic Factors.

Locus	Marker	Impact of Locus on Mean Pituitary mass (mg)[1]	Phenotypic Variance Determined (%)
Ept1	*D6Rat150*	16.8	6.0
Ept2	*D3Rat26*	24.2	11.0
Ept6	*D3MGH9*	-19.6	7.0
Ept9	*D10MIT7*	13.6	6.0
Ept10	*D1Rat119*	-15.8	6.0
Ept13	*D1Rat192*	14.6	5.0
Suggestive RNO4	*D4Rat196*		4.0
Suggestive RNO5	*D5Rat95*		3.0
Environmental Variance			34.0
Unexplained Genetic Variance			18.0

[1] Mean pituitary mass (mg) in those F2 rats that are homozygous for ACI alleles at the indicated polymorphic marker minus the mean pituitary mass in those F2 rats that are homozygous for COP alleles at that marker.